Aus der Medizinischen Klinik und Poliklinik III
Klinikum der Ludwig-Maximilians-Universität München
Direktor: Prof. Dr. Dr. Michael von Bergwelt

"Functional characterisation of Enhancer of Zeste-Homologue 2 (EZH2) in acute myeloid leukaemia"

Dissertation
zum Erwerb des Doktorgrades der Naturwissenschaften
an der Medizinischen Fakultät der
Ludwig-Maximilians-Universität zu München

vorgelegt von
Julia Maria Kempf
aus Baden-Baden
2019

Mit Genehmigung der Medizinischen Fakultät

der Universität München

Betreuer: Univ. Prof. Dr. Gunnar Schotta

Zweitgutachter: Prof. Dr. Wolfgang Enard

Dekan: Prof. Dr. med. dent. Reinhard Hickel

Tag der mündlichen Prüfung: 18.09.2020

Eidesstattliche Erklärung

Ich erkläre hiermit an Eides statt, dass ich die vorliegende Dissertation mit dem Thema „Functional characterisation of Enhancer of Zeste-Homologue 2 (EZH2) in acute myeloid leukaemia“ selbständig verfasst, mich außer der angegebenen keiner weiteren Hilfsmittel bedient und alle Erkenntnisse, die aus dem Schrifttum ganz oder annähernd übernommen sind, als solche kenntlich gemacht und nach ihrer Herkunft unter Bezeichnung der Fundstelle einzeln nachgewiesen habe.

Ich erkläre des Weiteren, dass die hier vorgelegte Dissertation nicht in gleicher oder in ähnlicher Form bei einer anderen Stelle zur Erlangung eines akademischen Grades eingereicht wurde.

_____

Julia Maria Kempf, den 04. Oktober, 2020

Content

Dedicated to my parents

Abstract

Background and Aim of this Work

Acute myeloid leukaemia (AML) is a fast proliferating haematologic cancer, causing death usually within weeks if untreated. Even though many patients achieve complete remission after initiating chemotherapy, relapse occurs frequently and is a main cause of therapy failure. The lysine-protein methyltransferase EZH2 is part of a repressive protein complex, mediating the tri-methylation on histone H3 lysine K27 and it has been reported to be overexpressed in many different types of cancer. Especially loss of function (LOF) mutations are prevalent in myeloid neoplasms and loss of EZH2 has been suggested to induce chemotherapy resistance in AML cell line models. Clinical observations and functional data in relapsed AML have shown that loss of EZH2 expression might contribute to drug resistance in AML. In this study we focussed on the functional characterization of *EZH2* mutations using different biological approaches applying patient material, patient-derived xenograft (PDX) models (*in vitro* and *in vivo*), human AML cell lines and clinical data.

Results and Conclusion

By analysing protein and mRNA expression levels, we found a decrease in EZH2 expression in 23-50% of AML patients. Additionally, low expression of EZH2 is correlated with a poor overall survival (OS) and a poor relapse free survival (RFS) interval. We found that EZH2 mutations, detected in AML patients, are loss of function (LOF) mutations and that protein loss of EZH2 induces resistance against cytarabine (AraC) in 293T cells and the myeloid cell line K652. Re-expression of EZH2-WT, but not of a LOF mutation is able to rescue drug sensitivity in K562 cells. Additionally, functional loss of EZH2 is associated with a drug resistant phenotype in a patient-derived xenograft (PDX) model, both *in vitro* and *in vivo*. In summary, we show that functional inactivation of EZH2 promotes chemotherapeutic resistance in AML *in vivo* and *in vitro* and is involved in clonal evolution and disease progression, highlighting its clinical relevance. Our data also indicate, that treatment with EZH2 inhibitors, which are currently applied in clinical trials might drive resistance mechanisms in a subset of AML patients.

Zusammenfassung

Hintergrund und Ziel der Arbeit

Die akute myeloische Leukämie (AML) ist eine maligne hämatologische Erkrankung, die unbehandelt zum Tod führt. Obwohl die meisten Patienten innerhalb der initialen Therapie eine Remission erreichen, treten häufig Rezidive auf, welche die Hauptursache für ein finales Therapieversagen sind. EZH2 ist eine Lysin-Protein Methyltransferase und Teil eines repressiven Protein-Komplexes, welcher die Tri-Methylierung von Histon3 Lysin27 (H3K27) vermittelt. Überexpression von EZH2 tritt in verschiedenen Tumorarten auf. In myeloischen Neoplasien werden im Speziellen Mutationen gefunden, welche zu einem Funktionsverlust führen. Klinische Beobachtungen deuten darauf hin, dass der Verlust von EZH2 einen Betrag zum Therapieversagen in der AML leisten könnte. Innerhalb dieser Arbeit wird daher die funktionale Charakterisierung von EZH2 unter Hilfenahme von Modellen wie humanen Zell-Linien, Patientenproben und patient-derived xenograft-(PDX)Zellen (*in vitro* und *in vivo*), thematisiert.

Ergebnisse und Fazit

Es konnte gezeigt werden, dass EZH2 mRNA- und Proteinexpressionslevel in 23-50% aller untersuchten AML Patienten zwischen Diagnose und Rezidiv verringert waren. Zusätzlich wurde gezeigt, dass eine niedrige Expression mit einem schlechten Überleben der Individuen mit AML korreliert. Es wurde gezeigt, dass mit Mutationen, welche in Patienten auftreten, ein Funktionsverlust einhergeht und dass der Verlust von EZH2 in 2 verschiedenen Zelllinien zu einer erhöhten Resistenz gegenüber dem Chemotherapeutikum Cytarabine (AraC) führt. Re-Expression des wildtyp Enzyms konnte dabei den resistenten Phänotyp wieder gänzlich aufheben, während eine LOF Mutante dazu nicht in der Lage war. Zusätzlich wurde in einem patient-derived xenograft (PDX) Modell gezeigt, dass eine LOF Mutante von EZH2 *in vivo* und *in vitro* resistenz-assoziiert ist. Zusammenfassend konnte in dieser Arbeit gezeigt werden, dass ein Funktionsverlust der Methyltransferase EZH2 die Chemotherapie-Resistenz in Patienten mit AML fördert und dass EZH2 in die klonale Evolution und Krankheitsprogression involviert ist. Die Daten deuten außerdem darauf hin, dass EZH2 Inhibitoren, welche derzeit in klinischen Studien getestet werden, Resistenz-Mechanismen in bestimmten Subgruppen von AML Patienten fördern könnte.

1. Introduction

According to a 2018 World Health Organization (WHO) statement, cancer is the second most common cause of death worldwide, accountable for approximately 9.6 million deaths in that year[1]. Internationally, mortality is due to cancer in about one in six cases. Hence, the impact of cancer is significant and increasing worldwide. Haematological malignancies are widespread, being the fourth most frequently occurring cancer in economically developed areas of the world[2–5]. WHO has classified more than 60 haematological cancer subtypes. These differ substantially in clinical presentation and treatment requirements[6].

1.1. Acute Myeloid Leukaemia

1.1.1. Pathogenesis and Treatment

Leukaemias are malignant disorders of the haematopoietic system causing an increased amount of non-functional progenitor leucocytes. Clinically and pathologically, leukaemias can be divided into several groups, including chronic leukaemias, which are slow-growing or acute leukaemias, which are fast-growing and characterized by rapid disease progression. Both chronic and acute leukaemias are divided into two subgroups whereas the origin of malignant cell type determines whether they are termed myeloid or lymphatic. Acute myeloid leukaemia (AML) is the most frequent acute leukaemia in adults, responsible for approximately 80% of cases[7,8]. AML is a highly heterogeneous disease, typified by the clonal expansion of aberrant, undifferentiated myeloid precursor cells[9]. This results in alterations of the haematopoietic system, including normal haematopoietic differentiation. As a consequence, an immense increase of immature myeloid cells in the bone marrow and the peripheral blood emerges. These so-called “blasts” are able to proliferate, but unable to differentiate into mature haematopoietic cells such as neutrophils or monocytes[9]. As a consequence, the absence of functional cells causes bone marrow failure, which is accompanied by clinical symptoms associated with to anaemia, thrombyocytopenia and granulocytopenia[10]. Left untreated, AML leads to death within a few weeks to months[11]. Even though many patients with AML respond to induction chemotherapy, relapse is very common and exemplifies the most important cause of therapy failure[12,13]. Albeit several new therapeutic strategies have been proposed

within the last years (including alternative anthracycline treatment, alternative cytotoxic agents and high-dose cytarabine induction therapy[14–16]), treatment with cytarabine (AraC) and daunorubicin (DNR) stays the standard care for AML patients[17]. The usual induction treatment for younger adults is composed of the "3+7" regimen which includes DNR (60mg/m^2 intravenously for 3d) and standard-dose AraC (100mg/m^2 administered via continuous infusion over 7d). This therapy ends in remission rates of 65% and 75% in patients aged 18–60 years[18]. Prognosis for older patients is much worse due to death rates and resistance during therapy[13,19]. Complete remission (CR), which is defined as a bone marrow with less than 5% blasts, neutrophil count greater than 1000/µl and a platelet count greater than 100.000/µl is the only therapy response that leads to cure[20]. In an elongated treatment phase, the goal is to prolong CR status in order to achieve complete cure. When a patient reached CR for more than three years, the probability of relapse decreases to less than 10%[21].

1.1.2. Classification and Incidence

Two main systems have been introduced to classify AML subtypes. The "French-American-British" (FAB) classification and the more recent "World Health Organization" (WHO) classification. In the 1970s, a group of international experts divided AML into subtypes, M0 through M7. This classification system is founded on morphology and cyto-chemistry[22]. AML classification was modernized in 2002 when WHO proposed a new taxonomy considering morphology, genetics and clinical parameters. Subsequently, the initial classification[23] has been updated twice, most recently in 2016[24,25]. In 2014 the "Surveillance of Rare Cancers in Europe (RARECARE) project" aimed to summarize epidemiology of myeloid malignancies in Europe. The overall annual incidence of myeloid malignancies was 8.6 per 100,000 wherein AML and myeloproliferative neoplasm (MPN) were detected most frequently, with incidence rates of 3.7 and 3.1 per 100,000 year respectively, slightly higher in males than in females. The 5-year relative overall survival for AML is 19% and incidence grows with increasing age[26].

1.2. Clonal Evolution and Resistance in AML Relapse

The ability of cancers to evolve and adapt is one of the major challenges when treating tumour patients in general. Co-existence of multiple, heterogeneous subclones forming the tumour tissue provides the foundation of a dynamic evolutionary process. Consequently, the landscape of tumour tissue is always re-shaping during disease progression. Evidence supports the theory, that cancer clones are selected in an evolutional manner, relying on the simplest Darwinian evolution model[27]. Clones that persist post-chemotherapy are a serious challenge for the pharmacological treatment of AML patients as it was previously discussed a lot[13,19,28]. Clonal heterogeneity of AML therefore forms the basis of clonal evolution during disease progression and hypothetical explanations for treatment resistance. It is commonly accepted, that most cases of AML develop from a single pre-malignant transformed haematopoietic progenitor cell termed "leukemic stem cell" (LSC), which has specific characteristics, e.g., cytotoxic resistance properties[27]. Based on this concept many patients have residual AML within CR which is called "minimal residual disease" (MRD[29]). MRD is characterized by a small number of resistant cell clones that persist during treatment. One of the most explored mechanisms in treatment resistance is the deregulation of the drug efflux transmembrane ATPase P-glycoprotein (P-gp; which is encoded by the *MDR1* gene) which was investigated decades ago[30]. Detection of residual clones in CR might improve clinical outcome for patients where relapse is very likely since it has been recently shown, that approximately 75% of all patients already have pre-leukemic mutations in the peripheral blood, even 7 to 10 years before AML is diagnosed[31]. Fast progression in the development of highly sensitive diagnostic tools, such as gene- and microRNA-expression, genome-wide single nucleotide polymorphism-based (SNP) mapping arrays or next-generation sequencing (NGS) techniques offer more and more insight into the functional genomics of cancer and is encouraging for achieving a better understanding of the evolution of AML development.

a. Chemotherapy induced Mutagenesis

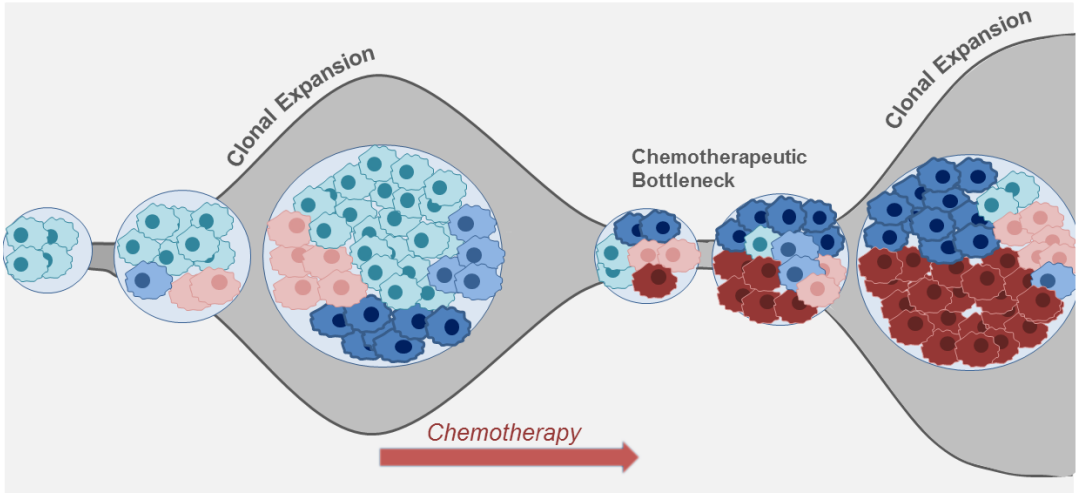

b. Selection of a Resistance accelerating Mutation

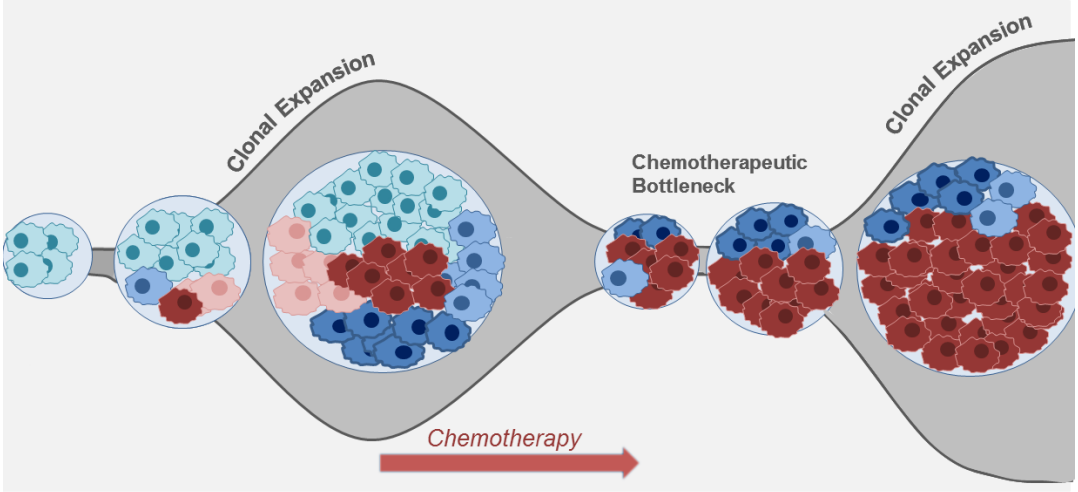

c. Competetive Selection after Cytotoxic Clearing

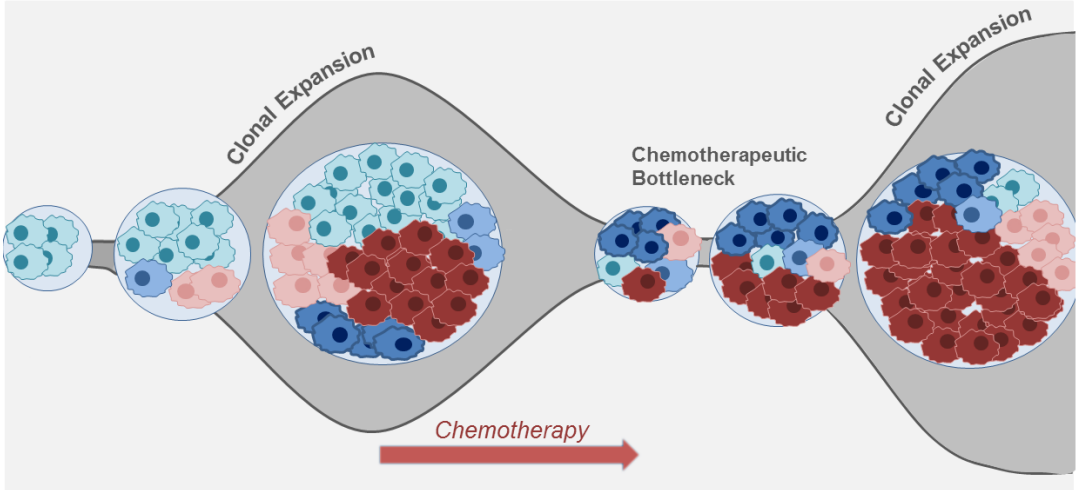

Figure Legend: See next page

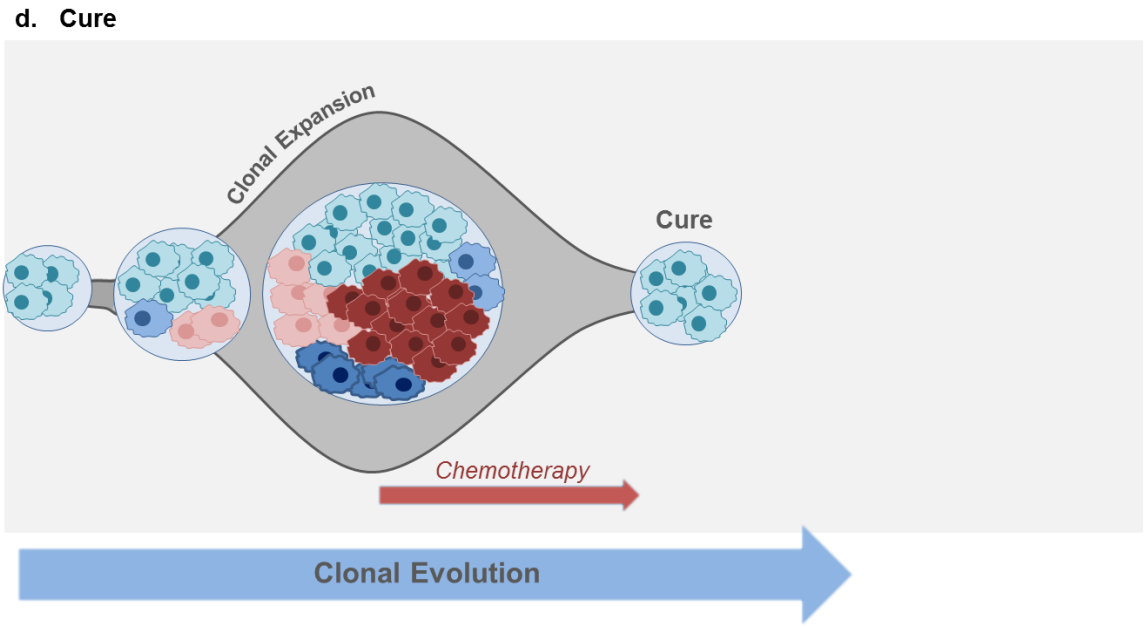

Figure 1: Hypothetical development of AML showing clonal fractions at AML diagnosis and relapse. In the first model, cytotoxic treatment induces mutagenesis (**a**). In the second model, one resistant clone arises from the tumour mass after chemotherapeutic treatment (**b**). In the third model, resistance of clones does not differ and the cleared niche after therapy is populated within a dynamic evolutionary pattern (**c**). Eradication of all malignant AML clones leads to cure (**d**) in the fourth model (adapted from Landau et. al[27]).

One question surrounding the difficult treatment of relapsed AML patients is how resistance develops during disease course. One major reason for resistance development is treatment with cytotoxic drugs. Several hypothetical possibilities can lead to resistance during chemotherapeutic treatment, founded on the model of clonal evolution of cancer cells[27] (Figure 1). It is accepted that exposure to a certain chemotherapeutic drug can lead to the development of resistant clones. Whereas treatment with cytotoxic agents such as AraC minimizes the cell number in remission, therapy associated mutations arise during treatment and resistant clones offer the basis for clonal expansion in AML relapse (chemotherapy induced mutagenesis). In another scenario, resistant clones exist from the beginning of AML induction and these persist during chemotherapy, due to specific resistant characteristics. These clones survive treatment and re-expand after therapy is completed (selection of a resistance accelerating mutation). In a third model, the outgrowth of relapse associated cells is not founded by a single clone, but different cell clones repopulate the cleared niche, which has been created by cytotoxic clearing. In a dynamic pattern, which is influenced by evolutional selection pressure (competitive selection after cytotoxic clearing) repopulation takes place. In the last scenario, AML can

be completely cured through the eradication of all malignant clones by chemotherapeutic treatment.

1.3. Genetic and Epigenetic Factors with Prognostic Impact in AML

1.3.1. Molecular Markers in AML

In 2010, international leukaemia experts comprising the "European leukaemia Net" (ELN) published recommendations for diagnosis, prognosis and treatment of AML patients. These guidelines consider the prognostic value of cytogenetic and molecular abnormalities[32]. The newest ELN recommendation[33] classifies AML into the three prognostic risk categories: favourable, intermediate, and adverse. Even though functional consequences of many recurrent genetic alterations are not yet completely defined, mutations have become useful molecular markers for diagnosis and prognosis and are used routinely in the clinics[33]. The most recurrent mutations that appear in cytogenetically normal (CN)-AML patients are the fms-like tyrosine kinase *FLT*3 (39%), nucleophosmin *NMP*1 (33%) and the DNA methyltransferase *DNMT3A* (31%)[34]. Yet, several other mutations can be observed to originate from kinases, which are involved in cellular signalling processes to diverse transcription factors. Moreover, the combination of different mutations or rearrangements has an immense effect on patient outcomes. For example patients harbouring *FLT3*-ITD alongside *NPM-1* wildtype alleles have a much poorer prognosis than patients with *FLT3*-ITD and mutated *NPM-1*[33].

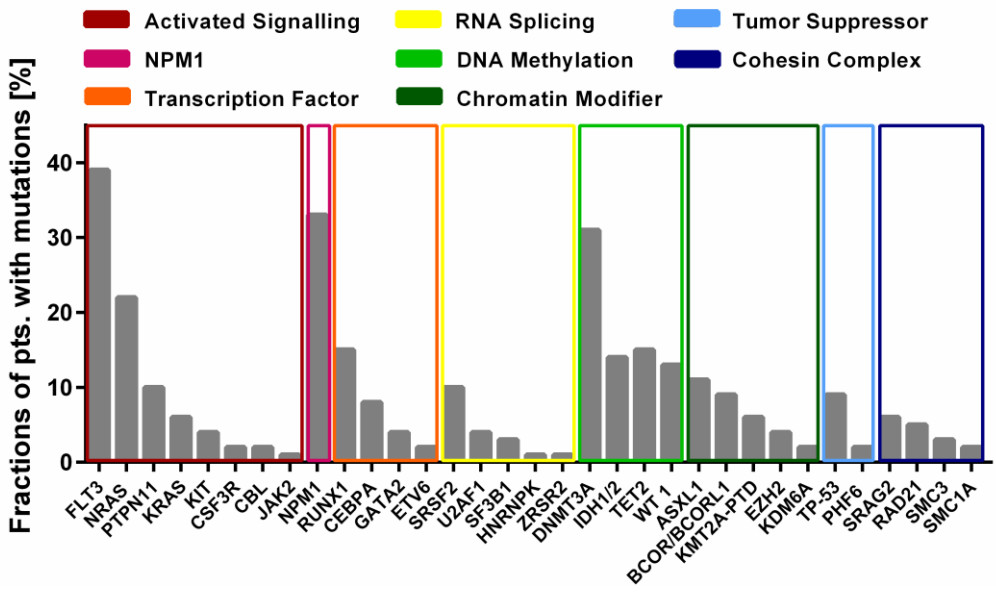

Figure 2: Histogram illustrating the spectrum of driver mutations detected in AML patients according to specific classification groups. Data obtained from Metzeler et al., 2016[34].

In a cohort of 664 patients Metzeler et al.[34] presented the spectrum of driver mutations in AML patients aged 18-86 years (Figure 2), summarized in specific functional groups, including chromatin modifiers. Mutations in genes which are involved in the regulation of epigenetics have been described frequently in the past decades[35–37] emphasizing the high importance of epigenetic regulation in the development and progression of cancer.

1.3.2. Epigenetics and AML

The term epigenetics refers to a heritable class of dynamic changes of chromatin structures and gene transcription, without altering the actual DNA sequence. Modification of chromatin structures which changes interaction between DNA and histones, are important physiological processes[38]. For example, these modifications permit transcriptional up- and downregulation of specific target genes, DNA repair, or replication. This includes DNA methylation, histone modifications, changes in nucleosome modelling, histone variants and non-coding RNAs[39,40] which indirectly affect gene transcription[38,41]. Epigenetic regulators can be broadly classified into "writers" (including methyltransferases or acetyltransferases), "erasers" (including demethylases and deacetylases) and "readers" (recognition enzymes, e.g. PHD- and bromodomain-containing proteins)[42].

Approximately 70% *de novo* AML patients show mutations in epigenetic modifiers that are involved in the methylation of DNA or histone modelling[43]. Methylation of DNA is associated with the transcriptional repression by formation of heterochromatin which is achieved through DNA methyltransferases (DNMTs)[44]. One of the most studied genes in AML is the DNA (cytosine-5)-methyltransferase 3A (*DNMT3A*) that catalyses *de novo* methylation of cytosine residues in DNA[45,45]. *DNMT3A* mutations occur in 20-30% of *de novo* AML patients and are associated with an adverse risk[46]. In addition, chromatin modelling enzymes, which mediate posttranslational histone methylation or acetylation in order to modify transcription, have been shown to affect tumour development[47].

1.3.3. Histone Modifications

In addition to DNA methylation, the posttranslational modification of histones plays a crucial role in epigenetic regulation. Histones offer a framework for storage space of DNA within eukaryotic nucleus. This complex of DNA and histone proteins is called chromatin. Histone proteins represent the core element of the nucleosome, the basic component of chromatin[48]. Modification of histone residues can be associated with either genetic repression or activation. For example, acetylation of H4K14, methylation of H3K4 or phosphorylation of H3S10 all infer genetic activation of specific target genes[49]. In contrast, the methylation of H3K9 and H3K27 is mostly associated with genetic repression[50]. The adjunct of methyl groups to lysine and arginine residues of histone proteins is accomplished by histone-lysine methyltransferases and histone-arginine methyltransferases, respectively[51,52]. Rearrangements of the lysine-methyltransferase 2A (*MLL/KMT2A)* gene are one of the first aberrations in methyltransferases that has been associated with leukemogenesis; alterations in this gene have been linked to a poor prognosis[53]. Subsequently, different kinds of modifiers coordinating histone methylation have been found to be altered in AML. The human lysine-methyltransferase protein family is a group of 52 described methyltransferases, sharing a catalytic domain which uses *S*-adenosyl-*l*-methionine (SAM) as methyl donor. Each histone-lysine-methyltransferase is highly specific for the associated histone residue[54,55] and the catalytic activity drives mono-, di- and tri-methylated lysine and causes specific downstream effects reliant on the residues' position and the level of methylation[56]. Enzymes, which control histone methylation can be classified in histone-methyltransferases and histone-demethylases, which both have been reported to be altered in different kinds of cancer[57–64].

1.3.4. Epigenetic Targeted Therapy

Given the importance of epigenetic regulation in the physiological background of cells, epigenetics plays an important role in the pathogenesis of many diseases. These include cancer[43,46,47,64–67], including haematopoietic malignancies[65,68], where they have been extensively studied. Since the understanding of epigenetic regulation in tumour emergence and maintenance is rapidly growing, epigenetic targeted therapy concepts are of high interest. Several therapeutic approaches targeting epigenetic regulators in AML have been productively tested in preclinical studies and some medications have been

passed, including, e.g., hypo-methylating agents such as azacytidine (AZA) or decitabine (DAC)[66,67]. Results have been disappointing considering these apporaches[69]. Both AZA and DAC are pyrimidine analogues functioning as inhibitors for DNA-methyltransferases, leading to global hypomethylation of cytosine residues[70]. Additionally, drugs affecting the activity of histone methyltransferases have been investigated extensively[71]. Several small molecule inhibitors for the DOT1-like histone H3K79 methyltransferase (DOT1L) showed a high suppression of *HOX* (homeobox) genes, leading to induction of differentiation and anti-leukemic activity in *DNMT3A* mutant AML[72]. Furthermore the development of specific inhibitors of the lysine-specific histone demethylase 1A (LSD1) have been the objective of many different recent studies[73] and have been proven to show anti-leukemic properties[64,74]. Additionally, combinatorial inhibition treatment of histone modifying proteins have been proposed, including e.g., combination treatment of LSD1 and EZH2 (Enhancer of zeste-homologue 2)[75] or LSD1 and pan-histone deacetylase (HDAC) inhibitors[75]. Epigenetic targeted therapy concepts therefore are of high importance and support patient-adapted therapy concepts in the future treatment of AML.

1.4. The Protein-Lysine Methyltransferase EZH2

Enhancer of zeste-homologue 2 (EZH2) is a protein-lysine methyltransferase and the central core unit of the polycomb repressive complex 2 (PRC2)[76]. Through its catalytic Su(var)3-9, Enhancer-of-zeste and Trithorax (SET) domain, the methylation of histone H3 lysine K27 (H3K27me) is achieved, whereby the generation of heterochromatin limits the accessibility for the transcription machinery (Figure 3)[77]. As a result, EZH2 mediates transcriptional repression of associated target genes[78]. EZH2 is capable of mono-, di- and tri-methylation of H3K27, which has been linked to a large range of biological functions such as transcriptional regulation in haematopoiesis, cellular differentiation and development[79–81]. For example, EZH2 activity is highly important for the maintenance of normal differentiation in ES cells[79]. EZH2 and H3K27 methylation also play a crucial role in X-inactivation[82], the silencing of one X-chromosome in female development.

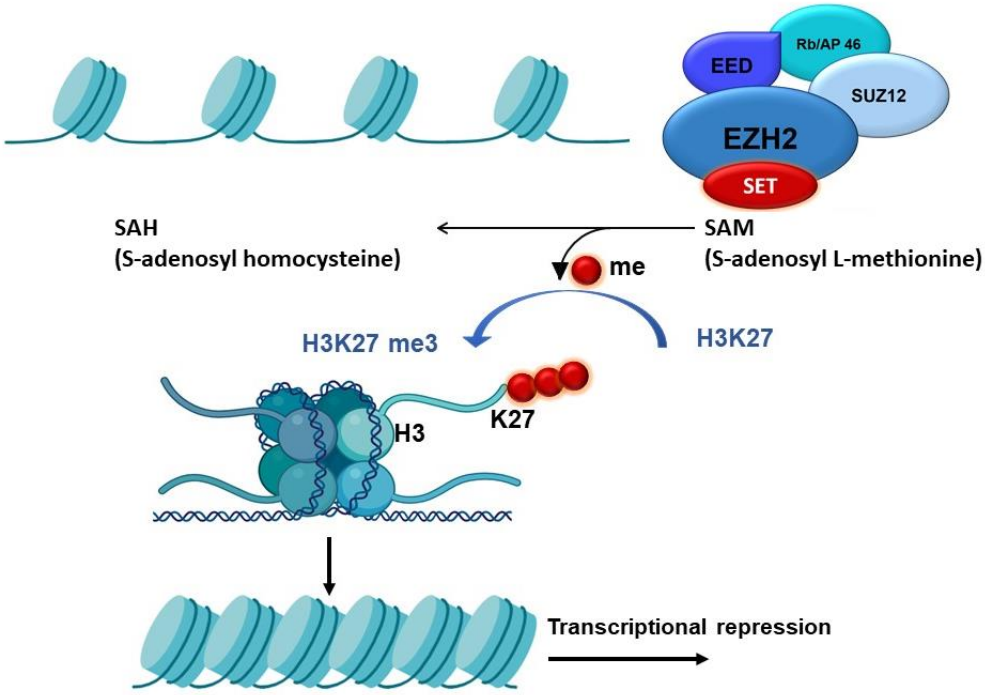

Figure 3: PCR2 mediated gene repression through catalytic activity of EZH2. By its catalytic SET domain EZH2 controls H3K27me3 and thereby promotes gene repression of associated target genes through changes in chromatin condensation by transmitting a methyl group from the cofactor S-adenosyl-L-methionine (SAM)[80].

EZH2 as part of PRC2 is primarily responsible for the methylation of H3K27. Therefore it is important that all PRC2 members are present, although the function of EED, RB/AP46/48 and SUZ12 is not yet completely characterized[78]. It has been discussed for years that PRC2 fulfils important roles in normal haematopoiesis by maintaining pluripotency and self-renewal capabilities in adult stem cells[76,83], therefore indicating that EZH2 expression is important for maintaining the stemness of HSCs. Meanwhile, it has been proposed that PRC2 mediated tri-methylation marks on H3K27 recruit PRC1 to mono-ubiquitinylate lysine 119 of histone H2A in order to establish a higher condensation of the chromatin[76] revealing an epigenetic signalling pathway downstream of H3K27 methylation by EZH2.

1.4.1. EZH2 and Cancer

To date, an oncogenic role of EZH2 (Figure 4) is well established in many diverse kinds of cancers[84–86], whereas the value of *EZH2* in haematopoietic malignancies remains unclear. High expression of EZH2 in patient samples was first detected in breast[87] and prostate[88] cancer in the early 2000s and was connected with a poor prognosis. It has been shown, that high levels of EZH2 can be linked to aggressive cell proliferation in endometrial, cutaneous melanoma and prostate cancers[89]. High EZH2 expression is also associated with bladder cancer[90], a poor prognosis and cisplatin resistance in ovarian cancer[84], fast progression of lung cancer[86] and liver cancer[91]. Additionally, researchers have observed high levels of EZH2 in later stages of brain tumours[85], and to be associated to poor prognosis in renal[92] and gastric[93] cancer and chemo-resistance in pancreatic cancer[94]. Furthermore, in 2013, investigators described a link between high expression levels and invasion in nasopharyngeal carcinoma[95]. Especially in lymphomas, high expression levels correlate with rapid and aggressive tumour growth[96,97].

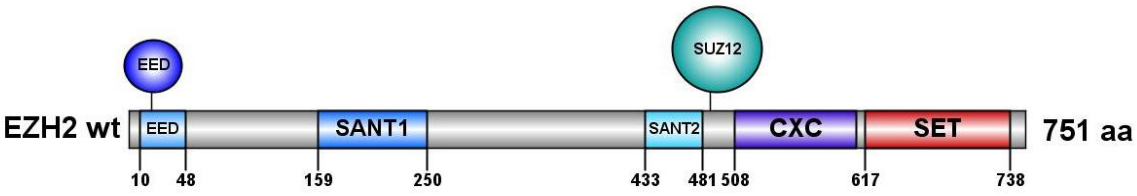

Figure 4: Schematic illustration of the protein-lysine methyltransferase EZH2. Functional domains are coloured, the catalytic SET domain is located C-terminal. Binding domains for the PRC2-proteins EED and SUZ12 are indicated above.

Strikingly, hot spot mutations (mainly located in the SET domain) causing increased levels of H3K27me3 have been found in 22% of diffuse large B-cell lymphoma (DLBCL) and 7.5-25% follicular lymphoma (FL)[98,99]. Y646 mutations occur most frequently in lymphomas; significantly higher levels of tri-methylated H3K27 are observed in mutated patient samples. Surprisingly, decreased levels of di-methylated H3K27 can be detected, which were found to be based on a diminished recognition of unmodified and mono-methylated H3K27[100]. Y646 was first thought to act as LOF mutation, since *in vitro* testing revealed decreased tri-methylation levels of H3K27. In 2010, Sneeringer et al. investigated known lymphoma associated *EZH2* mutations and found that mutated EZH2 alleles are always found associated with one wildtype allele. Thus, wildtype and mutant alleles collaborate

to hyper-tri-methylate H3K27, highlighting the importance of a heterozygous status[101]. Referring to this, potent small-molecule inhibitors have been developed and provide a promising therapeutic value in phase 1 trials (NCT02082977, NCT01897571). It has been definitely shown, that loss or inhibition of H3K27me3 contributes to the development of malignancies. In contrast to lymphomas, *EZH2* LOF mutations have been found in myeloid malignancies such as MDS or AML[43,102,103]. Ernst et al. described 7q deletions occurring in combination with homozygous *EZH2* deletions in 9 out of 12 patients, suggesting that EZH2 acts as a tumour suppressor in the context of myeloid malignancies. Additionally, loss of functional EZH2 has also been detected in patients suffering from myelodysplastic syndrome (MDS)[103] and *EZH2* LOF mutations were likewise correlated with a poor prognosis in a cohort of patients with myelofibrosis[104].

These data lead to the hypothesis, that EZH2 can act as a tumour suppressor and oncogene – strongly dependent on the cellular context. Within the last few years, contradictory results have been presented, also discussing an oncogenic role of EZH2 in MLL-rearranged leukaemias[105]. A recent study investigated opposing roles of EZH2 in initiation and maintenance of AML, suggesting that expression of EZH2 is highly dependent on the stage of disease[106].

2. Materials and Methods

2.1. Material

2.1.1. Laboratory Equipment

Table 1: Applied equipment

Equipment	Provider
ABI 3730 XL Sequencer	Applied Biosystems (Foster City, CA, USA)
Amaxa Nucleofector II device	Lonza (Basel, CH)
Analytical balance ABJ 220-4NM	Kern & Sohn (Balingen-Frommern, Germany)
BioPhotometer	Eppendorf (Hamburg, Germany)
Bio-Rad Mini Protean Tetra blotting system	Biorad (Hercules, CA, USA)
Centrifuge 5415D, 5424R	Eppendorf (Hamburg, Germany)
CO2 incubator C 170	BINDER (Tuttlingen, Germany)
E-BOX VX2	Vilber Lourmat (Eberhardzell, Germany)
FACS Vantage SE	BD Biosciences (Franklin Lakes, NJ, USA)
Fluorescent microscope DMi8	Leica Microsystems (Wetzlar, Germany)
Freezer -20°C	Liebherr (Bulle FR, Switzerland)
Freezer -80°C, TLE	Thermo Fisher Scientific (Waltham, MA, USA)
Freezing container Mr. Frosty	Thermo Fisher Scientific (Waltham, MA, USA)
Fusion SL4 imaging system	Vilber Lourmat (Eberhardzell, Germany)
Heating block Thermomixer compact	Eppendorf (Hamburg, Germany)
X1R Centrifuge Hareaus	Thermo Fisher Scientific (Waltham, MA, USA)
Ice machine FM-170AKE	Hoshizaki (Amsterdam, NL)
Incubator 9040-0013	Binder (Tuttlingen, Germany)
Liquid Nitrogen Tank	Cryoson (Schöllkrippen, Germany)
Magnetic stirrer MR3001	Heidolph (Schwabach, Germany)
Microplate reader GloMax® Discover	Promega (Madison, WI, USA)
Microscope ID03	Carl Zeiss (Oberkochen, Germany)
PCR cycler PeqSTAR 2xGradient	Peqlab (Wilmington, DE, USA)
pH meter inoLab® pH 7110	WTW (Weilheim, Germany)
Pipettes (0.25-2.00µL, 2.0-20.0µL, 20-200µL, 200-1000µL)	Gilson (Limburg, Germany)
Pipetus accu-jet pro	Brand (Wertheim, Germany)
High precision scale PCB 2500-2	Kern & Sohn (Balingen-Frommern, Germany)
RS-TR 5 Tube-roller	Phoenix instrument (Garbsen, Germany)

Nanodrop spectrophotometer 1000	Thermo Fisher Scientific (Waltham, MA, USA)
Ultrapure water system Milli-Q System	Merck Millipore (Darmstadt, Germany)
VARIOKLAV Type 500	HP Medizintechnik (Oberschleißheim, Germany)
Vertical Autoclave VX-150	Systec (Linden, Germany)
Vi-CELLTM Cell Viability Analyser XR	Beckman Coulter (Krefeld, Germany)
Vortexer	Cenco (Breda, NL)
Water Bath Type 1003	GFL (Burgwedel, Germany)
Xcell SureLock Mini Cell	Invitrogen (Darmstadt, Germany)

2.1.2. Consumables

Table 2: Used consumables

Consumable	Provider
5mL Round Bottom Polystyrene Tube	Thermo Fisher Scientific (Waltham, MA, USA)
5mL Stripette serological Pipets	Corning (Corning, NY, USA)
10mL Stripette serological Pipets	Corning (Corning, NY, USA)
25mL serological Pipets	Greiner Bio One (Frickenhausen, Germany)
96-well PCR plate	Brand (Wertheim, Germany)
96-well V-bottom	Greiner Bio One (Frickenhausen, Germany)
Amersham Protran Nitrocellulose membrane, 0.45µM	GE Healthcare (Little Chalfont, UK)
Combitips advanced 0.5mL	Eppendorf (Hamburg, Germany)
Combitips advanced 1.0mL	Eppendorf (Hamburg, Germany)
Combitips advanced 5.0mL	Eppendorf (Hamburg, Germany)
Diamond Tower Pack D10	Gilson (Middleton, WI, USA)
Diamond Tower Pack D200	Gilson (Middleton, WI, USA)
Diamond Tower Pack D1000	Gilson (Middleton, WI, USA)
Disposable bags	Brand (Wertheim, Germany)
DURAN GL 45 Lab Bottles (100mL, 250mL, 500mL, 1000mL)	DURAN Group (Mainz, Germany)
DURAN Erlenmeyer flasks (50 mL, 250mL, 500mL, 1000mL)	DURAN Group (Mainz, Germany)
Sorenson low binding standard tips	Sigma-Aldrich (St. Louis, MO, USA)

Gel-loading pipet tips	Sigma-Aldrich (St. Louis, MO, USA)
Micro tube 1.5mL SafeSeal	Sarstedt (Nümbrecht, Germany)
Micro tube 2.0mL SafeSeal	Sarstedt (Nümbrecht, Germany)
Novex Empty Gel Cassette, mini, 1.0 mm	Thermo Fisher Scientific (Waltham, MA, USA)
Cryo Tube Vial	Thermo Fisher Scientific (Waltham, MA, USA)
PARAFILM	Sigma-Aldrich (St. Louis, MO, USA)
PCR tubes 0.2mL	Biozym Scientific (Oldendorf, Germany)
Petri dish 10cm / 30 cm	Sarstedt (Nümbrecht, Germany)
TC Flask T25, T75, T175, standard	Sarstedt (Nümbrecht, Germany)
TC Flask T25, T75, T175, suspension	Sarstedt (Nümbrecht, Germany)
TC Plate 6-well - 96-well, standard	Sarstedt (Nümbrecht, Germany)
TC Plate 6-well - 96-well, suspension	Sarstedt (Nümbrecht, Germany)
Tube 15mL, 120x17mm	Sarstedt (Nümbrecht, Germany)
Tube 50mL, 114x28mm	Sarstedt (Nümbrecht, Germany)
Vasco Nitrile Blue Gloves	B. Braun (Melsungen, Germany)

2.1.3. Chemicals

Table 3: Used chemicals

Reagent	Provider
1 kb ladder	Promega (Madison, WI, USA)
ß-Mercaptoethanol	Sigma-Aldrich (St. Louis, MO, USA)
2-Propanol	AppliChem (Darmstadt, Germany)
Agarose	Carl Roth (Karlsruhe, Germany)
Albumin Fraction V (pH 7.0) (BSA)	AppliChem (Darmstadt, Germany)
APS (Ammonium persulfate)	Carl Roth (Karlsruhe, Germany)
Ampicillin sodium salt	Sigma-Aldrich (St. Louis, MO, USA)
Aprotinin	Sigma-Aldrich (St. Louis, MO, USA)
Bio-Rad Protein Assay Dye	Bio-Rad (Hercules, CA, USA)
Bromophenol blue	Sigma-Aldrich (St. Louis, MO, USA)
Calcium Chloride 2-hydrate	AppliChem (Darmstadt, Germany)
CutSmart Buffer	New England Biolabs (Frankfurt, Germany)
Coulter Clenz Cleaning Agent	Beckman Coulter (Krefeld, Germany)

Coulter Isoton II Diluent	Beckman Coulter (Krefeld, Germany)
DNase I	Roche (Basel, CH)
DEPC-treated water	Thermo Fisher Scientific (Waltham, MA, USA)
DH5α competent bacteria	Thermo Fisher Scientific (Waltham, MA, USA)
Dimethyl Sulfoxide (DMSO)	Sigma-Aldrich (St. Louis, MO,USA)
DMEM high glucose, Gibco	Thermo Fisher Scientific (Waltham, MA, USA)
Ethanol	Merck Millipore (Darmstadt, Germany)
Fetal Bovine Serum (FBS)	PAN-Biotech (Aidenbach, Germany)
Gel Loading Dye Purple 6x	New England Biolabs (Frankfurt, Germany)
HBS 2x	Sigma-Aldrich (St. Louis, MO, USA)
HEPES	AppliChem (Darmstadt, Germany)
Kanamycin Sulfate	Sigma-Aldrich (St. Louis, MO, USA)
LB-Agar	Carl Roth (Karlsruhe, Germany)
LB-Medium	Carl Roth (Karlsruhe, Germany)
Lipofectamine 3000	Thermo Fisher Scientific (Waltham, MA, USA)
Methanol	Carl Roth (Karlsruhe, Germany)
Milk powder (for blotting)	Carl Roth (Karlsruhe, Germany)
MyTaq Polymerase	Bioline (London, UK)
Opti-MEM I Reduced Serum Medium, Gibco	Thermo Fisher Scientific (Waltham, MA, USA)
PageRuler Prestained Protein Ladder	Thermo Fisher Scientific (Waltham, MA, USA)
PBS Dulbecco w/o Mg^{2+}, Ca^{2+}	PAN-Biotech (Aidenbach, Germany)
Penicillin-Streptomycin, Gibco	Thermo Fisher Scientific (Waltham, MA, USA)
Phenylmethylsulfonyl fluoride (PMSF)	Sigma-Aldrich (St. Louis, MO, USA)
Pierce ECL Plus Western Blotting Substrate	Thermo Fisher Scientific (Waltham, MA, USA)
Proteinase K	New England Biolabs (Frankfurt, Germany)
Quick-Load Purple 50bp DNA ladder	New England Biolabs (Frankfurt, Germany)
Recombinant Human FLT3 (rhFLT3) Ligand	R&D Systems (Minneapolis, MN, USA)
Recombinant Human IL3 (rhIL3) protein	R&D Systems (Minneapolis, MN, USA)
Recombinant Human Thrombopoietin (rhTPO) protein	R&D Systems (Minneapolis, MN, USA)

Recombinant Human SCF (rhSCF) protein	R&D Systems (Minneapolis, MN, USA)
RNase AWAY	Carl Roth (Karlsruhe, Germany)
Rotiphorese gel 30	Carl Roth (Karlsruhe, Germany)
RPMI 1640 + Glutamax, Gibco	Invitrogen (Darmstadt, Germany)
Sodium chloride (NaCl)	Carl Roth (Karlsruhe, Germany)
Sodium dodecyl sulfate (SDS)	Sigma-Aldrich (St. Louis, MO, USA)
Sodium fluoride NaF	Sigma-Aldrich (St. Louis, MO, USA)
Sodium Orthovanadate	Sigma-Aldrich (St. Louis, MO, USA)
Sodium pyruvate 100mM	Biochrom (Berlin, Germany)
S.O.C. Medium	Invitrogen (Darmstadt, Germany)
StemPro-34 SFM Media	Thermo Fisher Scientific (Waltham, MA, USA)
SYBR Safe DNA gel stain	Invitrogen (Darmstadt, Germany)
TAE Buffer 10x	Apotheke Klinikum der Universtität München (Munich, Germany)
TBS Buffer 10x	Apotheke Klinikum der Universtität München (Munich, Germany)
Tetramethylethylenediamine (TEMED)	Sigma-Aldrich (St. Louis, MO, USA)
Tris-(hydroxymethyl)-aminomethane (TRIS)	Carl Roth (Karlsruhe, Germany)
Triton X-100	Sigma-Aldrich (St. Louis, MO, USA)
Trypan Blue	Sigma-Aldrich (St. Louis, MO, USA)
Trypsin-EDTA (0.05%), phenol red	Thermo Fisher Scientific (Waltham, MA, USA)
Tween20	Sigma-Aldrich (St. Louis, MO, USA)

2.1.4. Kit Systems

Table 4: Applied kits

Kit	Application	Provider
Cell line Nucleofector Kit V	Transfection of suspension cell lines	Lonza (Basel, CH)
Endofree Plasmid Maxi Kit	Maxi preparation of plasmid DNA	Qiagen (Hilden, Germany)

EpiQuik Total Histone Extraction Kit	Isolation of histone proteins	Epigentek (Farmingdale, NY, USA)
InFusion HD Plus Cloning	Vector cloning	Takara Bio (Saint-Germain-en-Laye, France)
Mouse Cell Depletion Kit	Purification of human cells from PDX material	Miltenyi Biotec (Bergisch Gladbach, Germany)
MycoAlert Mycoplasma Detection Kit	Detection of mycoplasma contamination in cell culture	Lonza (Basel, CH)
QIAamp DNA Blood Mini Kit	Isolation of gDNA from cells and tissues	Qiagen (Hilden, Germany)
QIAprep Spin Miniprep Kit	Mini preparation of plasmid DNA	Qiagen (Hilden, Germany)
QIAquick Gel Extraction Kit	DNA extraction from agarose gels	Qiagen (Hilden, Germany)
QIAquick PCR Purification Kit	Amplicon purification	Qiagen (Hilden, Germany)
QuikChange II Site directed mutagenesis Kit	Gene mutagenesis	Agilent Technologies
RNAse-Free DNase Kit	DNase digest for RNA isolation pre-treatment	Qiagen (Hilden, Germany)
RNeasy Mini Kit	RNA isolation	Qiagen (Hilden, Germany)
SALSA MLPA MDS Kit	MLPA for human cell lines and patient material	MRC Holland (Amsterdam, Netherlands)

2.1.5 Buffers and Solutions

Table 5: Used buffers and solutions

Buffer	Composition
Agarose gels (1% - 1.5%)	1-1.5% agarose in 1x TAE buffer with SYBR Safe (1:10 000)
Western blot buffer (Transfer) 10x	15g Tris, 71g Glycine, 790 g Methanol

	Add up to 5000 mL d_2H_20
Gel electrophoresis buffer 10x	151.4mg Tris, 720.7g Glycine, 50g Sodiumdodecylsulfate (SDS), Add up to 5000mL d_2H_20
Gel electrophoresis buffer 1x	100 mL gel electrophoresis buffer 900 mL d_2H_20
KCM 5x	5mL 3 M KCl, 4,5mL 1 M CaCL2, 7,5mL 1M MgCl2
LB agar plates	32g Agar, add up to 1l d_2H_20
LB medium	Add up to 1l d_2H_20
$LB_{ampicillin}$ plates	LB-Agar 20mL 100µg/mL Ampicillin
LämmLi buffer 4x	50mM tris-HCL pH 6.8, 0.8g sodiumdodecylsulfate (SDS), 10% glycerol, 1% ß-mercatoethanol, 12.5mM EDTA, 8mg bromophenol blue
TAE buffer 1x	100mL TAE buffer 10x, 900mL d_2H_20
TBS 10x	60.57g Tris, 483.3g Sodium chloride
TBS-T	100mL TBS buffer 10x, 900mL $_d2H_20$, 1% Tween-20
Tris pH 6.8	5L: 908.55g Tris (pH 6.8), add H_20 dest.
Tris pH 8.8	5L: 908.55g Tris (pH 8.8), add H_20 dest.
Lysis buffer for whole cell lysis	25mL 1 M HEPES, pH 7.5, 15mL 5 M NaCl 2,5mL 200 mM EGTA, 100mL 50% Glycerol 5mL Triton X-100, 2.1g NaF, 2.2g $Na4P2O7x10H_2O$ add d_2H_20 freshly added before each lysis: 5mM PMSF, 25 µg/mL Aprotinin,, 50µg/mL Sodium Orthovanadate
FACS buffer	PBS, 1% FCS, 1mg/l propidium iodide Storage: Light protected, at 4°C
Freezing buffer	10% DMSO in FBS, stored at 4°C
Blocking solutions	5% non-fat milk in TBS-T or 5% BSA in TBS-T

2.1.6. Antibodies

Table 6: Used primary antibodies

Antibody	Host	Dilution	Blocked in	Provider
α-EZH2	Rabbit	1:1000	5% Milk	Cell Signaling Technology (Danvers, MA, USA)

α-ß-Actin	Mouse	1:20.000	5% Milk	Sigma-Aldrich (St. Louis, MO, USA)
α-H3K27me3	Rabbit	1:1000	5% BSA	Cell Signaling Technology (Danvers, MA, USA)
α-H3 total	Rabbit	1:30.000	5% Milk	Abcam (Cambridge, UK)
α-EED	Rabbit	1:500	5% Milk	MerckMillipore (Burlington, US)
α-SUZ12	Rabbit	1:1000	5% Milk	Cell Signaling Technology (Danvers, MA, USA)
α-RbAP46	Rabbit	1:1000	5% BSA	Cell Signaling Technology (Danvers, MA, USA)

Table 7: Used secondary antibodies

Antibody	Host	Dilution	Provider
Goat Anti Mouse m-IgGkappa HRP	Goat	1:10.000	Santa Cruz Biotechnology (Dallas, TX, USA)
Goat Anti Rabbit	Goat	1:10.000	Sigma-Aldrich (St. Louis, MO, USA)

2.1.7 Oligonucleotides

Table 8. Oligonucleotides for EZH2 sequencing

Name	5' → 3' sequence	Tm
EZH2-IsoA-FOR1	CCTTCTGATAAAATTTTTGAAGCC	59.6°C
EZH2-IsoA-FOR2	GACAATTTCTGTGCCATTGCT	60.1°C
EZH2-IsoA-FOR3	CGCAAGGGTAACAAAATTCG	60.5°C
EZH2-IsoA-REV1	GCTGCTGTTCGGTGAGTTCT	60.6°C

Table 9: Oligonucleotides for mutagenesis

Name	5' → 3' sequence	Tm
EZH2/A692G FOR	CCGTTAACCATCATAACTTTTCCATAGCAGTTTGGATTTACCG	79.7°C

EZH2/A692G REV	CGGTAAATCCAAACTGCTATGGAAAAGTTATGATGGTTAACGG	79.7°C
EZH2/Y646N FOR	TGAGAAATAATCTCTCCACAGTTTTCTGAGATGAATTCATTTTTCTG	78.1°C
EZH2/Y646N REV	CAGAAAAATGAATTCATCTCAGAAAACTGTGGAGAGATTATTTCTCA	78.1°C
EZH2/Y731F FOR	GCCTGGCTGTATCTGAAATCAAAAAACAGCTCTTCGC	79.4°C
EZH2/Y731F REV	GCGAAGAGCTGTTTTTTGATTTCAGATACAGCCAGGC	79.4°C
EZH2/I744fs FOR	CCCTGAAGTATGTCGGCATGGCATCGAAAGAGAAATGGA	78.0°C
EZH2/I744fs REV	TCCATTTCTCTTTCGATGCCATGCCGACATACTTCAGGG	78.0°C
EZH2/c.2195+1 FOR	AGCTGTTTTTTGATTACAGATTGATACAGCCAGGCTGATGC	78.3°C
EZH2/c.2195+1 REV	GCATCAGCCTGGCTGTATCAATCTGTAATCAAAAAACAGCT	78.3°C
EZH2/G743fs FOR	CCATTTCTCTTTCGATGCCGGGGCCCGACATACTTCAGGGC	79.2°C
EZH2/G743fs REV	GCCCTGAAGTATGTCGGGCCCCGGCATCGAAAGAGAAATGG	79.2°C
EZH2/K574E FOR	GCACGGGCACTGCTCGGTGTTGCACTGTG	80.2°C
EZH2/K574E REV	CACAGTGCAACACCGAGCAGTGCCCGTGC	80.2°C
EZH2/D293G FOR	ACGATGTAGGAAGCATTCATATTTAAAACATCGCCTACAGAAAAG	78.9°C
EZH2/D293G REV	CTTTTCTGTAGGCGATGTTTTAAATATGAATGCTTCCTACATCGT	78.9°C
EZH2/Q612X FOR	TCCTGCAAGAACTGCAGTATTTAGCGGGGCTCC	80.4°C
EZH2/Q612X REV	GGAGCCCCGCTAAATACTGCAGTTCTTGCAGGA	80.4°C
EZH2/D730_Y731FOR	CTGGCTGTATCTGTAATCAAAAAAACAGCTCTTCGCCA	78.3°C
EZH2/D730_Y731REV	TGGCGAAGAGCTGTTTTTTTGATTACAGATACAGCCAG	78.3°C

Table 10: Oligonucleotides for cloning

Name	**5' → 3' sequence**	**Tm**
InFuEZH2pcDNA6 FOR	CAGTGTGGTGGAATTCCGAAGAATAATCATGGGCCAGACT	78.0°C

InFuEZH2pcDNA6 REV	GCCCTCTAGACTCGAGGCAGATGTCAAGGGATTTCCATTTC	80.0°C
InFuEZH2piggy FOR	CTCTGAGGCCACCCGATAATCATGGGCCAGACTGGGAAGAA	82.0°C
InFuEZH2piggy REV	AGGCTTACCGCGGCCATGTCAAGGGATTTCCATTTCTCTTTCG	81.0°C

Table 11: Oligonucleotides for CRISPR/Cas9 mediated genome editing

Name	5' → 3' sequence	Tm
EZH2 guide upper	CACCGACCAAGAATGGAAACAGCGA	67.0°C
EZH2 guide lower	AAACTCGCTGTTTCCATTCTTGGTC	64.0°C
EZH2 Screening FOR	ACAATTTCTCCTTTCCTCTCCTTCA	63.0°C
EZH2 Screening REV	TGGACACCCTGAGGTCAATGAT	62.0°C

2.1.8 Vectors

Table 12: Used vector systems

Vector	Application	Origin
EZH2 (NM_004456)	Entry vector	Origene (Rockville, US)
pcDNA6/HisA	Expression-vector for transient expression	AG Spiekermann, Klinikum der Universität München
pcDNA6/HisA-EZH2	Re-expression of EZH2 mutations for tri-methylation activity test	This work
tet-3xFLAG-AsiSI-NotI-IRES-DsRed-Express-M2rtTA-P2A-PuroR	Expression vector for PiggyBac	AG Bultmann, LMU
tet-3xFLAG-AsiSI-NotI-IRES-DsRed-Express-M2rtTA-P2A-PuroR-EZH2	Stable/inducible re-expression of *EZH2* in K562 cells	This work
pSpCas9(BB)-2A-GFP-gRNA	Expression vector for Cas9 endonuclease	AG Bultmann, LMU
pSpCas9(BB)-2A-GFP-gRNA-EZH2	Generation of *EZH2* knockout cell clones	This work
Transposase	Helper plasmid for stable gene insertion via PiggyBac	AG Bultmann, LMU

2.1.9 Cytostatics and Inhibitors

Stock solutions of the cytostatic cytarabine (AraC, Selleck Chemicals, Houston, TX, USA) at 20mM and EZH2 inhibitor GSK126 (Selleck Chemicals, Houston, TX, USA) at 10mM were prepared by dissolving the drugs in DMSO. All steps were performed under sterile conditions. The anthracycline daunorubicin was prepared at 3.2mM dissolved in deionized water under sterile conditions. Aliquots were stored at -80°C to avoid freeze-thaw-cycles.

2.1.10 Software

Table 13: Applied software

Software	Application	Provider
Microsoft Office 2010	Data analysis (such as sequencing), text editing	Microsoft (Redmond, WA, USA)
SnapGene 3.3.4	Primer design, sequencing analysis, creation of vector maps	GSL Biotech LLC (Chicago, IL, USA)
IBS	Design and presentation of shown biological sequences	CUCKOO Workgroup, online
Benchling	Design of guideRNAs, sequencing analysis	Benchling Inc., online
E-Capt 15.06	Agarose gel recording and documentation	Vilber Lourmat (Eberhardzell, Germany)
GraphPad Prism 6.07	Data visualization, statistical analysis	GraphPad Software (La Jolla, CA, USA)
ImageJ version 1.50d	Western blot quantification	ImageJ developers, online
Genemarker V2.6.0	Analysis of MLPA results	Softgenetics LLC.(State College, USA)
FusionCapt Advance 16.11	Western blot recording and analysis	Vilber Lourmat (Eberhardzell, Germany)
Biorender	Illustration and design of biological figures	Biorender AG (Münchwilen TG, CH)

2.2. Methods

2.2.1. Cell Culture Methods

2.2.1.1 Cell lines and Patient Samples

All cell lines (Table 14) were acquired from DSMZ (Braunschweig, Germany) and cultured according to the supplier's recommendation. PDX-AML samples were engrafted and passaged in mice and re-isolated for *in vitro* cultivation as it has been previously described[107]. Exclusion of mycoplasma contamination was assessed continuously during cell culture using the MycoAlert Mycoplasma detection kit (Lonza, Basel, CH). Used patient material was derived from AML patients from the trials AMLCG-99 (NCT00266136) and AMLCG-2008 (NCT01382147), and the Department of Medicine III, University Hospital, LMU, Großhadern. Informed permission for utilization of sample material was obtained from all participants in agreement with the Declaration of Helsinki.

Adherent cells:

Adherent cells were incubated with DMEM (Dulbecco), supplemented with 10% FBS, 0.5% penicillin/streptomycin at 37°C and 5% CO_2. Before usage, cells were always re-suspended with pre-warmed medium and only used for further experiments when viability was more than 90%. Cell viability was measured with the Vi-Cell Cell Viability Analyser (Beckman Coulter, Krefeld, Germany). For sub-cultivation of cells were washed one with PBS (room temperature) and then covered with trypsin-EDTA at room temperature for 2-3 min to ensure detachment of the cells from the flask ground. Adding DMEM stopped the activity of trypsin and the cells can be passaged or harvested for further experiments. Adherent cells were sub-cultured in a ratio of 1:10 every 2-3d.

Suspension cells:

Human cell lines

All human AML cell lines were incubated with RPMI medium supplemented with 20% FBS and 0.5% penicillin and streptomycin at 37°C with 5% CO_2. Cell density was kept between 0.4–1.2 x 10^6 cells/mL (as recommended by the DSMZ (Braunschweig, Germany)). Cells were sub-cultured three times a week. For all experiments and cultivation condition pre-warmed medium was used. Cells were always re-suspended with pre-warmed medium and only used for further experiments when viability was more than 90%. Cell viability

was measured with the Vi-Cell Cell Viability Analyser (Beckman Coulter, Krefeld, Germany). The cell line K562, originally a CML cell line, was used for the cytotoxicity experiments in EZH2 KO cells. K562 originate from a CML patient in the last stage of the disease (blast crisis), which phenotypically shows a very high similarity to AML. For this reason, the line is particularly suitable for cytotoxicity studies.

Patient-derived xenograft (PDX) cells

PDX cells were cultured (according to Martin Wermke (Dresden, Blood 2015)) with StemPro-34 medium, supplemented with appropriate nutrient supplement, 0.5% penicillin/streptomycin, 0.5% L-Glutamine, 2% FBS, 0.02% SCF (stock 50µg/mL), 0.02% TPO (stock 50µg/mL), 0.02% IL-3 (stock 50µg/mL) and 0.01% FLT3L (stock 100µg/mL PBS + 0.1% BSA). Nutrient supplement was slowly thawed at 4°C. Medium was always prepared freshly before PDX cell cultivation. PDX cells were cultivated at 37°C and 5% CO_2 and medium was always pre-warmed for experiments. Cell viability was measured with the Vi-Cell Cell Viability Analyser (Beckman Coulter, Krefeld, Germany).

Table 14: Human cell lines in this thesis

Name	Cultivation	Organism	Tissue/Tumour	Origin
Hek293T	Adherent	Human	Embryonic kidney	DSMZ
HL-60	Suspension	Human	Acute myeloid leukaemia	DSMZ
K562	Suspension	Human	Chronic myeloid leukaemia	DSMZ
Kasumi1	Suspension	Human	Acute myeloid leukaemia	DSMZ
KG1a	Suspension	Human	Acute myeloid leukaemia	DSMZ
MM1	Suspension	Human	Acute myeloid leukaemia	DSMZ
MM6	Suspension	Human	Acute myeloid leukaemia	DSMZ
Molm13	Suspension	Human	Acute myeloid leukaemia	DSMZ
MV4-11	Suspension	Human	Acute myeloid leukaemia	DSMZ
Oci AML 3	Suspension	Human	Acute myeloid leukaemia	DSMZ
Oci AML 5	Suspension	Human	Acute myeloid leukaemia	DSMZ
Pl-21	Suspension	Human	Acute myeloid leukaemia	DSMZ
SKM-1	Suspension	Human	Acute myeloid leukaemia	DSMZ
THP-1	Suspension	Human	Acute myeloid leukaemia	DSMZ
U937	Suspension	Human	Histiocytic lymphoma	DSZM

2.2.1.2 Proliferation Assays

Suspension cells were treated with cytarabine (AraC, Selleck Chemicals, Houston, TX, USA), and daunorubicin (DNR, in-house). For short time assays, viable cell number was determined after 72h on Vi-Cell Cell Viability Analyser (Beckman Coulter, Krefeld, Germany). For long-term proliferation assays, cells were treated three times (d0, d4, d8) and viable cells were counted every second day. Unpaired, two-tailed Student's *t*-test and calculation of all IC_{50} values were performed using GraphPad Prism version 6.07 (GraphPad Software, La Jolla, CA, USA). PiggyBac[108](PB)/*EZH2* cells were pre-cultured with or without doxycycline (1µg/mL) for 72h followed by treatment with AraC +/- doxycycline, which was added every 48h. For knockdown experiments in PDX cells, siRNA EZH2 (#s4918, Thermo Fisher Scientific, Waltham, US) was transiently transfected (10nM) via nucleofection. Cells were pre-incubated for 48h and then treated with AraC for 72h.

2.2.1.3 Determination of Cell Viability by Trypan Blue Exclusion

To determine the cell viability and cell number, the trypan blue exclusion method was used as it is the most common method to define cell counts. The method is based on the simple principle, that viable cells actively exclude the dye whereas dead cells are stained blueish. Using of this staining viable cells can be distinguished from dead cells which is important for the evaluation of drug effects, such as inhibitors or cytostatics on the cell viability. Cell count was determined automatically with the Vi-Cell Cell Viability Analyser (Beckman Coulter, Krefeld, Germany). Cell number of untreated cells was always considered as 100% viability. All other conditions were normalized to the untreated cells in each experiment.

2.2.1.4. Freezing and Thawing of Cells

Cells in a density from 2-6 x 10^6 were made for long time storage in liquid nitrogen. The cell pellet was resolved in 1mL freezing medium (FBS supplemented with 10% DMSO) and frozen in 1.5mL cryotubes. These tubes were first delivered to -80°C in a suitable freezing container to gently cool down at a freezing rate of 1°C/minute. For long time storage, the cells were delivered to the liquid nitrogen at -196°C and thawed as required.

For thawing, cells were kept warm at 37°C for one minute and afterwards moved to a 50mL falcon, which contained pre-warmed medium in order to stop cytotoxic effects of the DMSO which is contained in the frozen cells. Cells were spun down for 5 min at 300g at room temperature and then cultured in the appropriate amount of pre-warmed medium.

2.2.1.5. Mycoplasma Detection Assay

All used cell lines were tested for mycoplasma contamination periodically during cell cultivation time. For detection the *MycoAlert Mycoplasma Detection Kit* from Lonza (Basel, CH) was used. Substrate and reaction solution were stored at room temperature for 30 min before usage. Only the supernatant of the tested cells were centrifuged at 200g for five min (approximately 0.5mL). 25µL of the supernatant was transferred to a luminescence compatible 96 well plate. Then 25µL of the reagent solution was added and incubated for 5 min at RT in order to lyse mycoplasma cells. Detection of luminescence was performed using the plate reader GloMax Discover (read A). After this first measurement 25µL substrate solution were added and incubated for 10 min in the dark. Luminescence was measured for a second time after this incubation step where mycoplasma enzymes react with the substrate solution. This reaction can be visualized due to luciferase enzyme activity. After 10 min, the solution is measured a second time (read B). Afterwards, the ratio (B/A) indicates whether cells are contaminated (>1.1.) or not (<0.9).

2.2.1.6. Transfection

Transient Transfection

For transient DNA and RNA transfection in 293T cells, *lipofectamine 3000* transfection reagent (Thermo Fisher Scientific, Waltham, US) was used. One day before transfection 293T cells were seeded at a density of 1 x 10^6 cells per 6-well and incubated at 37°C and 5% CO_2. After 24h medium was changed (2h before transfection). 2µg DNA were commonly transfected transiently, according to the suppliers' protocol.

Transient Transfection by Nucleofection

For transient induction of DNA and RNA into K562 cells the *2b Nucleofector* device from Lonza (Basel, CH) was used. This method offers cell-type specific nucleus targeted nucleotide transfer. For each cell line the recommended protocol which is provided from the manufacturer was applied. One day before transfection, cells were seeded out in low density 2d before nucleofection (approximately 0.2 x 10^6 cells/mL, depending on the cell type). For transfection procedure, cells were carefully spun down as described in each protocol and then suspended in the appropriate nucleofector solution (which was complemented with the suitable supplement solution) by carefully pipetting up and down. Afterwards, 2 µg DNA were added to the mix and the solution was carefully transferred to a provided cuvette. After nucleofection, cells were carefully transferred to a 24-well-plate.

Analysis of Transfection Efficiency

In order to evaluate the efficiency in each transfection assay the pmaxGFP vector, which is provided in the *2b Nucleofector* kits from Lonza (2µL from a 0.5µg/µL solution) was applied. After 16-18h the first GFP signal can be seen with the FITC channel (Fluorescence microscope *Leica DMi8* (Leica Microsystems (Wetzlar, Germany)).

2.2.2 Protein-Biochemical Methods

2.2.2.1. Whole Cell Lysis

Whole cell lysis was performed as it was described before[123]. For each lysate, a minimum cell amount of 4 x 10^6 cells was needed. Cells were spun down for 5min at 300g and 4°C and pellets were stored on ice for the whole lysis time. Cells were washed twice with ice cold PBS and re-suspended until a homogenous mixture was generated. Cells were spun down for another 5min at 300g and 4°C. For detachment of adherent cell lines a cell scraper was used, in order to generate a cell suspension. The pellet was re-suspended in the according amount of lysis buffer, which is supplemented with 5µL aprotinin/mL, 10µL PMSF/mL and 10µL orthovanadate/mL of lysis buffer. The pellet was vortexed every 5min. To remove cell fragments, the suspension was spun down after 30min on ice at 13.0000 rpm for 30min at 4°C and transferred to a pre-cooled tube. All whole cell lysates

were stored at -20°C for long time storage. For all further applications the lysates were always kept on ice.

2.2.2.2. Nuclear Cell Lysis

Nuclear cell lysis was performed as it was described before[123]. All steps were performed using the *EpiQuik Nuclear Extraction Kit II* (Nucleic Acid-Free) from Epigentek (Farmingdale, NY, USA) according to the manufacturers' protocol. After removing the medium, cell pellets were washed twice with ice cold PBS and spun down at 300g for 5min at 4°C. The appropriate amount of 10x pre-lysis buffer, which was diluted 1:10 in H_20 dest. was added and a homogenous suspension was generated. For nuclear pellet extraction the suspension was incubated for 10min on ice, followed by centrifugation at 12.000 rpm at 4°C. The supernatant was carefully removed and the pellet containing cell nuclei was incubated with nuclear lysis buffer for 30min on ice. Afterwards, the nuclear extracts were carefully removed and DTT (at a 1:1000 dilution) was added. Nuclear cell lysates were stored at -80°C for long time storage.

2.2.2.3. Determination of Protein Concentrations

Determination of protein concentration was performed as it was described before[123.] Protein concentration in cell lysates (whole cell and nuclear) was assessed by using a spectrophotometer and the Bradford method as previously described[109]. The calculated absorbance (595nm) correlates with the total protein concentration. First, the dye reagent was diluted 1:5 in H_2O and protein lysates were diluted 1:10 in H_2O. 20µl of these diluted lysates were then mixed with 980µl of diluted dye and stored for 5 min at RT. Absorption (595nm) was measured and compared to a blank control sample with only the dye and H_2O. A serial dilution of the BSA solution (200-1000µg/mL) was used as reference standard in order to evaluate final concentration.

2.2.2.4. Immunoblotting and SDS-PAGE

Immunoblotting, which is commonly known as Western Blotting (WB), was used for detection of proteins and was performed as it was previously described[123]. First, lysates from either whole cell or nuclear fractions were generated as described before. Then,

denaturing gel electrophoresis separates different molecular sized proteins. Subsequently, separated proteins are transferred to a nitrocellulose membrane. After blocking, the membrane is incubated with a solution containing a specific antibody against the protein of interest followed by a secondary antibody which is conjugated to a detection system. Between 2µg (for nuclear cell fractions) and 20µg (for whole cell fractions) of protein were loaded and a sodium dodecyl sulfate-polyacrylamide (SDS) gel electrophoresis was performed. Protein concentration was detected by Bradford assay with Bio-Rad Protein Assay reagent. Before electrophoresis 4x Lämmli buffer was added and samples were boiled for 10min at 95°C. After electrophoresis, separated proteins were moved to a nitrocellulose membrane by wet transfer procedure overnight at 100mA. The next day, membranes were blocked in Tris buffered saline (TBS-T) containing 5% non-fat dry milk. The same solution was prepared to dilute primary and secondary antibody, which were incubated with the membranes for 1h at room temperature. After antibody incubation the membranes were always washed three times with TBS-T for five min each. For protein detection, ECL method was applied. Seperating gel (here shown for 10%): H_2O dest. 6.9mL; 30% acrylamide/bisacrylamide 4mL; 1.5M Tris-HCl buffer (pH 8.8) 3.8mL; 10% SDS in H_2O dest. 0.15mL; 10% APS in H_2O dest. 0.15mL; TEMED 0.009mL. Stacking gel: H_2O dest. 3.4mL; 30% acrylamide/bisacrylamide 0.83mL; 1.5M Tris-HCl buffer (pH 6.8) 0.63mL; 10% SDS in H_2O dest. 0.05mL; 10% APS in H_2O dest. 0.05mL; TEMED 0.005mL.

2.2.2.5. Evaluation of Biochemical EZH2 Activity

To investigate the effect of mutations on the catalytic activity of EZH2, eight distinct mutations were characterized for their potential to tri-methylate H3K27. For this assay, HEK293T *EZH2*$^{-/-}$ cells were seeded out in a concentration of 1 x 10^6 cells per 6-well plate one day before transfection. *EZH2* mutant or wildtype constructs were transfected transiently in HEK293T/*EZH2*$^{-/-}$ cells. After 72h, nuclear or whole cell lysates were generated and global H3K27me3 levels were evaluated by immunoblotting. Levels of H3K27me3 were normalized to the wildtype control for each construct.

2.2.3. Genome Editing

2.2.3.1. CRISPR/Cas9 mediated EZH2 Silencing

Design of single guide RNAs (sgRNA) was performed with Benchling software, considering the sgRNA score which gives information about the predicted off-target effects. To ensure proper gene knockout, it is advisable to target exons at the anterior site of the gene. Therefore, *EZH2* sgRNA was designed to target Exon 3 of *EZH2*.

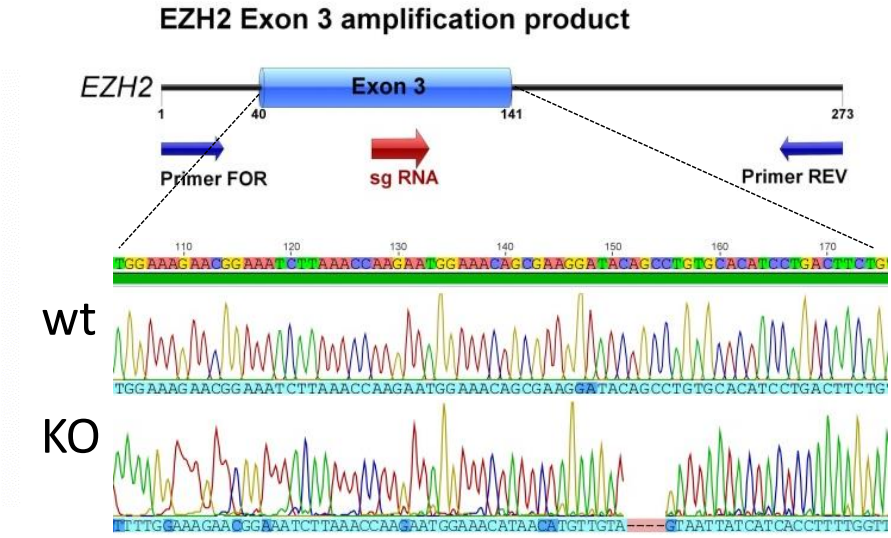

Figure 5: Targeting *EZH2* exon 3 for CRISPR/Cas9 mediated gene knockout. For the establishment of CRISPR/Cas9 mediated knockout (KO) clones, exon 3 of *EZH2* was targeted. Wildtype/KO clone sequences were confirmed by Sanger sequencing for each clone.

Genome editing procedures with CRISPR/Cas9 was performed as is was previously described by Stief et. al, 2019[123].Establishment of CRISPR/Cas9 mediated *EZH2* knockouts (KO,Figure 5) in the cell lines HEK293T and K562, cells were transiently transfected with 2µg pSpCas9(BB)-2A-GFP-gRNA-EZH2 by using electroporation (nucleofection). GFP positive cells were accumulated after 2d and single cell (SC) sorted into 96-well plates (V-bottom, K562) and in 30cm dishes (HEK293T) with the FACSVantage SE. For HEK293T cells, the colonies were separated manually using a 20µL sterile pipette tip and transferring each cell into wells of a 96-well plate. After that, cells were incubated at 37°C with 5% CO_2 for a few weeks, until colony formation was observed and sc clones were expanded. To screen for EZH2 loss, cells were lysed and amplified exon 3 PCR products[110] were sequenced by Sanger sequencing. gDNA was enriched with the QIAamp DNA Blood Mini Kit in a 96-well plate, re-suspended in 50µL lysis buffer SC, chilled for 30min at -80°C, incubated at 56°C for 3h and finally Proteinase K heat deactivated at 85°C for 30

min. 2.5µL/well of this lysate were directly subjected to the PCR mixture (25µL/rxn., 0.1µL MyTaq DNA Polymerase) and PCR was performed under following conditions: 95°C_5 min- (95°C_30s - 61°C_30s - 72°C_30s) x 45 - 72°C_40s - 4°C_∞. Genetic EZH2 KO was detected for each clone by RFLP analysis of PCR products using digestion with HpyAVI. After successful targeting, recognition sites are lost. Expression loss was always validated by immunoblotting for each clone. Primer and PCR design was performed using both, Geneious 8.1.7 and Benchling software.

2.2.3.2. Re-Expression by PiggyBac (PB)/Transposase System

For inducible re-expression of *EZH2* in HEK293T and K562 cells, cells were transfected either by lipofectamine (HEK293T) or nucleofection (K562) with tet-3xFLAG-AsiSI-NotI-IRES-DsRed-Express-M2rtTA-P2A-PuroR-EZH2[108]. Transposase was expressed transiently as helper plasmid. After transfection, cells were incubated for 48h at 37°C and 5% CO_2 and afterwards selected with 2µg/mL puromycin for 3d. Next, cells were sorted into 96-well-plates (with V-bottom) with the FACSVantage SE (single cell clones). Cells were incubated at 37°C with 5% CO_2 for a few weeks, until colony formation was observed and sc clones were expanded. To confirm inducible EZH2 protein expression by immunoblottting, clones were treated for minimum 24h with 1µg/mL doxycycline.

2.2.4. Molecular Biological Work

2.2.4.1. Cloning

For all cloning procedures In-Fusion Cloning (Takara-Bio, Kusatsu, JP) was performed. This technique provides a highly efficient, ligation-independent cloning method, which is based on the annealing of complementary ends of a cloning insert and linearized cloning vector. First, a base vector was chosen and cut by desired restriction enzymes. The insert of interest was amplified by specifically designed cloning primers which contain 15bp extensions (5') that are complementary to the ends of the linearized vector. Primer design for cloning was performed with the *SnapGene 3.3.4* software. After verification of the target DNA on an agarose gel, the amplicon was purified by the *QIAQuick PCR Purification* kit. Amplifying PCR was performed under following conditions: 5µL premix, 1µL primer FOR (10µM), 1µL primer REV (10µM), 10ng vector with desired insert (template) and xµL

H_20 dest., 20µL in total. Linearization of the base vector was achieved by restriction digest with specific restriction enzymes as followed: 500ng vector, 1.5µL enzyme A, 1.5µL enzyme B, 20µL in total. To ligate the amplified insert to the desired vector, a ligation was performed under following conditions: 2µL 5x InFusion HD enzyme premix, 50ng of amplified Insert, 150ng of linearized vector, xµL H_20 dest.; 10µL in total. Reaction was incubated for 15 min at 50°C. Transformation of the cloned construct was performed using *Stellar heat-shock competent cells* (Takara-Bio, Kusatsu, JP) as proposed in the protocol. For all transformations 2.5µL of the ligation mix was used. Stellar competent cells were thawed on ice and the ligation mix was added. After 30 min on ice the cells were heat-shocked for exactly 45 sec at 42°C to enforce DNA uptake to the bacterial strain. After two min on ice 500µL SOC medium was added and the bacteria mix was shaken for one hour at 37°C and 210 rpm. After that cells were spun down and re-suspended in 100µL fresh SOC medium. Diverse dilutions (1:20, 1:50, 1:100, 1:200) were spread out on LB_{amp} agar plates and incubated in an appropriate incubator overnight. After plasmid mini preparation, the sequence of the cloned insert was always verified.

2.2.4.2. Site-directed Mutagenesis

Site directed mutagenesis was used to induce point mutations, switch amino acids, and delete or insert single or multiple amino acids. This technique is a reliable tool which allows site-specific mutation insertion in any double-stranded plasmid. For mutation insertion the *Quickchange II Site directed mutagenesis kit* (Agilent Technologies, Santa Clara, US) was applied. The basic idea of the procedure relies on specific primers which both contain the desired mutation site. The primers are extending the template in a PCR reaction during temperature cycling by the *PfuUlta HF DNA polymerase,* which is provided in the kit. This extension produces mutated plasmid DNA of choice. The DPNI endonuclease (target sequence: 5'-Gm6ATC-3') is specific for methylated and hemi-methylated DNA and digests the parental DNA template, to enrich the mutation-containing fragments. Mutation inserting PCR was performed under following conditions: 5µL 10X reaction buffer, 20ng dsDNA template, 125ng Primer FOR, 125ng Primer REV, 1µL dNTP mix, xµL H_20 dest.; 50µL in total. Transformation of the mutated vector is recommended *in XL-10 blue supercompetent E.coli* cells, which are provided in the kit.

2.2.4.3. Chemical Transformation of Bacteria

Chemical transformation was used for re-transformation procedure in DH5α bacteria (Thermo Fisher Scientific, Waltham, US). This transformation step was used for all re-transformation procedures to multiply plasmid DNA. Competent bacteria were thawed on ice and then 1µL DNA was supplemented. In parallel, 10µL KCM and 14µL H_20 dest. were added. This mixture was incubated on ice for 20min, followed by 10min incubation at room temperature. Subsequent to this, 500µL LB medium were added and the cell suspension was shaken for one hour at 37°C and 210 rpm. After this procedure, 50–120µL of bacteria suspension were spread out on LB_{amp} plates by means of a drigalski spatula. Plates were incubated overnight at 37°C in an appropriate incubator.

2.2.4.4. Isolation of Plasmid DNA – Mini Preparation

Approximately 2mL of a single bacteria clone overnight culture was used for mini preparation of plasmid DNA. For all mini preparations the *QIAprep Spin Miniprep* kit (Qiagen, Hilden, Germany) was used. Cells were spun down for 3 min at 6800g and the supernatant was discarded. All further steps were performed according to the supplier's protocol. The DNA was eluted by addition of 30-50µL EB buffer and incubation for 3min. The eluted DNA was collected in a new 1.5mL tube and the concentration was determined by the Nanodrop. Plasmid DNA was stored at -20°C for long-term storage.

2.2.4.5. Isolation of Plasmid DNA – Maxi Preparation

In case that a higher amount of plasmid DNA was needed, a maxi preparation was conducted. Therefore, the *Endofree Plasmid Maxi* kit (Qiagen, Hilden, Germany) was applied. To increase bacteria and hence DNA material, a 2mL of a single bacteria clone was expanded to 100mL LBamp and shaked in a 1000mL Erlenmeyer flask at 37°C and 210 rpm overnight. The next day, bacteria were spun down at 6800g for 10 min at 4°C. All further steps were performed according to the supplier's protocol. The pellet was air dried for approximately 10 min and afterwards an appropriate amount of H_20 dest. (200–500 µL) were applied on the dried DNA. To increase concentration, an overnight incubation step was performed and concentration was determined the next day with the Nanodrop. Plasmid DNA was stored at -20°C for long-term storage.

2.2.4.6. DNA Restriction Digest

To assess correct cloning or mutagenesis, an enzymatic restriction digest was performed. All enzymes were acquired from New England Biolabs (Frankfurt, Germany). All digestion setups were applied as recommended by the producer. In a further step, the nucleic acids were separated on a 1% agarose gel for visualization with SYBR-Safe and UV light. The mix containing the following components were incubated for 2h at 37°C: 1µg plasmid DNA, 1µL of each restriction enzyme (10.000 u/µl or 20.000 u/µL), 2µL of the recommended restriction buffer (10X), x µL H_2O dest. in order to generate a total amount of 20µL.

2.2.4.7 Nucleic Acid Separation and Visualization by Electrophoresis

For visualization of different sized RNA and DNA fragments, nucleic acids were separated on a 0.7-1% agarose gel which contained 0.1µg/mL of the fluorescent dye SYBR-Safe. Nucleic acids were mixed with 6x gel loading buffer and applied on the gel. Additionally, a standard marker was applied to allow size orientation of the fragments. In case that an extraction was needed from the gel, the specific band was cut out under UV light and cleaned up with the *QIAquick Gel Extraction Kit* (Qiagen, Hilden, Germany) according to the supplier's recommendations. Purified DNA was eluted in 30µL of supplied elution buffer.

2.2.4.8. Isolation of Genomic DNA

For several applications the isolation of genomic DNA (gDNA) from whole cells was affordable. Therefore, the *QIAamp DNA Blood Mini Kit* was applied. At least approximately 5 x 10^6 cells were spun down for five min at 300g and room temperature and then resolved in 200µL PBS by gently pipetting up and down. As recommended in the protocol, a 1.5mL tube holding 20µL Proteinase K was prepared and the cells suspension was added. This procedure ensures protein digestion for the following nucleic acid extraction. For efficient lysis, 200µL of buffer AL were supplemented and the suspension was vortexted for 15sec and then incubated for 10min at 56°C in a heat block. All further steps were performed as recommended by the supplier. Concentration of gDNA was determined by measurement with the Nanodrop machine.

2.2.4.9 Isolation of RNA

For RNAseq analysis, isolation of RNA was affordable. This was performed with the *RNeasy Kit* (Qiagen, Hilden, Germany). All pipetting steps were performed with filtered tip to decrease the eventual degradation of the RNA. Additionally, the whole work space was cleaned with EtOH (70%) and *RNase Away* solution. The optional DNAse digest step was always performed.

2.2.4.10 Multiplex Ligation-dependent Probe Amplification (MLPA)

Multiplex ligation-dependent probe amplification (abbreviated with MLPA (Figure 6)) is a method to detect copy number variation and it was applied for examination of different patient/PDX samples. The principle of MLPA is based on probes which bind a specific DNA sequence of approximately 60nt length. The reaction results in a set of unique PCR amplicons between 64–500nt which can be separated through capillary electrophoresis. In a multiplex PCR each gDNA sample can be investigated for deletions in a specific gene set. The gDNA was denatured and specific hybridization primers (probes) attached to a linker sequence bind specific loci. One PCR primer is fluorescently labelled enabling the amplicon fragments to be visualized during the fragment separation. Fragment analysis was carried out in cooperation with the "Zentrum für Humangenetik und Laboratoriumsdiagnostik" (MVZ, Martinsried, Germany). The analysis followed with *Genemarker V2.6.0* software in order to compare different patients. For all experiments, the *SALSA MLPA P414 MDS* probemix (MRC Holland, Amsterdam, NL) was applied and carried out according to the protocol.

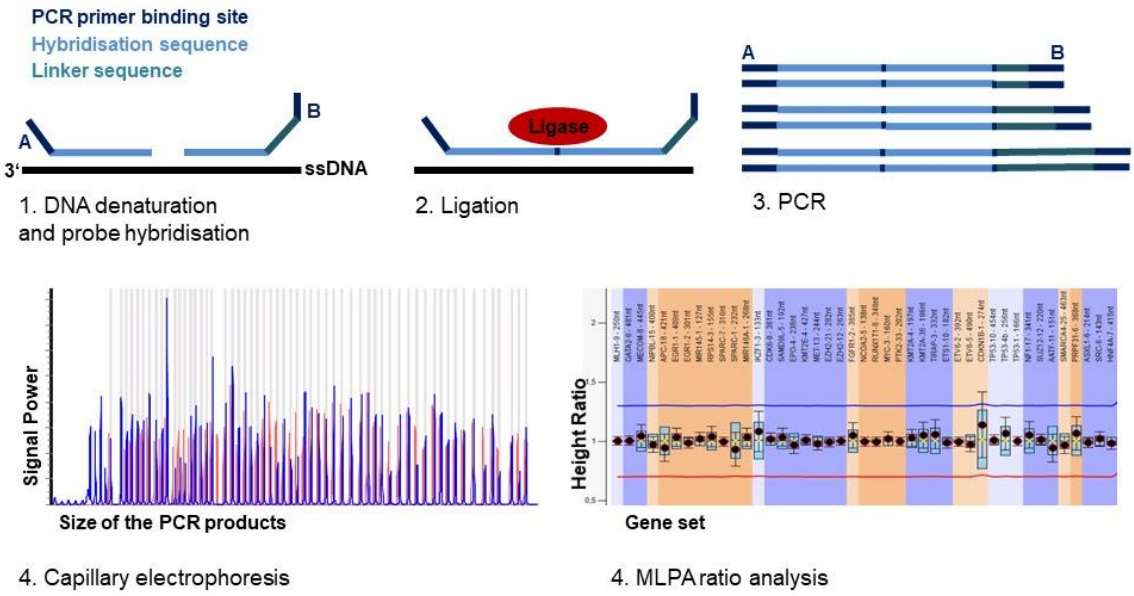

Figure 6: Multiplex ligation-dependent probe amplification. Stepwise explanation of the MLPA procedure, where chromosomal microdeletions can be detected: After DNA denaturation, specific probes can bind to distinct regions in the genomic DNA. In a PCR step these regions can be amplified and afterwards detected by capillary electrophoresis. Further ratio analysis provides information about genomic deletions.

First, DNA was denatured by heating the sample up to 98°C for five min. Hybridization of the probes was performed by adding 3µL of the hybridization mixture after cooling down the sample to room temperature. The mixture was incubated at 95°C for one minute and hybridization followed for 16h at 60°C. Hereinafter, the cycler's temperature was decreased to 54°C followed by adding 32µL of the ligase mixture. The suspension was incubated for 15min at 54°C. To inactivate the ligase, the suspension was heat up to 98°C for 15min. For product amplification, the samples were cooled down at room temperature first. 10µL of the polymerase master mix induce amplification setup. PCR thermocycler program is shown below. For evaluation of the PCR fragments, relative peaks were determined in each probe. For evaluation of patient samples, control fragments and binning DNA controls (provided in the kit) were used as probe binding controls and cell line experiments were used as last control to evaluate EZH2 status.

2.2.4.11 Digital Droplet PCR (ddPCR)

Digital droplet PCR (ddPCR) is a special PCR method which allows direct quantification and amplification of nucleic acid strands. The method is based on water-oil emulsion droplet technology which makes it more precise than conditional PCR. One sample is fractioned into thousands of droplets and amplification occurs in each individual droplet.

This enormous sample partitioning is a key feature of the technique. For ddPCR, a special kit was designed (ddPCR MUT FAM/HEX-EZH2/p.A692G) in cooperation with Bio-Rad (Hercules, US) for the precise detection of the time point the EZH2 mutation raised in the patient. All steps for ddPCR were performed as recommended in the manufacturers' protocol.

2.2.5. Sequencing

2.2.5.1. Sanger Sequencing

For the validation of correct PCR products and plasmid DNA fragments, sanger sequencing was executed external by Sequiserve (Vaterstetten, Germany). Verification of correct cloning and site-directed mutagenesis was confirmed for each maxi-preparation with full-length sequencing.

2.2.5.2. RNA Sequencing

Complete RNA sequencing procedure was performed as is was previously described by Stief et. al, 2019[123]. Experiments and data evaluation were done by Sabrina Weser (ELLF, Klinikum der Universität München). In short, a modified protocol from the SCRB-seq technique was used[111]. All wetlab and bioinformatic analyses were performed as described in Stief et al., 2019[123].

2.2.6. Statistical Analysis

Statistical analysis of all assays (proliferation and biochemical assays) was performed using *GraphPad Prism 6.07 (GraphPad Software (La Jolla, CA, USA))* software. All presented results include the mean ± SD of a minimum of three biological replicates, except if indicated otherwise. For biochemical and proliferation assays, the statistical significance was calculated by an unpaired, two-tailed *t*-test. All graphs shown were created with *GraphPad Prism 6.07* software. The association of *EZH2* mRNA expression with clinical, genetic and outcome variables was analysed in publicly available data sets. Patients of the AMLCG1999 trial were used as discovery cohort (GSE37642)[117,118] and results were validated in patients intensively treated in trials of the HOVON (Haemato

Oncology Foundation for Adults in the Netherlands) group (GSE14468)[119,120]. Maximally selected rank statistics[121] were used to dichotomize *EZH2* expression in the discovery cohort. The identified cut point was independently validated in the HOVON data set. KaplanMeier estimates for overall survival (OS) were calculated using the R survival package with standard parameters. p-values were calculated using the log-rank test. Statistical analysis was performed using the R-3.4.1 software package (R Core Team. R A language and Environment for Statistical Computing).

2.2.7. In vivo Therapy Trial

All trials including animals were performed in conformity with the present ethical guidelines of the formal committee on animal experimentation (Regierung Oberbayern, Nummer 55.2-1-54-2531-95-2010 and ROB- 55.2Vet-2532.Vet_02-16-7). Patient-derived xenograft (PDX) cells were established as it was described previously[107]. For *in vivo* therapy trials, $1x10^5$ PDX-491 or $8x10^5$ PDX-661 cells were injected intravenously into NSG mice (NOD scid gamma, The Jackson Laboratory, Bar Harbour, USA), and tumour burden was repeatedly examined by bioluminescence imaging (BLI) as described previously[107]. 21d after transplantation, animals were treated with cytarabine (100mg/kg, i.p., days 1-4, 15-18, 29-32, and 43-46) and DaunoXome (1mg/kg, i.v., days 1, 4, 15, 18, 29, 32, 43, 46). Tumour burden was regularly monitored by BLI.

3. Results

3.1. Recurrent *EZH2* Mutations at AML Diagnosis

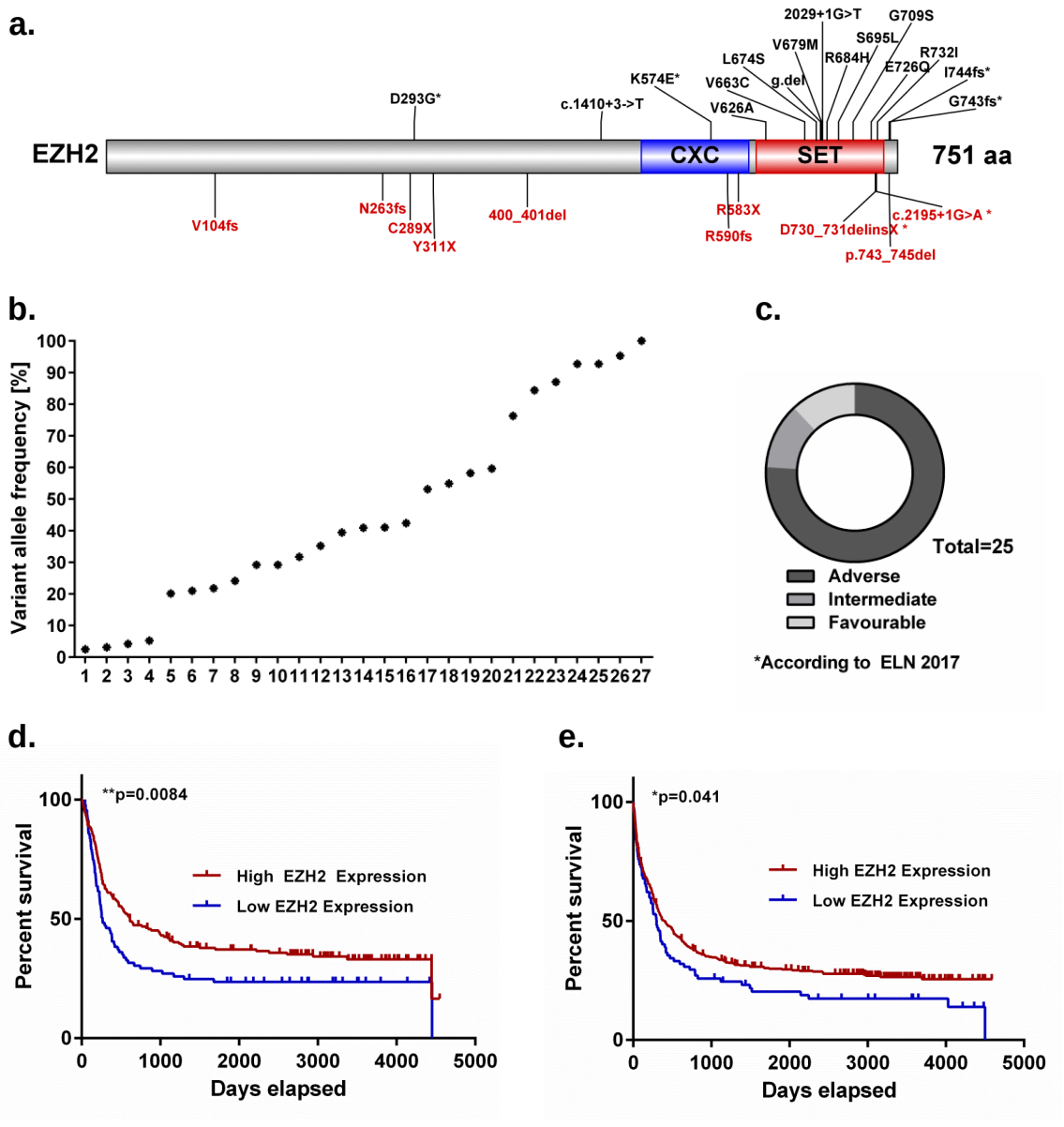

Figure 7: Recurrent *EZH2* mutations at AML diagnosis. a, Schematic illustration of EZH2 protein structure (NM_004456.4) and identified mutations (27 in total, c.2195+1G>A appeared twice) in AML patients at diagnosis. Presented *EZH2* mutations were found in AML-CG-99 trial (NCT00266136) and AML-CG-2008 trial (NCT01382147). Functional domains are indicated at distinct locations and truncating mutations are displayed in red. Asterisks indicate mutations, that were further investigated; **b,** Histogram showing VAF (in %) of detected EZH2 mutation; **c,** Plot presenting the prognostic subgroups of 25 patients with *EZH2* mutation according to the ELN classification; **d,** Survival plot showing overall survival (OS) in patients with low or high mRNA EZH2 expression; **e,** Survival plot showing relapse-free survival (RFS) in patients with low or high mRNA EZH2 expression.

A few years ago, Metzeler et al. from our department described *EZH2* mutations within a broad spectrum of driver mutations in AML patients[34] in the clinical trials AML-CG-1999 (NCT00266136, n = 390) and AML-CG-2008 (NCT01382147, n=274). 27 *EZH2* mutations were detected in 25 AML patients at diagnosis (Figure 7a), referring to a mutation rate of 4% (n=25/664). 74.07% (n=20/27) of these mutations are located in the SET ([Su(var)3-9, Enhancer-of-zeste and Trithorax]) or CXC domain (cysteine-rich region, sometimes referred to as pre-SET domain) at the C-terminus of the protein, which are responsible for the catalytic activity of the methyltransferase. 11 (40.7%) mutations cause a stopgain or frameshift leading to a truncated protein. Moreover, 2 (7.4%) frameshift mutations result in an elongated protein variant. Most frequently detected additional mutations in *EZH2* mutated patients are *EZH2*/*RUNX1* (44%, n=11/25), *EZH2*/*ASXL1* (44%, n=11/25), *EZH2*/*DNMT3A* (20%, n=5/25) and *EZH2*/*TET2* (20%, n=5/25). Interestingly, mutations in *NPM1* can only be found in 12% (n=3/25) of all patients with *EZH2* mutation (Supplementary Figure 1a). A wide range of variant allele frequencies (VAF) reaching from 2.5%-100% (Figure 7b) was detected. In order to compare the prognostic relevance of EZH2 mutations, *EZH2* mutated patients were classified in risk groups, according to the ELN classification from 2017[33]. 76% (n=19/25) of *EZH2* mutated patients can be assigned to an adverse risk category (Figure 7c). To evaluate the impact of *EZH2* status on patient survival, the survival of individuals with *EZH2* mutation in the cohorts which are described above were compared. Even though a poor overall survival (OS) for patients with monosomy 7 could be confirmed (Supplementary Figure 1b), where *EZH2* is located, a difference in the OS of patients harbouring *EZH2* mutations could not be observed (Supplementary Figure 1c). A significant difference could be observed when *EZH2* mutated patients in the adverse risk group were compared to patients with intermediate or favourable phenotype but not when *EZH2* mutated patients (adverse risk group) are compared to the *EZH2* wildtype control group (Supplementary Figures 1d-e). Next, expression levels in AML patients were compared and the survival of individuals with low/high EZH2 expression was compared. Low EZH2 mRNA expression was significantly associated with poor relapse free survival (RFS) and OS in publicly available independent data sets of the AML-CG (GSE37642, Figure 7d-e) and HOVON (GSE14468, supplementary Figure 2b) study groups[119,120,122].

3.2. EZH2 Expression is Often Altered in AML Patients Between Diagnosis and Relapse

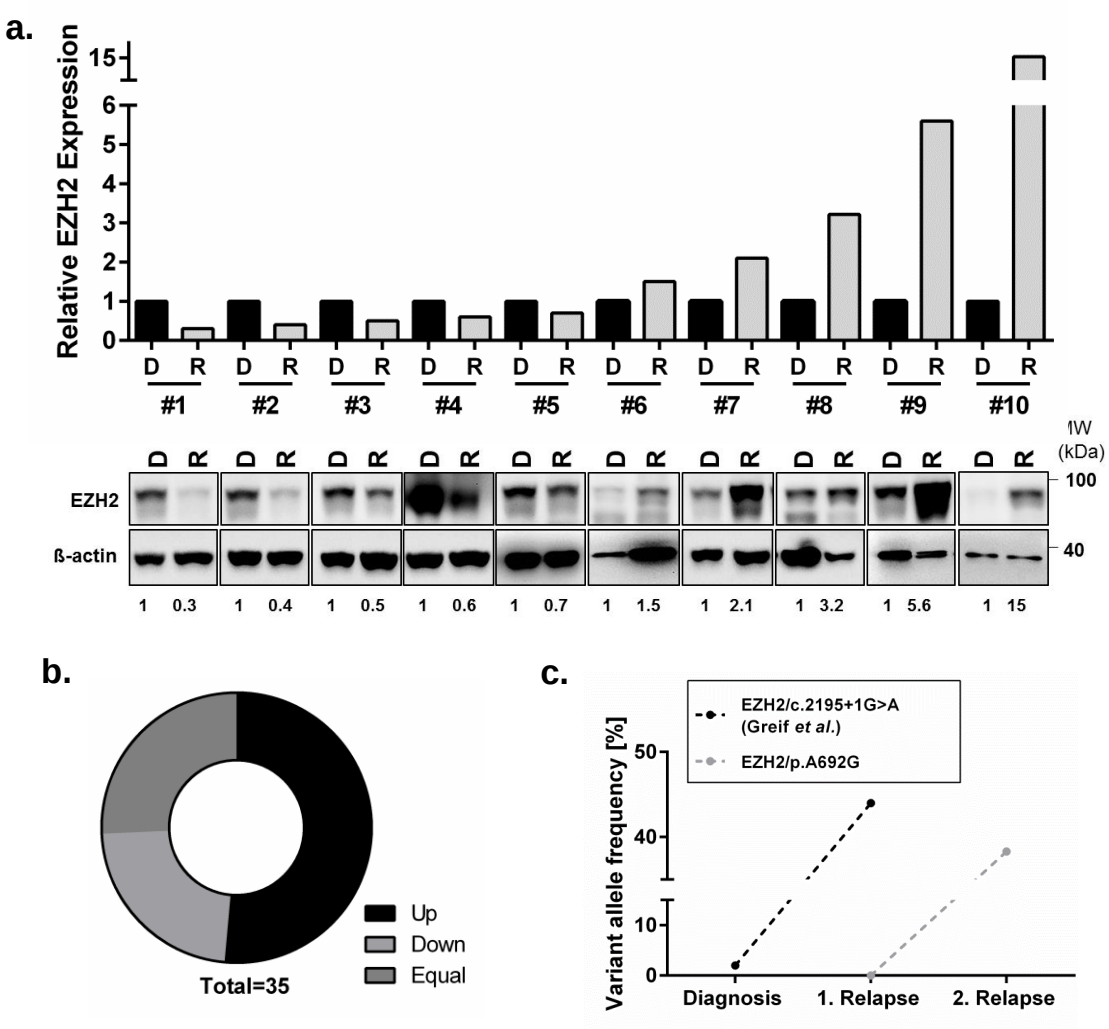

Figure 8: Relevance of *EZH2* status in AML relapse. a, Immunoblotting for EZH2 protein expression in 10 AML patients[123] at diagnosis and relapse. Molecular weight (MW); β-actin: loading control. The ratio of EZH2 to β-actin expression is indicated below and presented in the histogram above. Each relapse value was normalized to the corresponding diagnosis sample; **b,** Plot showing EZH2 mRNA expression in 35 CN-AML patients between diagnosis and relapse; **c,** Graphs showing VAF (in %) of two *EZH2* mutations with outgrowth in first/second relapse in AML patients.

Because a poor RFS was observed in patients with low EZH2 mRNA expression, protein expression in a set of relapsed AML patients[123] was investigated. In a screening of ten patients (Table 15: Patient characteristics from samples shown in Figure 8a), matched diagnosis-relapse samples were compared to evaluate the change of EZH2 expression during disease progression (Figure 8a-b). In 50% of these patients, decreased levels of EZH2 protein expression were observed, whereas 50% revealed increased protein expression levels at relapse. A strong decrease of protein expression could be found in three patients (UPN#1 - UPN#3), whereas a strong increase of protein expression was observed in two patients (UPN#9 and UPN#10). An additional analysis of EZH2 mRNA regulation in 35 CN-AML patients resulted in an alteration of EZH2 expression in 74.3% (n=26/35) of all relapsed patients. Only 25% (n=9/35) patients did not show any significant alteration in EZH2 mRNA levels between diagnosis and relapse (Figure 8b; Supplementary Figure 2a). In addition to changes in expression, two relapse-associated *EZH2* mutations were found in AML-CG study. *EZH2*/p.A692G could be confirmed in the second relapse of a patient and *EZH2*/c.2195+1G>A in the first relapse of another patient. Both mutations revealed subclonal outgrowth during AML treatment and increasing variant allele frequencies (VAF) in relapsed AML samples (Figure 8c).

Table 15: Patient characteristics from samples shown in Figure 8 (adapted from Stief et. al, 2019[123])

UPN	Age at Diagnosis	Sex	Karyotype at Diagnosis	Karyotype at Relapse	Time to Relapse	Induction Therapy
#1	76	m	CN	CN	176	s-HAM
#2	57	f	CN	CN	468	TAD9-HAM
#3	56	f	CN	CN	2294	sHAM+TAD
#4	38	f	47,XX,+8[15]//46,XX[2]	47,XX,+8[6]/47,sl,t(2;13)(p21;p11)[2]/47,sl,t(1;13)(p36;q?3),t(1;20)(q21;?q13),t(1;8)(q21;q22),t(3;4)(q2?8;q3?4),t(3;5)(q1?;q3?5),t(5;9)(q31;p22),t(6;13)(q2?;q?3),t(9;15)(q3?4;q1?5)[cp8]//46,XX[2]	137	sHAM
#5	33	f	NA	NA	728	NA
#6	62	m	CN	CN	680	sHAM+TAD
#7	71	m	CN	46,XY,t(1;22)(p13;q11),der(5)t(5;19)(q12;?),der(15)t(5;15)(q?;q?),der(19)t(15;19)(q?:q?)[5]/46,XY,t(11;13)(p1?;q1?)[3]/46,XY[1]	209	sHAM
#8	44	m	47,XY,+21[16]/46,XY[6]	46,XY,i(7)(q10),der(9)(p?),del(9)(p1?)[9]	860	TAD-HAM
#9	68	f	47,XX,+8 [25]	NA	245	TAD-HAM
#10	80	m	46,XY,t(2;14)(q1?;q3?2),del(16)(q1?3q22)[8].ishder(2)t(2;14)(q1?;q3?2)(ALK+,IGH+),del(16)(q1?3q22)(CBFB,MAF+)/46,XY [1]	NA	392	sHAM

3.3. Pharmacological Inhibition of EZH2 Induces Sensitivity in MLL-Rearranged AML Cell Lines

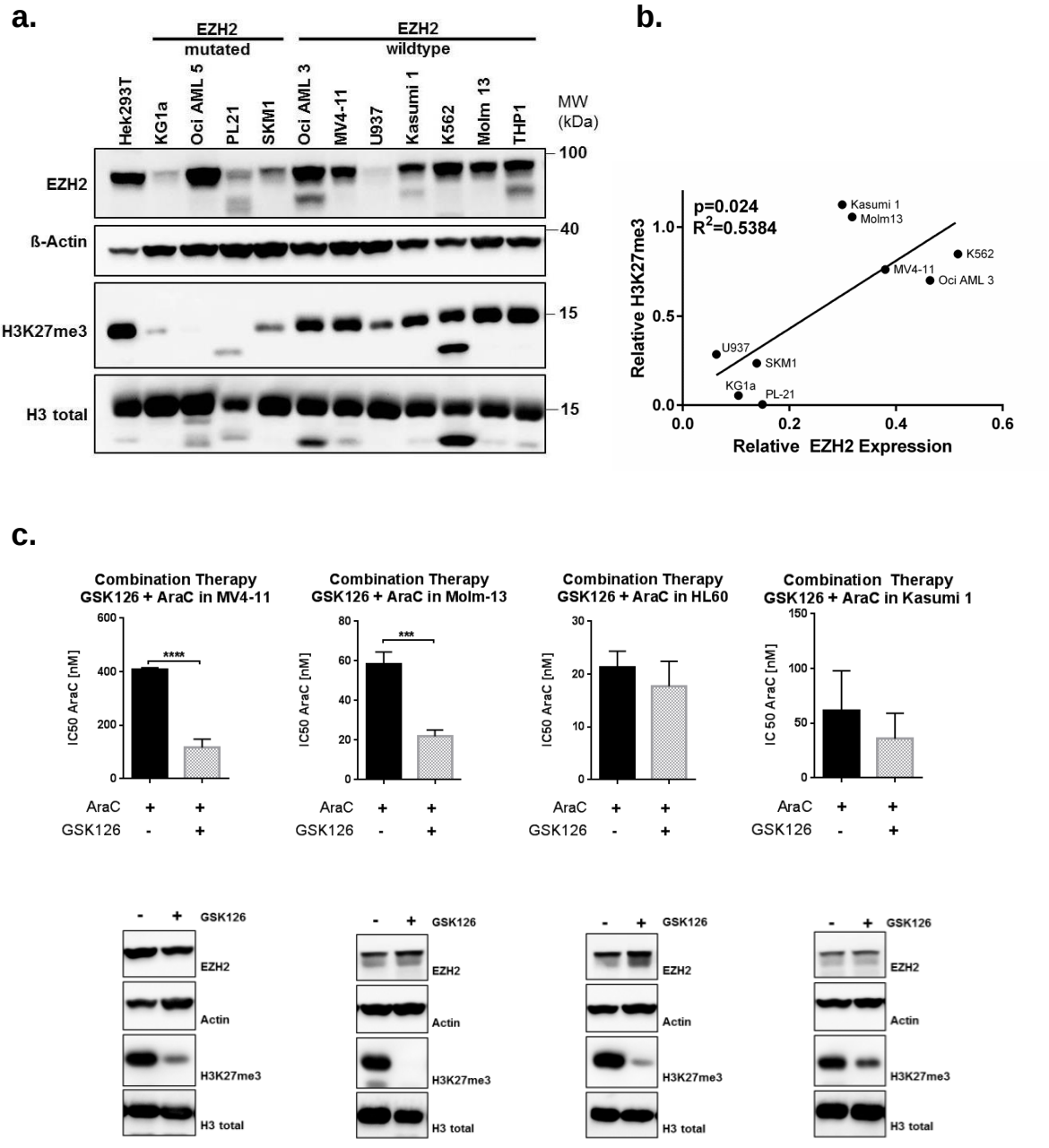

Figure 9: EZH2 in human AML cell lines. **a,** Immunoblotting for EZH2 expression and global H3K27me3 in 11 AML cell lines. Molecular weight (MW); β-actin and H3 total: loading controls. **b**; Correlation between EZH2 protein expression and global H3K27me3 in haematopoietic cell lines (Expression levels normalized to HEK293T control; Pearson`s correlation; R^2=0.5384, *p=0.024); **c,** Graphs showing IC_{50} values of AraC treatment in AML EZH2 wildtype cell lines with combinatorial treatment with GSK126 for 72h. Cells were first pre-incubated with 1µM GSK126 for 72h and then treated with 1µM GSK126 and AraC for 72h. Mean (including s.d) are shown for three biological replicates. Unpaired, two-tailed Student's t-test; *p<0.05; **p<0.01; ***p<0.001; ***p<0.0001.

Because a difference in protein and mRNA expression patterns of EZH2 in AML patients between diagnosis and relapse was found, EZH2 protein expression was evaluated in human AML cell lines (Figure 9a). Four cell lines with *EZH2* mutation and seven *EZH2* wildtype cell lines were investigated in a protein expression screening. Two clusters could be observed, cell lines with comparatively high expression and cell lines with comparatively low expression. A low protein expression was observed in 75% (n=3/4) of all mutated cell lines. OCI-AML 5 revealed high expression levels even though EZH2 is mutated. This mutation was previously described to show a strong LOF phenotype[124], which could be confirmed in our screening, since global H3K27me3 levels are completely absent. As expected, EZH2 was strongly expressed, whereas methylation of H3K27me3 was completely absent. Expression was in general stronger in wildtype cell lines with exception of the cell line U937. Global H3K27me3 levels were lower in all mutated cell lines, which could be confirmed in a linear regression plot (Figure 9b).

In order to evaluate the effect of impaired EZH2 function on drug resistance, human AML cell lines were treated with a combination of the highly specific EZH2 inhibitor GSK126 and the cytostatic drug AraC. A significant decrease in IC_{50} values could be observed in the cell lines MV4-11 and Molm13 (Figure 9c), both characterized by MLL-rearrangements, confirmed by DSMZ (Braunschweig, Germany). For two additional EZH2 wildtype cell lines (HL-60 and Kasumi1) no alteration in the sensitivity against AraC was observed under GSK126 treatment. In summary, pharmacological inhibition of EZH2 by GSK126 sensitizes against AraC treatment in two MLL-rearranged cell lines.

3.4. *EZH2* Mutations in AML Patients are LOF Mutations

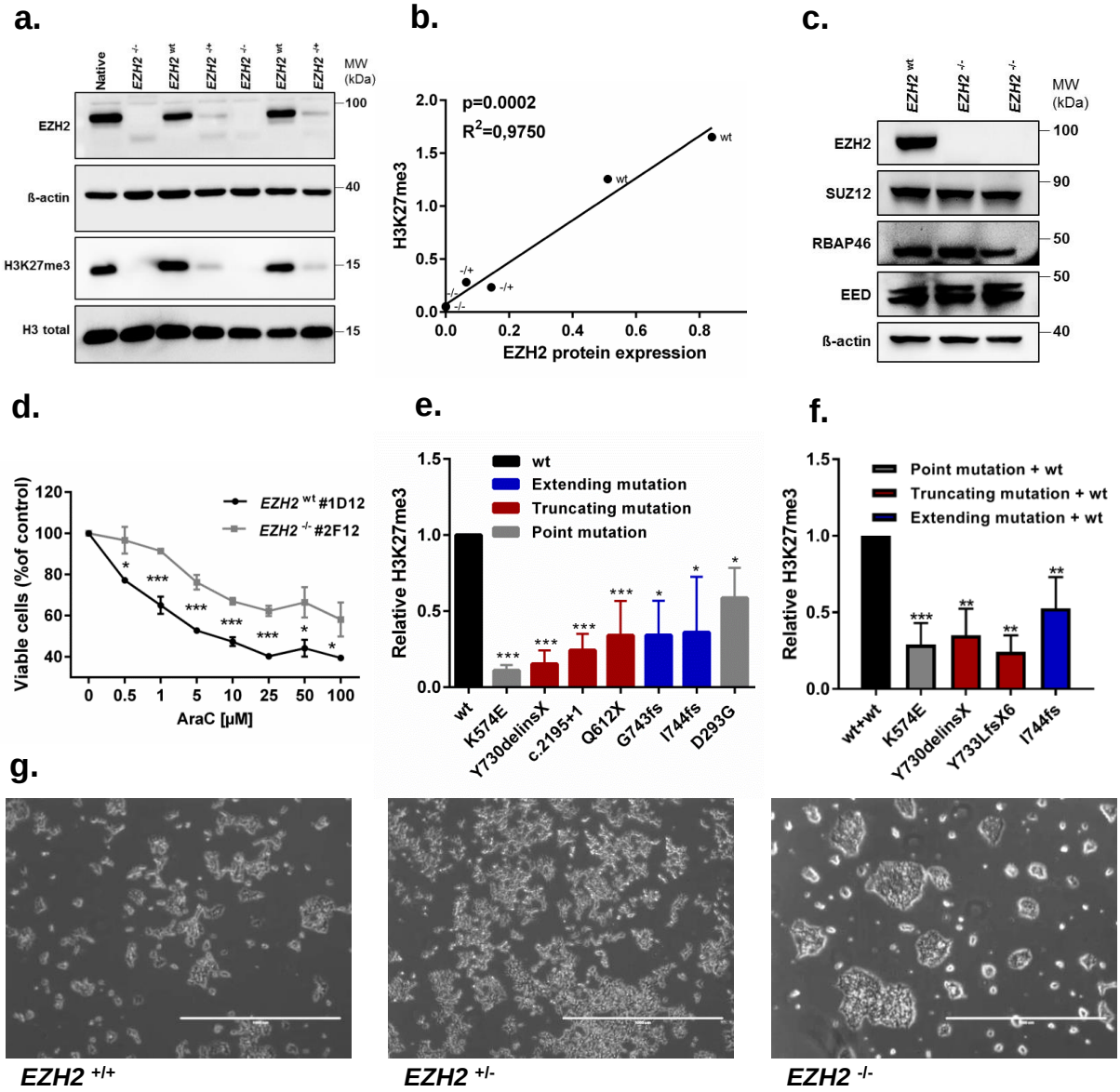

Figure 10: Evaluation of *EZH2* mutations found in AML patients at diagnosis. a, Immunoblotting for EZH2 expression and global H3K27me3 in HEK293T sc clones. Molecular weight (MW); β-actin and H3: loading controls; **b,** Correlation between EZH2 expression and global H3K27me3 in HEK293T/ *EZH2*$^{-/-}$ sc clones (Pearson`s correlation; R^2=0.975, *p=0.002); **c,** Immunoblotting for EZH2, SUZ12, RBAP46 and EED in HEK293T/*EZH2*$^{-/-}$ sc clones. Molecular weight (MW); β-actin: loading control; **d,** Graph showing AraC resistance in a HEK293T/*EZH2*$^{-/-}$ clone. Cells were treated for 72h with AraC. Mean (including s.d.) are shown for three biological replicates. Unpaired, two-tailed Student's t-test; *p<0.05; **p<0.01; ***p<0.001; **e,** Histogram showing the biochemical H3K27me3 activity of different *EZH2* mutations which were detected at diagnosis. Colours refer to different protein structures caused by the mutation. Mean (including s.d.) are shown for minimum three biological replicates. Unpaired, two-tailed Student's t-test; *p<0.05; **p<0.01; ***p<0.001; **f,** Histogram showing the biochemical activity of different *EZH2* mutations in the context of wildtype background. Mean (including s.d.) are shown for minimum three biological replicates. Unpaired, two-tailed Student's t-test; *p<0.05; **p<0.01; ***p<0.001; **g,** Microscopic imaging of HEK293T sc clones. Representative images are shown for each status of zygosity.

In order to evaluate the importance of *EZH2* LOF in myeloid malignancies, the biochemical activity of mutated EZH2 variants, which were found at diagnosis and relapse, was investigated. Therefore, the global H3K27 tri-methylation potential was tested *in vitro*. For this purpose, a HEK293T/*EZH2* knockout (KO) model (Figure 10a) was established. Therefore, CRISPR/Cas9 mediated genome editing was applied, targeting exon 3 of *EZH2.* Thereby, different clones (homozygous KO (*EZH2*$^{-/-}$), heterozygous KO (*EZH2*$^{+/-}$) and wildtype (*EZH2*$^{+/+}$)) could be established. It should be noted, that EZH2 protein expression levels strongly correlated with global H3K27me3 levels in HEK293T single cell (sc) clones (Figure 10b). Whereas protein expression and global H3K27me3 levels were present in *EZH2*$^{+/+}$ clones, they were completely absent in all *EZH2*$^{-/-}$ clones. *EZH2*$^{+/-}$ clones exposed decreased EZH2 expression levels and, compatible, diminished global H3K27me3 levels. To evaluate whether endogene loss of *EZH2* is leading to a destabilized protein complex in HEK293T/*EZH2*$^{-/-}$ sc clones, the presence of PRC2 components was analysed. Expression of all PRC2 components (including SUZ12, RBAP46 and EED) could be shown in both HEK293T/*EZH2*$^{-/-}$ clones (Figure 10c). Interestingly, both homozygous KO clones showed an increased resistance against AraC compared to the 293T/*EZH2*$^{+/+}$ clone (Figure 10d; Supplementary Figure 3a) and a slightly reduced proliferative potential (Supplementary Figure 3b). Re-expression of seven different EZH2 variants which were found in the studies AML-CG-1999 (NCT00266136, n=390) and AML-CG-2008 (NCT01382147, n=274) could only partially rescue global H3K27me3 levels compared to the re-expressed wildtype protein (Figure 10e). To validate these results, the experiment was performed with a known GOF mutation (EZH2/p.Y646N), which is well characterized in lymphomas[98,99] and a LOF mutation, which was described in MDS (EZH2/Y731F[122]). We showed, that p.Y646N mediates increasing global H3K27me3 levels (Supplementary Figure 10c), while p.Y731F has a LOF phenotype (Supplementary Figure 3d). Summarized, all seven tested mutations showed decreased global H3K27me3 levels compared to the wildtype enzyme, referring to a LOF phenotype. Four mutations additionally showed dominant-negative characteristics on the wildtype (Figure 10f). Interestingly, HEK293T sc clones revealed different phenotypes concerning morphology and growth behaviour. Homozygous sc KO clones formed stucked colonies, the formation of pseudopodia was reduced and cells were round-shaped (Figure 10g). Of note, this phenotype was not observed in a heterozygous background.

3.5. EZH2 Depletion is Associated with AraC Resistance in the Myeloid Cell Line K562

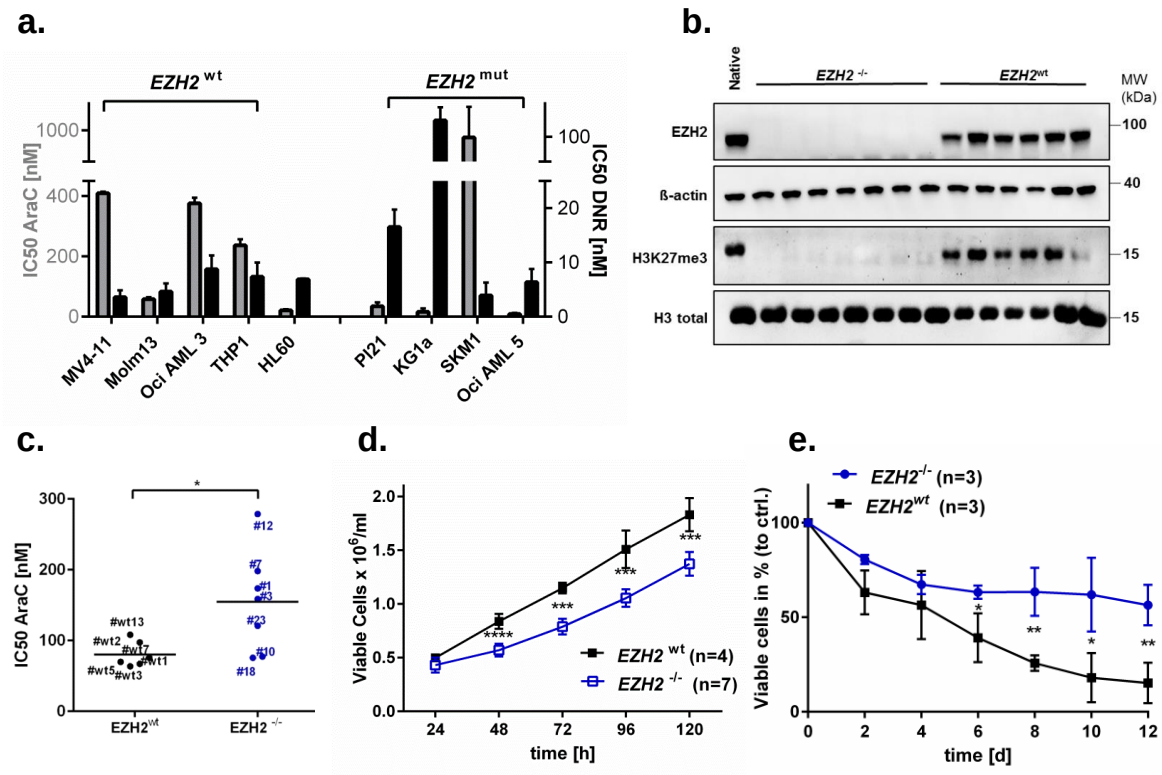

Figure 11: EZH2 depletion is associated with AraC resistance in the myeloid cell line K562. **a,** Graph comparing IC_{50} values for DNR and AraC in 9 haematopoietic cell lines. Cells were treated with AraC/DNR for 72h. Mean are shown for three biological replicates; **b,** Immunoblotting for EZH2 expression and global H3K27me3 in 13 K562 sc clones. Molecular weight (MW); β-actin and H3: loading controls; **c,** Plot comparing AraC IC_{50} values in in *EZH2*$^{+/+}$ (n=6) and *EZH2*$^{-/-}$ (n=7) clones. Cells were treated with AraC/DMSO for 72h. Each clone represents the mean of three biological replicates. Unpaired, two-tailed Student's t-test; *p<0.05; **p<0.01; ***p<0.001; **d,** Comparison of proliferation potential in *EZH2*$^{+/+}$ (n=4) and *EZH2*$^{-/-}$ (n=7) clones for 7d. Medium was changed every 48h. Mean are shown for three biological replicates for each clone. Unpaired, two-tailed Student's t-test; *p<0.05; **p<0.01; ***p<0.001; **e,** Long-term low dose AraC treatment in in *EZH2*$^{+/+}$ (n=3) and *EZH2*$^{-/-}$ (n=3) clones. Cells were treated with 30nM AraC/DMSO for 12d. Mean (including s.d.) are shown for three biological replicates for each clone. Unpaired, two-tailed Student's t-test; *p<0.05; **p<0.01; ***p<0.001

Since a drug resistant phenotype was observed in 293T/*EZH2*$^{-/-}$ cells, we aimed to verify these results in a haematopoietic context. Even though diminished global H3K27me3 levels were detected in all *EZH2* mutated cell lines (Figure 9a), no difference in drug sensitivity against DNR (daunorubicin) and AraC (Figure 11a) was observed. In order to evaluate complete loss of EZH2 in a myeloid system, seven K562/*EZH2*$^{-/-}$ sc clones were established by using CRISPR/Cas9 mediated gene silencing (Figure 11b) and compared

to wildtype sc clones concerning the response to AraC and DNR treatment. Notably, a difference between K562/*EZH2*$^{+/+}$ and K562/*EZH2*$^{-/-}$ in DNR resistance could not be confirmed (Supplementary Figure 4c). Nevertheless, a significant increase of IC_{50} values for AraC in K562/*EZH2*$^{-/-}$ sc clones when treated for 72h was observed (Figure 11c) and Supplementary Figure 4a). Yet, the IC_{50} values showed a broad range in K562/*EZH2*$^{-/-}$ sc clones. Additionally, a reduced proliferation was observed in K562/*EZH2*$^{-/-}$ clones compared to K562/*EZH2*$^{+/+}$ clones (Figure 11d). Taking this into consideration, we decided to investigate treatment resistance against AraC in a long-term proliferation assay. Therefore, six sc clones were consequently treated for 12d with 30nM AraC. As a result, K562/*EZH2*$^{+/+}$ clones show a more sensitive phenotype against AraC compared to K562/*EZH2*$^{-/-}$ clones (Figure 11e). Data of each sc clone is additionally shown in Supplementary Figure 4b. In summary, CRISPR/Cas9 mediated KO promotes treatment resistance against AraC in the myeloid cell line K562.

3.6. EZH2 Re-Expression Sensitizes to AraC Treatment in the Myeloid Cell Line K562

Even though a significant difference in the resistance against AraC was observed in K562/*EZH2*$^{-/-}$ clones, sc clones revealed to be highly heterogeneous concerning the behaviour during AraC treatment. To overcome this effect, a stable doxycycline inducible EZH2 re-expression via PB/Transposase was established in K562/*EZH2*$^{-/-}$ sc clones. Thereby, EZH2 re-expression can be induced by doxycycline treatment to native expression levels (Figure 12a). EZH2 expression is induced by doxycycline treatment for a minimum of 24h and additional selection by puromycin treatment increases positive cells (Supplementary Figure 5).

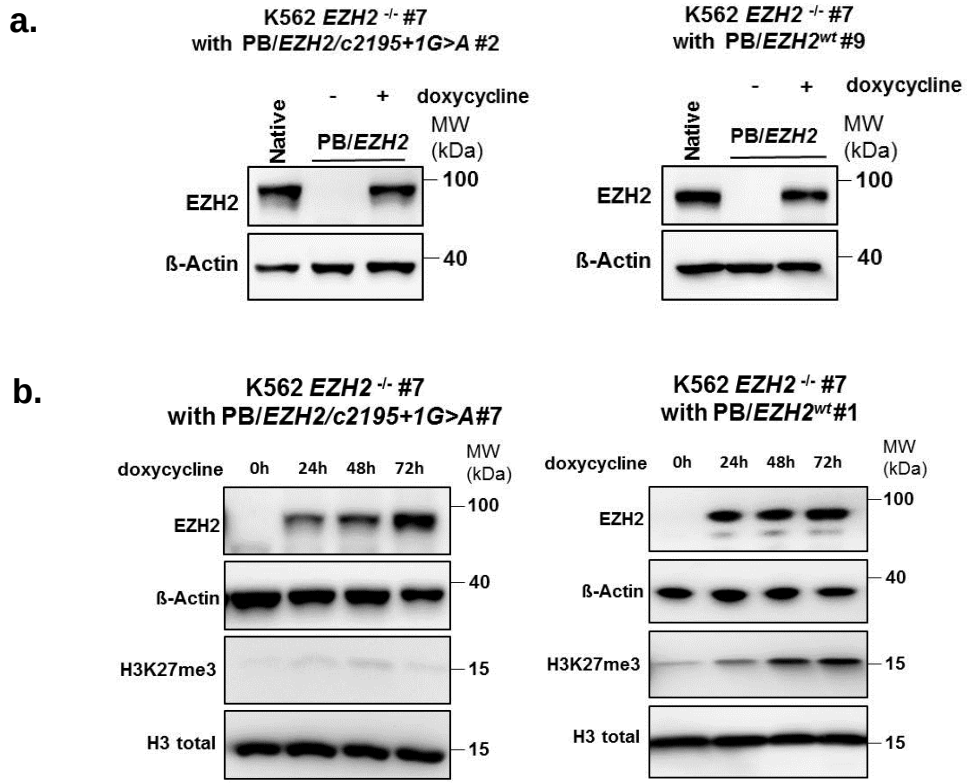

Figure 12: Inducible EZH2 re-expression via PB/Transposase system. **a;** Immunoblotting for EZH2 expression in two K562 *EZH2*$^{-/-}$/PB/*EZH2* sc clones. Cells were treated with 1µg/mL doxycycline for 24h. Right: *EZH2*/wildtype. Molecular weight (MW); β-actin: loading control; Left: *EZH2*/ c.2195+1G>A. Molecular Weight (MW); β-actin: loading control; **b,** Immunoblotting for EZH2 expression and global H3K27me3 levels in two K562 *EZH2*$^{-/-}$/PB/EZH2 sc clones. Cells were serially treated for 3d with 1µg/mL doxycycline. Right: *EZH2* wildtype; Left: *EZH2*/c.2195+1G>A;. Molecular weight (MW); β-actin and H3: loading controls.

We decided to establish *EZH2*/wildtype (AA1-751) as it was expected, that re-expression was able to rescue the resistant phenotype of *EZH2*$^{-/-}$. Additionally, EZH2/c2195+1G>A was established since this relapse-associated mutation appeared twice in the investigated cohorts (diagnosis and relapse) and a strong LOF phenotype was observed in the biochemical assay (Figure 10e). *EZH2*/c.2195+1G>A (AA1-737) was previously described in MDS[103]. This frameshift mutation leads to a sequence variation in the SET domain and results in a premature stop codon and loss of the C-terminal part of the protein[103]. Nevertheless, an impaired and dominant negative methylation activity was observed while transiently transfected (Figure 10f). Consequently, the effect of c.2195+1G>A on AraC resistance was investigated.

First, the catalytic activity in PB/*EZH2* sc clones was analysed. Therefore, global H3K27me3 levels were examined after doxycycline induction either in *EZH2*/wildtype and *EZH2*/c.2195+1G>A clones. Serial re-induction with doxycycline every 24h leads to stable global H3K27me3 after 72h in *EZH2*/wildtype clones. Importantly, global H3K27me3 cannot be rescued in *EZH2*/c.2195+1G>A clones (Figure 12b). To estimate the value of mutated *EZH2* on chemotherapeutic resistance in leukemic cells, PB sc clones were studied in a long-term low dose AraC treatment for 12d. It could be confirmed that wildtype EZH2 is capable to re-induce sensitivity against AraC (Figure 13c-d, Supplementary Figure 6a). As expected, re-expression of *EZH2*/wildtype restored sensitivity to AraC whereas the LOF (c.2195+1G>A) mutation did not (Figure 13a-b, Supplementary Figure 6a). To estimate the effect of doxycycline in this assay, two control sc clones (one *EZH2*$^{+/+}$ and one *EZH2*$^{-/-}$) were tested, which were treated with the same experimental settings (Figure 13e-f, Supplementary Figure 6b). No significant effects were observed in both control sc clones during treatment with doxycycline.

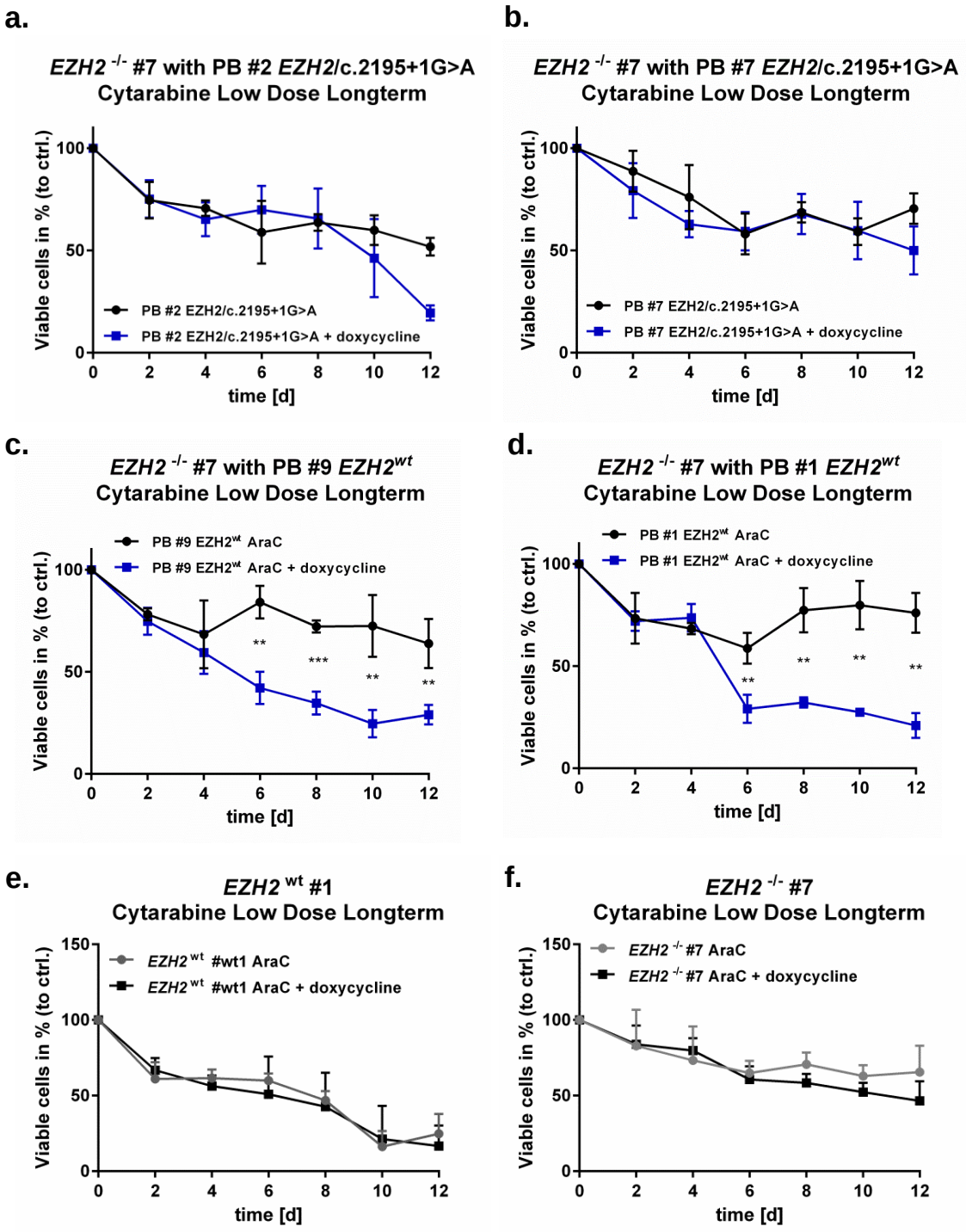

Figure 13: EZH2 re-expression sensitizes to AraC treatment in the myeloid cell line K562: Graphs showing AraC low dose long-term treatment in PB/*EZH2* clones; **a-b,** two *EZH2*/ c.2195+1G>A (LOF) sc clones; **c-d,** two *EZH2*/wildtype sc clones; **e-f,** two control sc clones (one $EZH2^{+/+}$ and one $EZH2^{-/-}$). Cells were pre-treated for 3d with doxycycline and then treated with 30nM AraC/DMSO for 12d. Cells were splitted and treated every 4d and doxycycline was added every 48h to ensure stable expression of EZH2. Mean (including s.d.) are shown for three biological replicates for each clone. Unpaired, two-tailed Student's t-test; *p<0.05; **p<0.01; ***p<0.001

3.7. EZH2 Mutation Induces Resistance in a Patient-Derived Xenograft (PDX) Model *in vivo*

To validate the findings of treatment resistance in haematopoietic cell lines which was caused by *EZH2* loss, a patient-derived xenograft (PDX) model[107] was used (Figure 14, Establishment of patient-derived xenografts). Here, primary leukemic patient cells are engrafted in immune-deficient NSG mice and can be passaged or analysed *in vivo* as it was previously described[107].

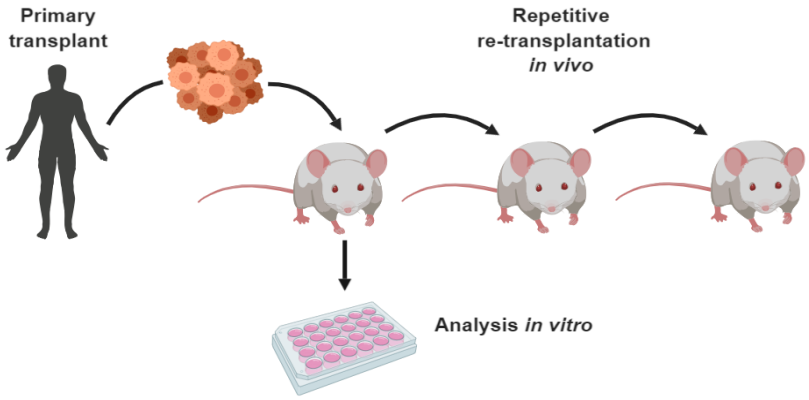

Figure 14: Establishment of patient-derived xenografts. Primary patient samples engraft in immuno-deficient NSG mice and can be cultured and analysed *in vivo*. Cells can be harvested and cultured *in vitro* for a few days for further analysis.

A 54-year old AML patient from an AML-CG cohort was identified who gained an *EZH2* mutation (p.A692G) at second relapse. To confirm that the mutation was relapse-associated, a sensitive digital droplet PCR (ddPCR) assay (customer designed with Bio-Rad, Hercules, US) for this mutation was established in patient material. The arise of the mutation in the second relapse and the absence in earlier stages could be confirmed (Figure 15a; see fractional abundance). Furthermore, the patient gained a heterozygous 7q deletion at first relapse, as analysed by MLPA (Figure 15a; see 7q del status). A summary of the patients' AML course is shown in Figure 15a. Cells of the first (PDX-AML-491) and second (PDX-AML-661) relapse were serially transplanted into immune-deficient mice, establishing patient-derived xenograft (PDX) cells[107]. Furthermore, PDX cells were lentivirally transduced for transgenic expression of luciferase, enabling disease monitoring *in vivo*[26]. Unfortunately, leukaemia cells of initial diagnosis sample did not engraft in the model.

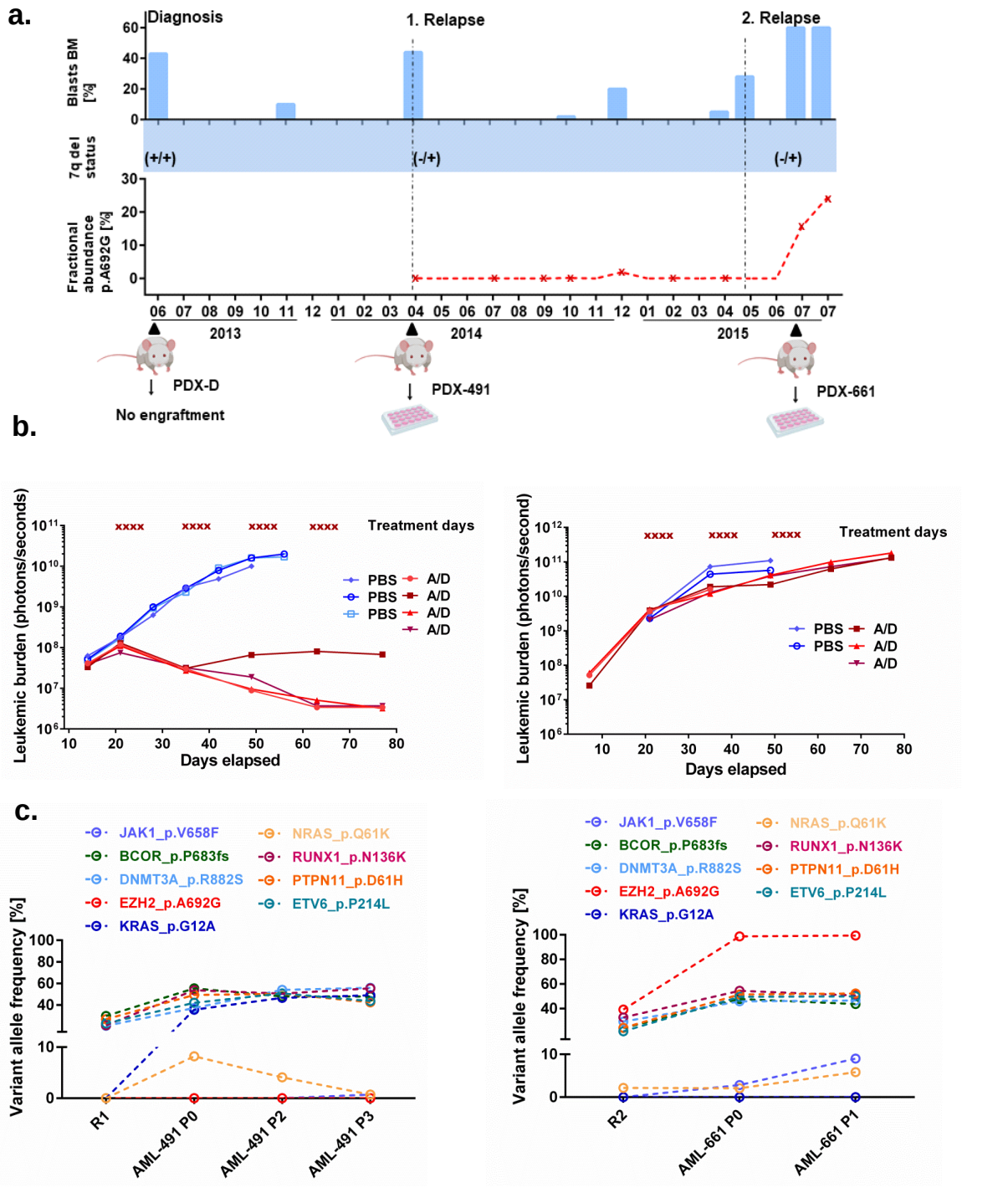

Figure 15: Resistance in an *EZH2* mutated patient-derived xenograft (PDX) model *in vivo*. a, Illustration of the course of an AML patient with two relapses (indicated with dashed lines). 7q deletion was confirmed with MLPA, arise of p.A692G mutation was verified by digital droplet PCR. Sampling time points for PDX engraftment is indicated below with arrows. Blast count of each sampling time point from bone marrow is given above; **b,** *In vivo* treatment of PDX xenograft mice. NSG mice were injected with PDX-AML-491 PDX cells (left) or PDX-AML-661 PDX cells (right) expressing luciferase. 21 days after injection, mice were treated with AraC (100 mg/kg) and DaunoXome (1mg/kg) as indicated above. Leukemic burden was supervised by bioluminescence imaging. Treated mice are presented in red, control mice in blue; **c,** Graphs showing VAF in % of mutations found in PDX and patient material analysed with NGS.

EZH2 mutation status was confirmed in established PDX cells by performing next-generation sequencing (NGS) in patient and PDX cells. *EZH2*/p.A692G abundance could be confirmed in the second relapse of the patient (VAF: 39.2%) with clonal outgrowth in PDX-AML-661 cells growing in mice (VAF: 98.8%). Further mutations identified by targeted NGS (Figure 15c) included (i) BCOR, DNMT3A, ETV6, PTPN11, and RUNX1, where VAF remained stable at all time points analysed, indicating that these alterations are present in the founder clone; (ii) a subclonal NRAS mutation that could be found at all time points analysed; (iii) a subclonal KRAS mutation that grew out in the PDX cells of PDX-AML-491 but was undetectable in PDX-AML-661 cells; (iv) and a subclonal JAK1 mutation that was detectable in PDX-AML-661 cells.

To analyse if the gain of the *EZH2*/p.A692G mutation elicits resistance towards chemotherapy *in vivo*, mice engrafted with either *EZH2*^{wt} PDX-AML-491 cells or *EZH2*/p.A692G PDX-AML-661 cells were treated with a combination of AraC and DNR (DaunoXome). Interestingly, tumour burden in *EZH2*^{wt} PDX-AML-491 bearing animals dropped under therapy, with a complete cure of 3 out of 4 animals, whereas treatment of *EZH2*/p.A692G PDX-AML-661 bearing animals showed only a minimal effect in comparison to control treated animals (Figure 15b). These data support the *in vitro* findings that LOF mutations of *EZH2* lead to chemotherapy resistance.

3.8. Knockdown of EZH2 Promotes Drug Resistance in Patient-Derived Xenograft (PDX) Model *in vitro*

To validate the connection between *EZH2* mutation and therapy resistance, PDX-cells were screened for AraC response *in vitro,* and a resistant phenotype of PDX-AML-661 compared to PDX-AML-491 was confirmed (Figure 16a). Moreover, global H3K37me3 levels were completely depleted in PDX-AML-661 cells, while EZH2 protein expression was stable (Figure 16b). In order to further confirm a LOF phenotype, *EZH2/*p.A692G was transiently expressed in the 293T/*EZH2*$^{-/-}$ model with the result, that global H3K27me3 levels were decreased compared to wildtype EZH2 (Figure 16c). Because loss of functional EZH2 seems to be of high importance, a siRNA knockdown (kd) targeting EZH2 in PDX-AML-491 cells was established. EZH2 levels can thereby be reduced to approximately 20% of the native levels (Figure 16d). In order to evaluate the behaviour

against chemotherapy, cells were treated for 72h with AraC, where a slower proliferation (Figure 16e) and an increased resistance (Figure 16f) in EZH2 kd cells compared to control-siRNA transfected cells was observed.

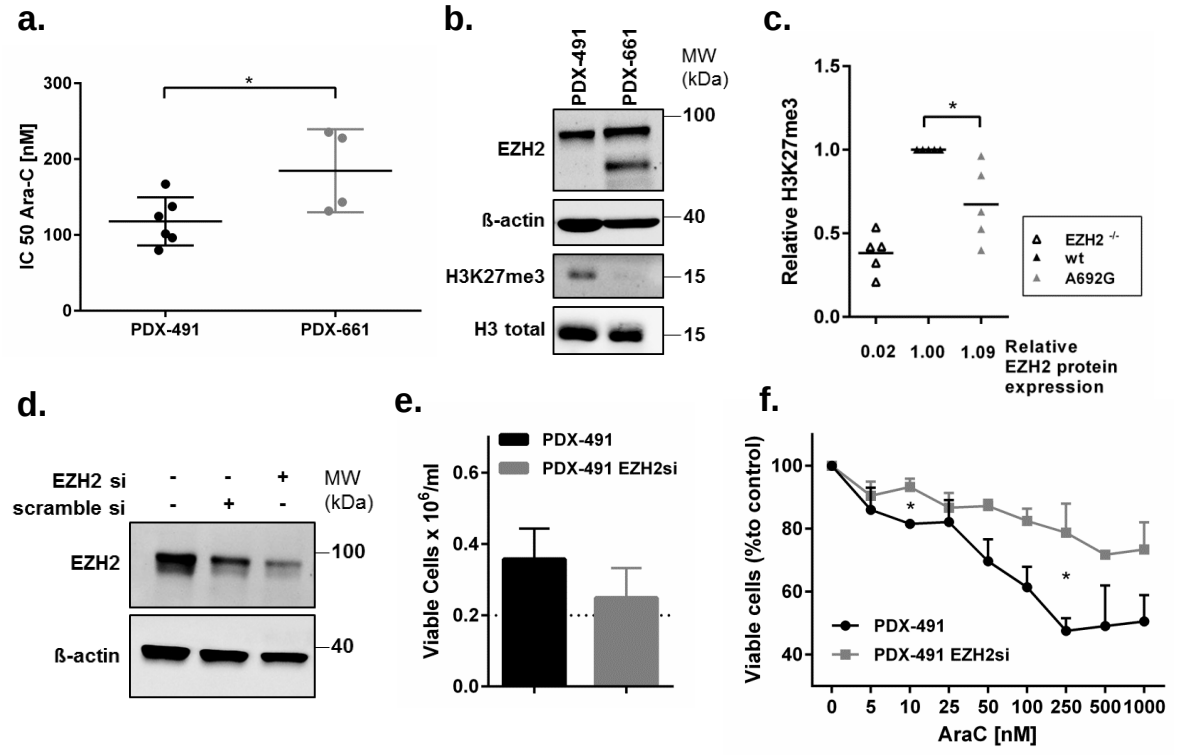

Figure 16: Knockdown of EZH2 in a patient-derived xenograft (PDX) model *in vitro*. a, Plot comparing IC_{50} AraC values for PDX-AML-491 and PDX-AML-661 *in vitro.* Mean (including s.d.) are shown for minimum four biological replicates. Unpaired, two-tailed Student's *t*-test; **p*<0.05; ***p*<0.01; ****p*<0.001; **b,** Immunoblotting of EZH2 expression and global H3K27me3 in PDX-AML-491 and PDX-AML-661. Molecular weight (MW); β-actin and H3 total: loading controls; **c,** Plot presenting the biochemical H3K27me3 activity of *EZH2*/p.A692G. Mean are shown for five biological replicates. Unpaired, two-tailed Student's *t*-test; **p*<0.05; ***p*<0.01; ****p*<0.001; **d,** Immunoblotting of EZH2 expression in PDX-AMAL-491 cells treated with 10nM siRNA. Molecular weight (MW); β-actin: loading control. Representative blot shown for two biological replicates; **e,** Histogram showing the proliferation of PDX-AML-491 cells with 10nM siRNA. Cells were pre-treated for 2 days with siRNA and then incubated for another 3 days for the proliferation assay. Mean (including s.d.) are shown for two biological replicates; **f,** Graph showing AraC treatment in PDX-AML-491 cells with 10nM siRNA. Cells were pre-treated for 2 days with siRNA and then treated for 72h with AraC. Mean (including s.d.) are shown for two biological replicates. Unpaired, two-tailed Student's *t*-test; **p*<0.05; ***p*<0.01; ****p*<0.001

4. Discussion

Clinical observations and functional data in relapsed AML have shown that loss of EZH2 expression might contribute to drug resistance. *EZH2* mutations were examined using different biological approaches applying patient material, patient-derived xenograft (PDX) models (*in vitro* and *in vivo*), human AML cell lines and clinical data. The aim of this work was to investigate the functional and prognostic impact of mutations in the methyltransferase EZH2 in AML. It was hypothesized that functional loss of EZH2 is associated with resistance to treatment with chemotherapeutic agents in patients suffering from AML. We showed, that *EZH2* mutations found in AML patients are loss of function (LOF) mutations and that functional inactivation of EZH2 is associated with resistance to the chemotherapeutic drug AraC.

4.1. Importance of *EZH2* Mutations for AML Patients

In a patient cohort of 664 AML patients[23], *EZH2* mutations were found in approximately 4%. Regarding those mutations, a wide variety of variant allele frequencies (VAF) were detected, ranging from 2.5% - 100%. More than 74% of the detected mutations in this cohort can be found in the catalytic SET domain at the C-terminal portion of the protein. Approximately 41% of *EZH2* mutations cause structural aberrations, some are truncating and a few cause an elongated protein variant due to frameshift mutations. Even though 76% of AML patients with *EZH2* mutation can be assigned to an adverse phenotype, increased mortality was not observed for these patients, even though this was recently shown for another cohort[106]. One explanation may be that our small sample size was insufficiently powered to detect a survival difference as compared with the larger cohort studied by Basheer et al[106].

In this work, it was observed that *EZH2* mutations frequently occur in patients with concurrent *RUNX1*, *ASXL1*, *TET2* or *DNMT3A* mutations. In a 2017 paper, Ernst et al. reported that *EZH2* mutations in patients with myeloid disorders frequently co-occur with *TET2* (58%), *RUNX1* (40%) and *ASXL1* (34%) mutations[102]. Additionally, *EZH2* was found to be most frequently mutated simultaneously with *RUNX1* and *ASXL1* in myelodysplastic and myeloproliferative neoplasm, as previously described[125]. The results of this work confirm these observations, since the same mutation pattern was observed

in the examined cohort. Additionally, a 2018 study reports that combined *Ezh2* and *Runx1* mutations initiate lympho-myeloid leukaemia in early thymic progenitors. Notably, the authors report that therapy-resistant leukaemia was associated with the frequent co-occurrence of *EZH2* and *RUNX1* inactivating mutations[126]. In this work, an increased mortality was not detected in patients with *EZH2* and *RUNX1* mutation as compared to the control group.

4.2. EZH2 Mutations in AML Patients Are LOF Mutations

The catalytic EZH2 SET domain has been shown to be a hot spot for mutations in several cancers including lymphomas and other myeloid malignancies like MDS[102–104]. Although inactivating mutations of *EZH2* are described in MDS, little is known about the impact of *EZH2* mutations in patients suffering from AML. Even though 74% of all *EZH2* mutations were found to be located in the SET domain, this work detected several mutations that are located N-terminal from the catalytic domains. In order to evaluate the importance of *EZH2* mutations in AML patients, different patient associated mutations were investigated to assess their methyltransferase activity. Thereby, a biochemical assay was established to evaluate the potential of EZH2 variants (Figure 17) to maintain global H3K27me3 levels.

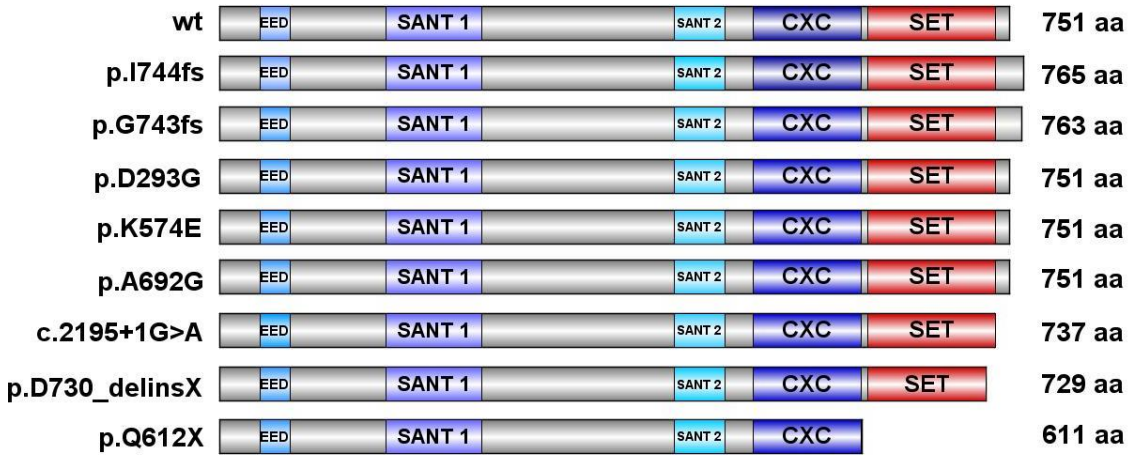

Figure 17: Illustration of investigated *EZH2* mutations: Illustration indicates structural aberrations which are caused by point or frameshift mutations.

Transient expression of patient associated *EZH2* mutations in 293T/*EZH2*$^{-/-}$ cells resulted in different global H3K27me3 levels detectable by immunoblotting. Previously described LOF and GOF mutations were used as controls, revealing diminished or hyper-trimethylation levels at H3K27 compared to the wildtype control. Seven different *EZH2* mutations were chosen, which have been found in patients in the cohorts studied. These include point mutations or different impacts on the natural protein structure, such as truncating or extending mutations. In some patients, mutations that lead to a complete loss of the C-terminal part of EZH2 were found. One mutation (EZH2/p.Q610X) was chosen to analyse a representative mutation lacking the entire SET domain. As expected, H3K27me3 levels were completely absent when these mutations were expressed.

Furthermore, one variant with a premature stop codon at p.Y730 was investigated (EZH2/p.D730_731DelinsX), found in one patient. This resulted in a strong decrease in measured global H3K27me3 levels, as expected, considering that Y731 of EZH2 is highly conserved and also essential for the SAM cofactor binding site[127,127]. These findings support the hypothesis that the C-terminal portion of the SET domain is essential for maintaining global H3K27me3 levels. EZH2/c.2195+1G>A (Y733LfsX6) was previously described in 2010 in MDS[103]. This mutation causes an alternate sequence in the SET domain and the absence of the C-terminal portion of the enzyme. This was of critical importance for the methylation activity of EZH2, since global H3K27me3 levels are completely abolished when this mutation was re-expressed.

In summary, the C-terminal part of the SET domain was indispensable for the catalytic activity of the enzyme. Nevertheless, the point mutations EZH2/p.K574E and EZH2/p.D293G revealed impaired catalytic activity with EZH2/p.K574E showing the most severe impact on global H3K27me3 in our experimental settings. Missense mutations at residues coordinating the first and second zinc ion of the CXC domain were reported in AML (p.H525N) and in MDS (p.C571N). This suggests that a disruption of the CXC domain of EZH2 also has a strong impact on the catalytic activity of the methyltransferase[102,128]. It was shown that EZH2 CXC domain is involved in the nucleosome interaction and that mutations in this region perturbate proper binding of the histone tail[129]. We therefore hypothesize, that histone tail interaction is impaired by p.K574E, whereby H3K27 cannot be methylated due to abrogated H3 tail binding.

In this work, LOF phenotypes were also detected in frameshift mutations, which cause an elongated transcript variant. EZH2/p.I744fs has been previously described in AML[130,130], but without further information concerning the biochemical activity. EZH2/p.G743fs and p.I744fs both have impaired catalytic activity, even though the SET domain sequence is unchanged. This leads to the conclusion that, not only a correct protein sequence is necessary for methyltransferase activity, but also the steric integrity of the C-terminal part is highly critical for the functionality of the EZH2. Changes causing an elongated protein might influence the interaction with PRC2 members or induce steric hindrance within the enzymatic reaction.

In summary, *EZH2* LOF mutations seem to play an important role in the pathogenesis and progression of AML. As expected, different AML-related mutations were found to be determined as LOF mutations, both truncating and non-truncating mutations. Catalytic loss of H3K27me3 by *EZH2* mutations support the hypothesis that the functional activity of EZH2 plays a relevant role in these AML patients. Additionally, a dominant negative effect in 50% of all tested mutation was observed, highlighting the importance of a heterozygous mutation status. Since *EZH2* mutations most frequently occurred in a heterozygous background in our cohorts this fact is of importance. We therefore hypothesize that also a heterozygous mutation status is also sufficient to induce loss of H3K27 methylation and thereby cause drug resistance in a subset of patients.

4.3. Loss of EZH2 Expression is Associated with Poor Survival

In this work, EZH2 mRNA expression levels were shown to be altered in more than 70% of matched diagnosis-relapse pairs of AML patients. Additional analysis of protein expression levels revealed both increasing and decreasing levels of EZH2 expression in relapsed patients. Overall, EZH2 decrease was observed in 23-50% of relapsed patient samples.

In a 2016 publication, Göllner et al. reported altered EZH2 protein levels in AML patients[131]. In that study, a decrease of EZH2 protein and global H3K27me3 levels was detected in 45% of relapsed samples in matched diagnosis-relapse pairs. The results of that work are consistent with our findings since a decreased expression of EZH2 was found in 23-50% of AML patients by analyzing mRNA and protein expression levels. It

was also shown by Göllner et al. in a cohort of 124 patients, that low expression levels of EZH2 correlate with a poor prognosis. The results shown here confirm that generally low EZH2 expression correlates with a poor OS and a poor RFS in AML patients. In addition to low expression levels, two relapse-associated *EZH2* mutations were detected in patients, which show clonal outgrowth in AML relapse. *EZH2*/c.2195+1G>A (Y733LfsX6) and *EZH2*/p.A692G are both located in the SET domain and were observed in a first and a second relapse of two patients. We therefore hypothesize, that in addition to protein loss, *EZH2* mutations might also play an important role in the development of drug resistance in AML.

4.4. Loss of EZH2 is Associated with Chemotherapeutic Drug Resistance and Provides Selective Advantage in Relapsed AML Patients

Loss of EZH2 expression was shown to be associated with treatment resistance in AML patients by Göllner et al. in 2016. They proposed that proteasomal degradation of the EZH2 protein results in chemotherapeutic resistance by de-repression of downstream EZH2 target genes such as *HOXA9* and *HOXB8*[131]. Göllner et al. further found that loss of EZH2 induces resistance against standard chemotherapeutic drugs such as AraC and tyrosine kinase inhibitors (Midostaurin), which results from degradation of the EZH2 protein. They showed that application of proteasome inhibitors was able to rescue the sensitivity in AML cell lines and patient samples[131]. At the genetic level, loss of chromosome 7 or partial deletions such as 7q deletions are common in AML patients and have been shown to be an adverse prognostic factor (ELN classification from 2017[33]). Since EZH2 is located on 7q36, partial loss of chromosome 7 or the q arm of chromosome 7 directly impacts EZH2 protein expression.

In this work, two *EZH2*$^{-/-}$ cell lines were established by using CRISPR/Cas9 genome editing in order to evaluate resistance towards cytotoxic agents in cells lacking EZH2 expression. We could show that complete loss of EZH2 results in a resistance against AraC in HEK293T cells and in the myeloid cell line K562. These data are therefore supportive of the previous work from Göllner et al. The findings were extended with respect to *EZH2* mutations which are recurrently found in AML and MDS patients, by showing that re-expression of wildtype EZH2, but not EZH2 LOF mutations restore sensitivity, showing

that the catalytic activity might influence chemotherapeutic drug resistance. In order to confirm whether *EZH2* mutation status might also drive resistance mechanisms in AML patients, an inducible EZH2 mutated model was established in this work. It was shown that wildtype EZH2 was able to re-induce sensitivity in *EZH2*$^{-/-}$ cells, but LOF mutation, where global H3K27me3 was completely lost, did not. It is therefore assumed that loss of the catalytic activity of EZH2 plays a major role in a resistance mechanism in AML patients.

To extend these results to an *in vivo* system, a patient-derived xenograft (PDX) model was used[107], which uses patient-derived primary leukaemia cells that engraft in immuno-deficient NSG mice. Matched patient samples from a first (PDX-AML-491) and second (PDX-AML-491) relapse of an AML patient were compared, where *EZH2* is mutated (EZH2/p.A692G) in the second relapse. Importantly, this mutation shows subclonal outgrowth to up to 98.8% VAF *in vivo* in mice, suggesting that the mutation is selected by a clonal evolution process during tumour development. We hypothesize that functional inactivation of EZH2 drives mechanisms allowing the resistant clone to grow within the tumour mass. Loss of EZH2 provides a selective growth advantage, which might be explained by an increased resistance to chemotherapeutic drugs since drug resistance could be detected in the *EZH2* mutated relapsed PDX (PDX-AML-661) both *in vivo* and *in vitro*. In these cells, global H3K27me3 levels were strongly reduced, indicating a LOF phenotype of the mutation which was confirmed in an additional biochemical assay.

Interestingly, *EZH2/*p.A692 was previously described as a mutational hot spot that occurs in lymphoma patients[99]. A similar mutation (p.A692V) was formerly characterized as a GOF mutation in a heterozygous background[132]. In this work, the mutation was detected in a hemizygous background, since an additional deletion of 7q was present in this patient. It has been known for years that EZH2 GOF mutations in lymphomas require a wildtype EZH2 (heterozygous background) to induce a hyper-trimethylation phenotype[101]. Thus, wildtype and mutant alleles collaborate to elevate H3K27 methylation, highlighting the importance of the heterozygous status. The experimental setting of our PDX model has limitations since additional mutations co-occur in the second relapse of the patient (PDX-AML-661), which could be verified by NGS. To overcome these restrictions, a knockdown of EZH2 in PDX-AML-491 cells was established to investigate EZH2 dependence *in vitro*. It was shown that downregulation of EZH2 is responsible for the drug resistant phenotype

in vitro, supporting the hypothesis that loss or functional inactivation of EZH2 directly induce chemotherapy resistance in AML.

4.5. Downstream Effects of Genetic De-Repression Caused by EZH2 Loss

Since *EZH2* mutations are rare events in AML, more clinical studies are necessary to address the importance of *EZH2* mutations and expression status in order to evaluate the prognostic relevance of its up or downregulation. Even though EZH2-dependent resistance could be confirmed in different models, the origin of drug resistance which is dependent on the presence of EZH2 remains unclear. EZH2, a transcriptional repressor, is responsible for the suppression of thousands of genes. This requires further investigation in order to completely understand how loss of the catalytic activity might promote chemotherapy resistance in AML patients.

It has been shown, that repressive marks which are mediated by EZH2 lead to silencing of *HOX* gene clusters[131,133]. *HOX* gene clusters encode a huge variety of highly conserved transcription factors, which regulate cellular fate during embryogenesis. It is therefore generally accepted that homozygous *Ezh2* KO is lethal in early stages of mouse development[134]. Generally, *HOX* gene expression decreases during haematopoietic cell maturation[135]. During haematopoiesis, *HOX* genes are expressed in lineage- and stage-specific combinations which are tightly regulated. It has been shown, that overexpression of *HOXA5* causes an increase in the amount of myeloid progenitors and stopped erythroid differentiation[136]. Another study revealed that upregulation of *HOXA10* in $CD34^+$ haematopoietic progenitors leads to a significant assembly of blast cells and myelopoiesis in parallel with a total block of erythroid differentiation[137].

HOXA9 is the most frequently expressed *HOX* gene in human $CD34^+$ HSCs and early haematopoietic progenitors and it is consequently downregulated during cell differentiation[139]. *Hoxa9* overexpression was shown to boost the growth of HSC and myeloid progenitor cell proliferation and linked to the induction of leukaemia[138]. As stated atop, *HOXA9* is a key controller of haematopoietic programs and it acts as oncogene in leukaemia, driving leukemogenesis[139]. It is comprehensible that *HOXA9* initiates the transcription of genes, which control cell proliferation and survival. Consequently, myeloid differentiation is stopped and proliferation is enhanced[140].

HOXA9 upregulation by EZH2 loss and association with chemotherapeutic resistance has also been described by Göllner et al. in 2016. They additionally showed, that knockdown of HOXA9 was able to restore sensitivity against TKIs and AraC[131]. The complex network of *HOX* genes and the fact that there is a wide range of oncogenes and tumour suppressors that are targeted by EZH2 (some even independent on the trimethylation of H3K27) uncovers the necessity to investigate EZH2 downstream mechanisms in more detail.
Additionally, inhibition of EZH2 and subsequent loss of H3K27me3 has been shown to induce cell cycle arrest[106] and lower proliferation rates in different cancer associated cell models[141]. One study showed, that depletion of EZH2 leads to DNA damage repair and induction of cell senescense[142]. In that study, the loss of H3K27me3 marks led to upregulation of p16 (CDKN2A), which induces DNA repair.

In this work, impaired proliferation was observed in both *EZH2*$^{-/-}$ cell line models and in an *EZH2* mutated (LOF) PDX sample. In addition to *HOX* genes, another set of genes that are relevant for cell cycle processes and differentiation are known targets of EZH2. Among these, major targets are the Ink4b/Arf/Ink4a loci (encoding the tumour supressors p15INK4b, p16INK4a and p14ARF proteins). Inhibition of these genes promotes cell proliferation[143–145]. Hence, de-repression which is caused by EZH2 loss of these targets, impairs normal cell proliferation by the induction of cell cycle arrest and apoptosis[146]. EGR1 is another key transcription factor that is directly affected by EZH2 loss. The zink finger transcription factor EGR1 (encoded by the *EGR-1* (Early growth response protein 1) gene) is a key transcription factor which mediates important differentiation processes[147,148]. It was found that de-repression and subsequent overexpression of *EGR-1* caused by EZH2 loss promoted differentiation and profoundly diminished AML cell growth[149]. Even though decelerated cell proliferation is not a hallmark of cancers, this phenotype might also promote decelerated uptake of chemotherapeutic drugs, such as AraC, since their uptake is cell-cycle dependent.

4.6. EZH2 Might Act as Tumour Suppressor and Oncogene – Depending on the Cellular Context

Many studies within the last years describe EZH2 (or PRC2 in general) in the context of an oncogene. This concept is related to the fact that EZH2 overexpression promotes the repression of tumour suppressor genes by repressive H3K27me3 marks. In contrast, a few years ago an association between EZH2 loss and tumour development was observed in pancreatic cancer. In that study, EZH2 loss led to a 6-fold increase in the development of pancreatic intraepithelial neoplasia, suggesting a protective role of EZH2 in the carcinogenesis of pancreatic cancer[150].

The results of this work highlight a tumour suppressor role of EZH2 in AML. Nevertheless, high expression levels of EZH2 have been previously found in AML patient samples[151] and inhibition of EZH2 has been shown to exert anti-leukemic effects in MLL-rearranged leukaemias[105], as verified for two AML cell lines in this work. It was also reported that simultaneous inhibition of the histone demethylase LSD1 and EZH2 was synergistic for anti-leukemic activity in AML[152]. Moreover, recent reports show that concordant inhibition of EZH1 and EZH2 has anti-leukemic effects. Specifically, combination therapy with both inhibitors reduced the number of LSCs, impaired leukaemia progression and prolonged survival times in mouse models[153]. Additionally, it has been reported that loss of EZH2 promotes MDS development, but prevents transformation from MDS to AML in MDS mouse models[154]. These results support an oncogenic role of EZH2 in context of AML.

A novel mouse study showed opposite roles of the methyltransferase EZH2 in initiation and maintenance of AML, suggesting that expression of EZH2 is highly dependent on the disease stage[106]. In that work, stage-specific and entirely opposite roles for Ezh2 at the initial and advanced stages of AML were described[106]. Basheer et al. found that Ezh2 exerts an oncogenic function in AML maintenance that can be targeted therapeutically in patients. Conversely, Ezh2 can also act as a tumour suppressor during disease induction. They found the oncogene PLAG1 to be de-repressed by EZH2 loss. This gene is also involved in cell cycle programs by affecting the activity of cycle-related genes such as *Cyclin D3* and *Cyclin D1*, as well as genes, that are linked to apoptosis, such as *Caspase-8,*[155] associated with AML induction[156].

In summary, the results of this work demonstrate that functional loss of the methyltransferase EZH2 is associated with a drug resistant phenotype in AML. On the other hand, increasing EZH2 expression levels were also observed in more than 50% of patients in matched diagnosis-relapse samples, which might lead to the assumption that diverse subgroups of *EZH2* mutated patients might benefit from different treatment recommendations, guided by their EZH2 status. Treatment with small-molecule inhibitors has been shown to provide promising results in the treatment of *EZH2* mutated lymphoma (NCT02082977, NCT01897571) also in addition to AML patients[105,153]. Despite the useful potential of EZH2 inhibitors, further study is needed to address their target specificity. In this thesis, EZH2 inhibitors induce sensitivity towards the chemotherapeutic drug AraC in two MLL-rearranged leukaemia cell lines. Nevertheless, there is also evidence, that lacking activity of EZH2 also drives resistance mechanisms in leukaemia cells. The data presented in this work therefore counsels caution in the treatment of AML patients with EZH2 inhibitors, since this might promote chemotherapeutic resistance in a subgroup of patients.

5. Annex

5.1. Supplementary Material

Supplementary Figures

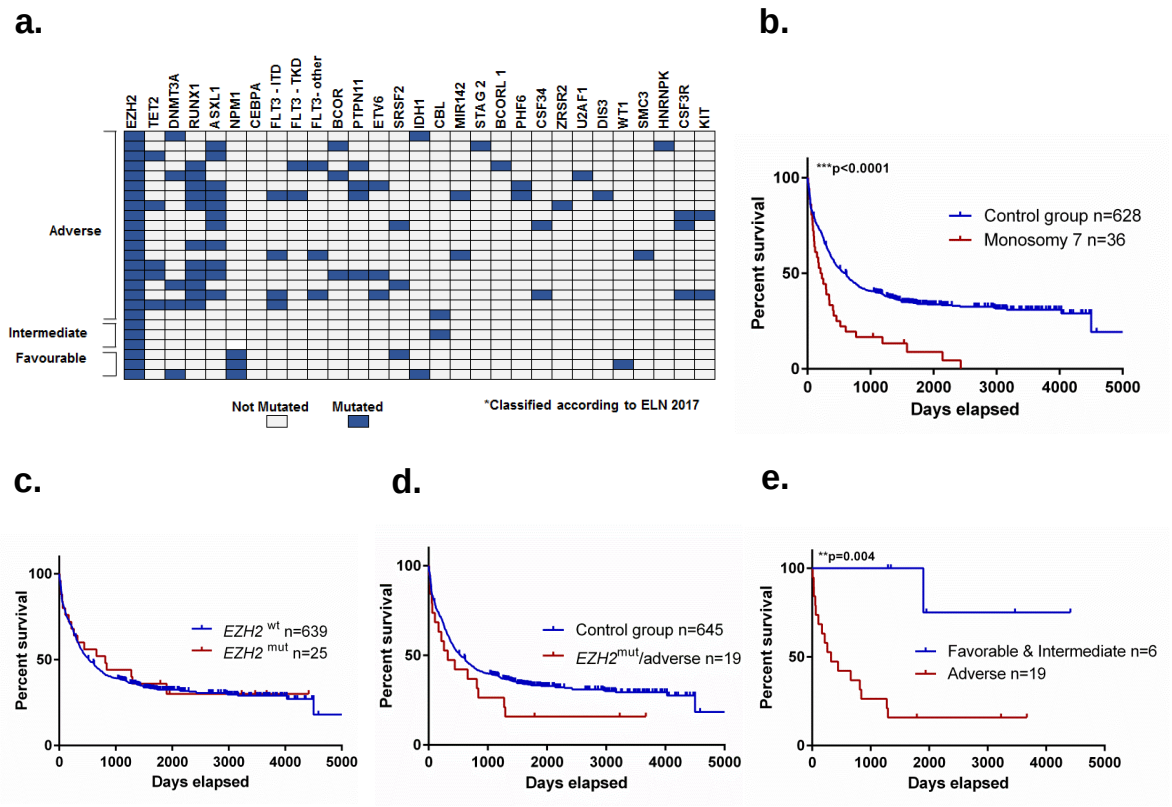

Supplementary Figure 1, related to Figure 7: Recurrent EZH2 mutations at diagnosis. a, Illustration of mutation pattern in 25 AML patients at diagnosis. Classification was performed in consideration of ELN 2017. Status includes also multiple mutations in one patient. **b-e,** Overall survival plots of patients with monosomy 7 (**b**), patients with EZH2 mutation (**c**), patients with EZH2 mutation and an adverse phenotype (**d**) and a comparison of patients with EZH2 mutation and adverse or favourable/intermediate phenotype (**e**).

a.

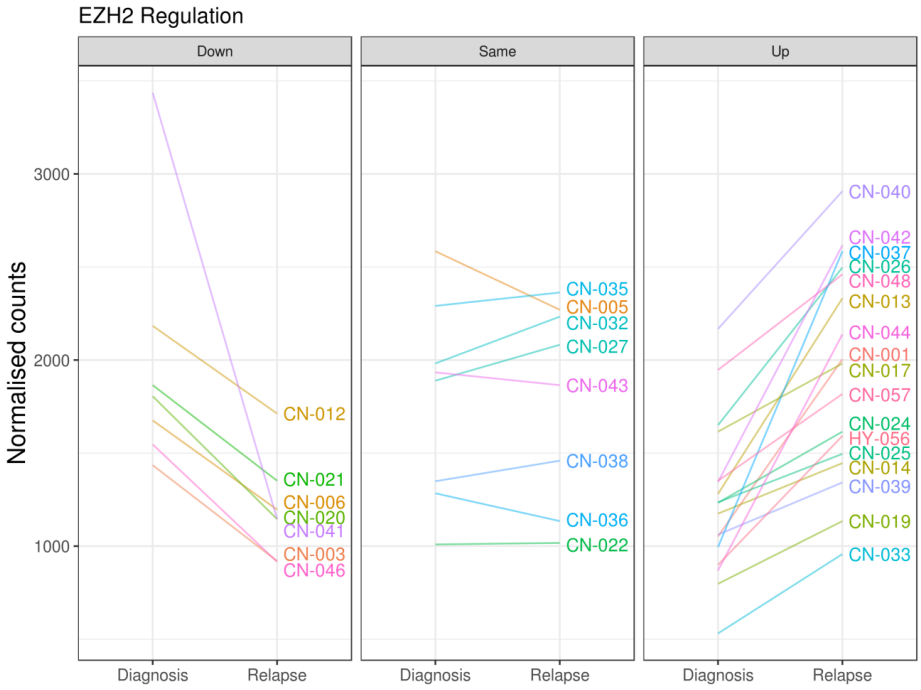

b.

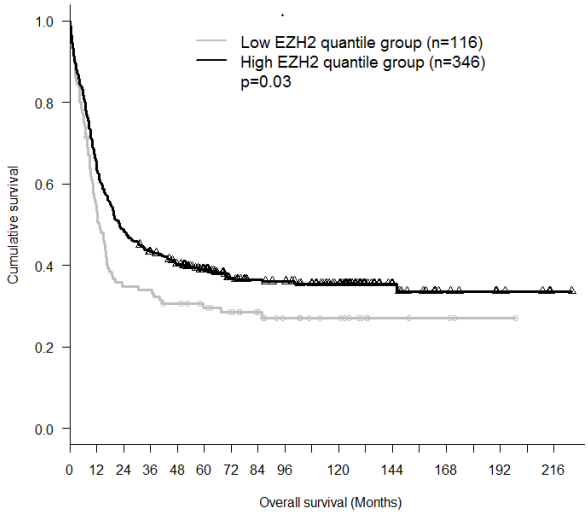

Supplementary Figure 2, related to Figure 8: Relevance of EZH2 in AML relapse. a, EZH2 mRNA expression levels of 35 CN-AML patients between diagnosis and relapse. **b,** OS in patients with low/high EZH2 expression; HOVON cohort.

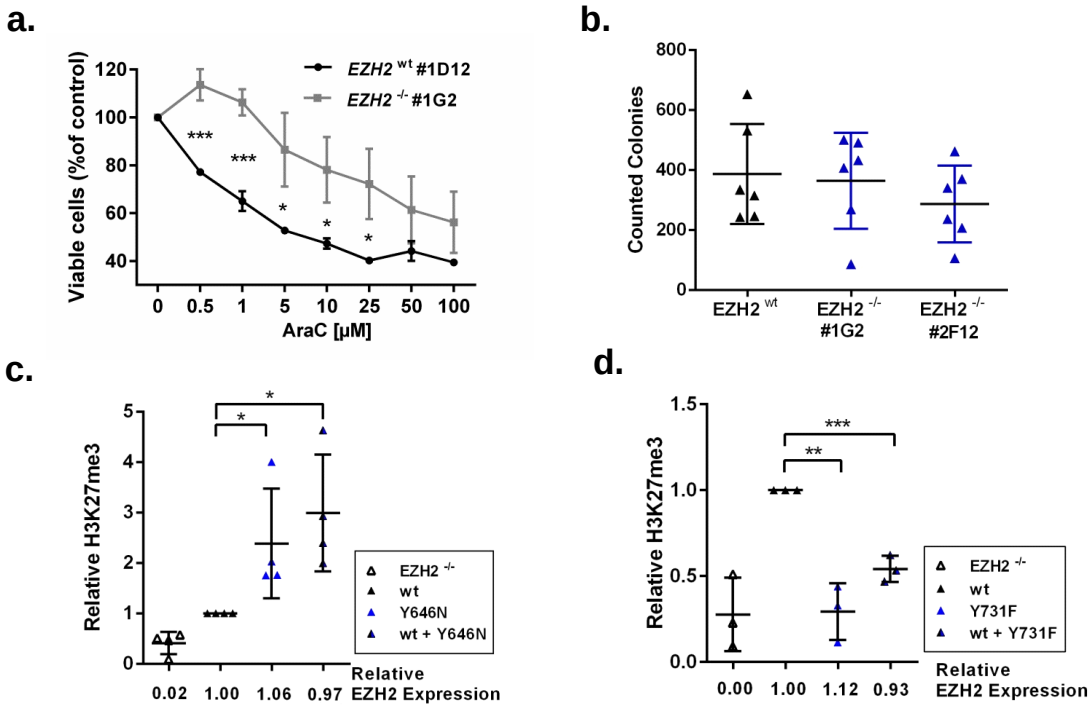

Supplementary Figure 3, related to Figure 10: Evaluation of *EZH2* mutations found in AML patients at diagnosis. a, Graph showing AraC resistance in one 293T/EZH2$^{-/-}$ sc clone. Mean (including s.d.) are shown for three biological replicates. Unpaired, two-tailed Student's *t*-test; *p<0.05; **p<0.01; ***p<0.001**. b,** Plot showing the colony formation of 3 293T sc clones. Mean (including s.d.) are shown for 6 biological replicates. **c,** Plot showing the biochemical H3K27me3 activity of EZH2/p.Y646N which was previously described[99]. Mean (including s.d.) are shown for four biological replicates. EZH2 expression was confirmed in the same experimental setting and the ratio of ß-actin and EZH2 is shown below. Unpaired, two-tailed Student's *t*-test; *p<0.05; **p<0.01; ***p<0.001. **d,** Plot showing the biochemical H3K27me3 activity of EZH2/p.Y731F which was previously described[122]. Mean (including s.d.) are shown for three biological replicates. Unpaired, two-tailed Student's *t*-test; *p<0.05; **p<0.01; ***p<0.001.

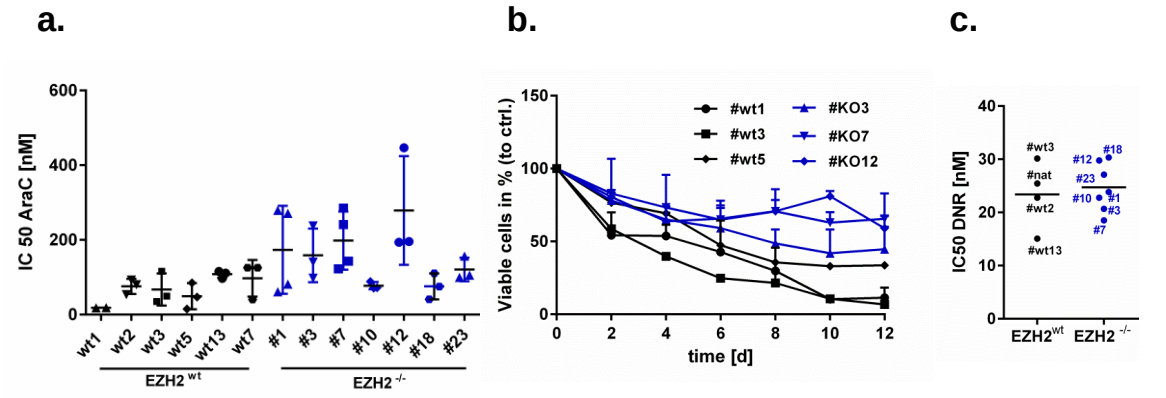

Supplementary Figure 4, related to Figure 11: EZH2 depletion is associated with AraC resistance in the myeloid cell line K562. a, Plot comparing AraC IC_{50} values in *EZH2*^{wt} (n=6) and *EZH2*$^{-/-}$ (n=7) clones. Mean (including s.d.) are shown for three biological replicates for each clone. **b,** Long-term low dose AraC treatment in *EZH2*^{wt} (n=3) and *EZH2*$^{-/-}$ (n=3) clones. Cells were treated with 30nM AraC/DMSO for 12d. Cells were splitted and treated every 4d. Mean (including s.d.) are shown for three biological replicates for each clone; **c,** Plot showing DNR IC_{50} values for *EZH2*^{wt} (n=4) and *EZH2*$^{-/-}$ (n=7) sc clones. Cells were treated with DNR/DMSO for 72h. Each clone represents the mean of three biological replicates.

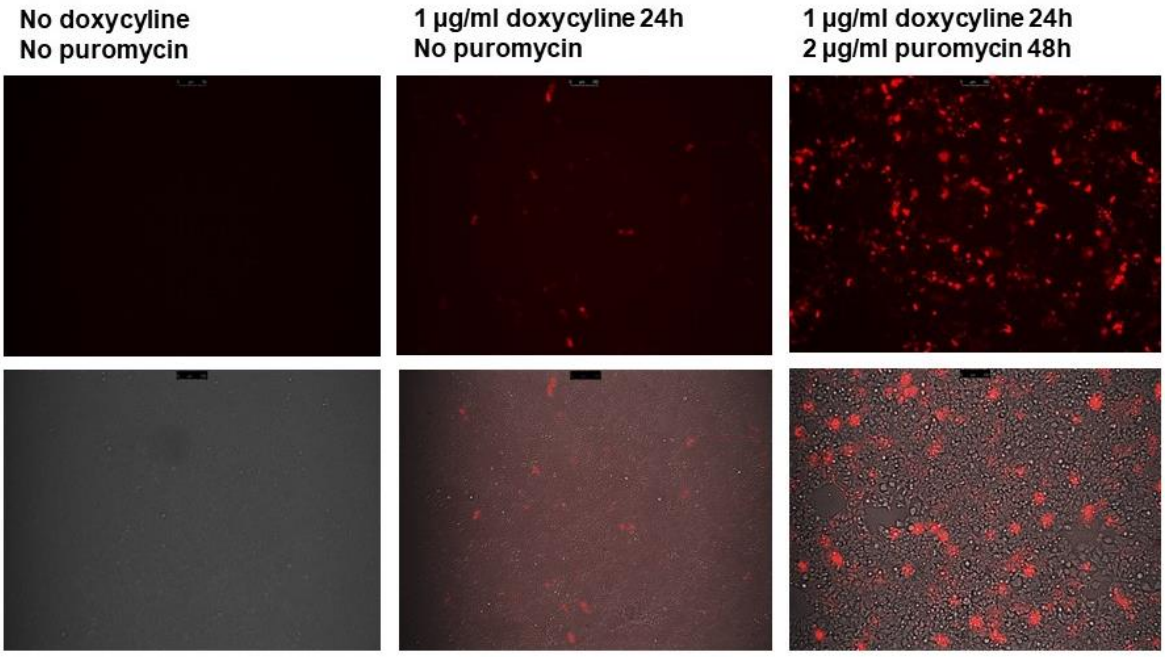

Supplementary Figure 5, related to Figure 12: Inducible EZH2 re-expression via PB/Transposase system; here shown in HEK293T cells. Transient co-expression of PB/*EZH2* and transposase induces stable integration of *EZH2* into the genome, accompanied by a fluorescent marker to visualize positive expression after doxycycline treatment. Additionally, integrated puromycin resistance offers the possibility to select positive cells. Cells were transiently transfected with both vectors (PB/*EZH2* and Transposase) for 24h. Immediately after transfection, 1µg/ml doxycycline was added. Selection via puromycin (2µg/ml) followed 48h later for 7d. K562 clones were sc sorted.

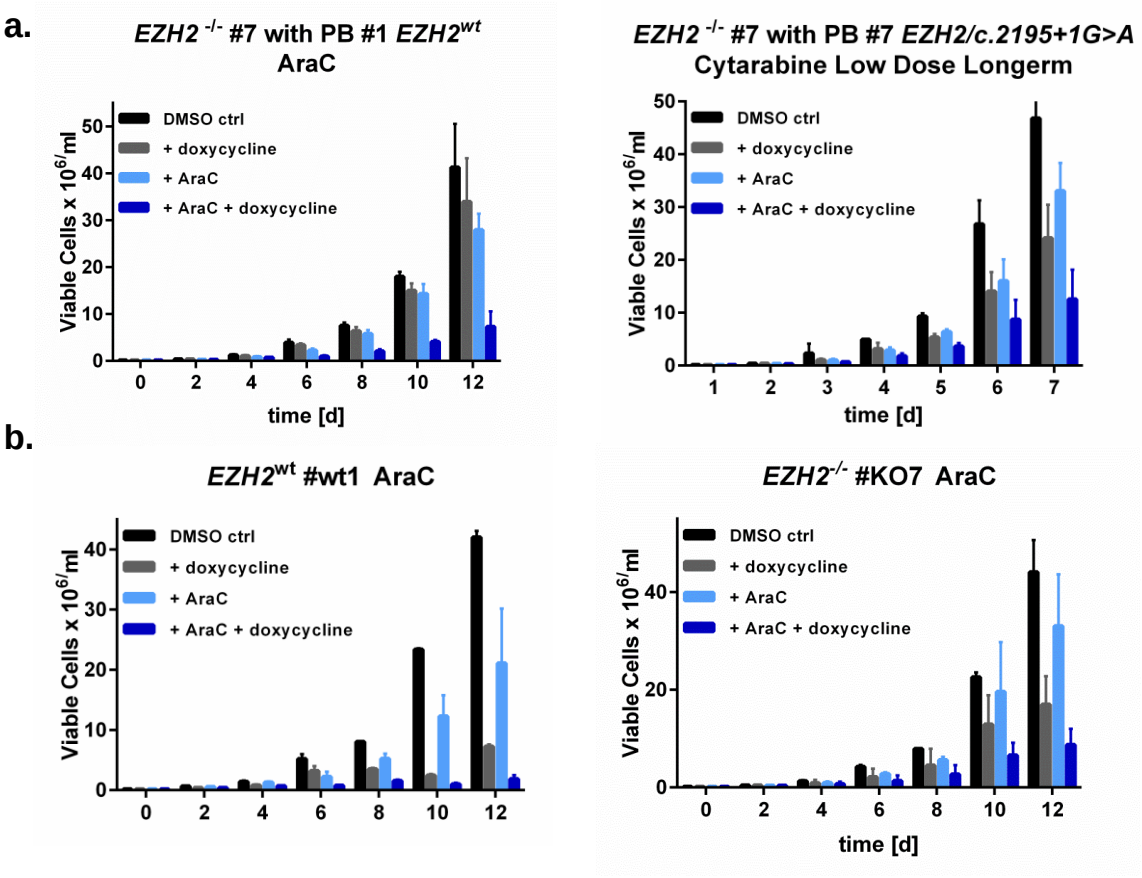

Supplementary Figure 6, related to Figure 13: EZH2 re-expression in the myeloid cell line K562 via PB. a-b Graphs showing AraC low dose long-term treatment in K562 sc clones. Cells were pre-treated for 3d with doxycycline and then treated with 30nM AraC/DMSO for 12d. Cells were splitted and treated every 4d and doxycycline was added every 48h to ensure stable expression of EZH2 (**a,** PB/EZH2; **b,** ctrl clones). Mean (including s.d.) are shown for three biological replicates for each clone.

5.2. References

1 World Health Organization (WHO), International Agency for Research on Cancer. [Latest global cancer data: Cancer burden rises to 18.1 million new cases and 9.6 million cancer deaths in 2018]. 12.09.18. Updated 12.09.18.

2 Westlake S. Cancer incidence and mortality in the United Kingdom and constituent countries, 2004–06. *Health Stat Q*. 2009;43(1):56-62. doi:10.1057/hsq.2009.28.

3 Jemal A, Siegel R, Ward E, et al. Cancer statistics, 2008. *CA Cancer J Clin*. 2008;58(2):71-96. doi:10.3322/CA.2007.0010.

4 Parkin DM, Bray F, Ferlay J, Pisani P. Global cancer statistics, 2002. *CA Cancer J Clin*. 2005;55(2):74-108.

5 Smith A, Howell D, Patmore R, Jack A, Roman E. Incidence of haematological malignancy by sub-type: a report from the Haematological Malignancy Research Network. *Br J Cancer*. 2011;105(11):1684-1692. doi:10.1038/bjc.2011.450.

6 Campo E, Swerdlow SH, Harris NL, Pileri S, Stein H, Jaffe ES. The 2008 WHO classification of lymphoid neoplasms and beyond: evolving concepts and practical applications. *Blood*. 2011;117(19):5019-5032. doi:10.1182/blood-2011-01-293050.

7 Yamamoto JF, Goodman MT. Patterns of leukemia incidence in the United States by subtype and demographic characteristics, 1997-2002. *Cancer Causes Control*. 2008;19(4):379-390. doi:10.1007/s10552-007-9097-2.

8 Kouchkovsky I de, Abdul-Hay M. 'Acute myeloid leukemia: a comprehensive review and 2016 update'. *Blood Cancer J*. 2016;6(7):e441. doi:10.1038/bcj.2016.50.

9 Alan G. Rosmarin. Pathogenesis of acute myeloid leukemia. 2017.

10 Cline A, Jajosky R, Shikle J, Bollag R. Comparing leukapheresis protocols for an AML patient with symptomatic leukostasis. *J Clin Apher*. 2018;33(3):396-400. doi:10.1002/jca.21588.

11 Chang HY, Rodriguez V, Narboni G, Bodey GP, Luna MA, Freireich EJ. Causes of death in adults with acute leukemia. *Medicine (Baltimore)*. 1976;55(3):259-268.

12 Ferrara F, Lessi F, Vitagliano O, Birkenghi E, Rossi G. Current Therapeutic Results and Treatment Options for Older Patients with Relapsed Acute Myeloid Leukemia. *Cancers (Basel)*. 2019;11(2). doi:10.3390/cancers11020224.

13 Burnett AK, Mohite U. Treatment of older patients with acute myeloid leukemia--new agents. *Semin Hematol*. 2006;43(2):96-106. doi:10.1053/j.seminhematol.2006.01.003.

14 Hann IM, Stevens RF, Goldstone AH, et al. Randomized comparison of DAT versus ADE as induction chemotherapy in children and younger adults with acute myeloid leukemia. Results of the Medical Research Council's 10th AML trial (MRC AML10). Adult and Childhood Leukaemia Working Parties of the Medical Research Council. *Blood*. 1997;89(7):2311-2318.

15 Bradstock KF, Matthews JP, Lowenthal RM, et al. A randomized trial of high-versus conventional-dose cytarabine in consolidation chemotherapy for adult de novo acute myeloid leukemia in first remission after induction therapy containing high-dose cytarabine. *Blood*. 2005;105(2):481-488. doi:10.1182/blood-2004-01-0326.

16 Wang J, Yang Y-G, Zhou M, et al. Meta-analysis of randomised clinical trials comparing idarubicin + cytarabine with daunorubicin + cytarabine as the induction chemotherapy in patients with newly diagnosed acute myeloid leukaemia. *PLoS ONE*. 2013;8(4):e60699. doi:10.1371/journal.pone.0060699.

17 Roboz GJ. Novel approaches to the treatment of acute myeloid leukemia. *Hematology Am Soc Hematol Educ Program*. 2011;2011:43-50. doi:10.1182/asheducation-2011.1.43.

18 Tallman MS, Gilliland DG, Rowe JM. Drug therapy for acute myeloid leukemia. *Blood*. 2005;106(4):1154-1163. doi:10.1182/blood-2005-01-0178.

19 Bhatt VR. Personalizing therapy for older adults with acute myeloid leukemia: Role of geriatric assessment and genetic profiling. *Cancer Treat Rev*. 2019;75:52-61. doi:10.1016/j.ctrv.2019.04.001.

20 Cheson BD, Bennett JM, Kopecky KJ, et al. Revised recommendations of the International Working Group for Diagnosis, Standardization of Response Criteria, Treatment Outcomes, and Reporting Standards for Therapeutic Trials in Acute Myeloid Leukemia. *J Clin Oncol*. 2003;21(24):4642-4649. doi:10.1200/JCO.2003.04.036.

21 Lima M de, Strom SS, Keating M, et al. Implications of potential cure in acute myelogenous leukemia: development of subsequent cancer and return to work. *Blood*. 1997;90(12):4719-4724.

22 Bennett JM, Catovsky D, Daniel MT, et al. Proposals for the classification of the acute leukaemias. French-American-British (FAB) co-operative group. *Br J Haematol*. 1976;33(4):451-458.

23 Vardiman JW, Harris NL, Brunning RD. The World Health Organization (WHO) classification of the myeloid neoplasms. *Blood*. 2002;100(7):2292-2302. doi:10.1182/blood-2002-04-1199.

24 Vardiman JW, Thiele J, Arber DA, et al. The 2008 revision of the World Health Organization (WHO) classification of myeloid neoplasms and acute leukemia: rationale and important changes. *Blood*. 2009;114(5):937-951. doi:10.1182/blood-2009-03-209262.

25 Arber DA, Orazi A, Hasserjian R, et al. The 2016 revision to the World Health Organization classification of myeloid neoplasms and acute leukemia. *Blood*. 2016;127(20):2391-2405. doi:10.1182/blood-2016-03-643544.

26 Visser O, Trama A, Maynadié M, et al. Incidence, survival and prevalence of myeloid malignancies in Europe. *Eur J Cancer*. 2012;48(17):3257-3266. doi:10.1016/j.ejca.2012.05.024.

27 Landau DA, Carter SL, Getz G, Wu CJ. Clonal evolution in hematological malignancies and therapeutic implications. *Leukemia*. 2014;28(1):34-43. doi:10.1038/leu.2013.248.

28 Karjalainen E, Repasky GA. Molecular Changes During Acute Myeloid Leukemia (AML) Evolution and Identification of Novel Treatment Strategies Through Molecular Stratification. *Prog Mol Biol Transl Sci*. 2016;144:383-436. doi:10.1016/bs.pmbts.2016.09.005.

29 Ossenkoppele G, Schuurhuis GJ. MRD in AML: time for redefinition of CR? *Blood*. 2013;121(12):2166-2168. doi:10.1182/blood-2013-01-480590.

30 Hu XF, Slater A, Kantharidis P, et al. Altered multidrug resistance phenotype caused by anthracycline analogues and cytosine arabinoside in myeloid leukemia. *Blood*. 1999;93(12):4086-4095.

31 Abelson S, Collord G, Ng SWK, et al. Prediction of acute myeloid leukaemia risk in healthy individuals. *Nature*. 2018;559(7714):400-404. doi:10.1038/s41586-018-0317-6.

32 Döhner H, Estey EH, Amadori S, et al. Diagnosis and management of acute myeloid leukemia in adults: recommendations from an international expert panel, on behalf of the European LeukemiaNet. *Blood*. 2010;115(3):453-474. doi:10.1182/blood-2009-07-235358.

33 Döhner H, Estey E, Grimwade D, et al. Diagnosis and management of AML in adults: 2017 ELN recommendations from an international expert panel. *Blood*. 2017;129(4):424-447. doi:10.1182/blood-2016-08-733196.

34 Metzeler KH, Herold T, Rothenberg-Thurley M, et al. Spectrum and prognostic relevance of driver gene mutations in acute myeloid leukemia. *Blood*. 2016;128(5):686-698. doi:10.1182/blood-2016-01-693879.

35 Greif PA, Hartmann L, Vosberg S, et al. Evolution of Cytogenetically Normal Acute Myeloid Leukemia During Therapy and Relapse: An Exome Sequencing Study of 50 Patients. *Clin Cancer Res*. 2018;24(7):1716-1726. doi:10.1158/1078-0432.CCR-17-2344.

36 Shen Y, Zhu Y-M, Fan X, et al. Gene mutation patterns and their prognostic impact in a cohort of 1185 patients with acute myeloid leukemia. *Blood*. 2011;118(20):5593-5603. doi:10.1182/blood-2011-03-343988.

37 Sandoval JE, Huang Y-H, Muise A, Goodell MA, Reich NO. Mutations in the DNMT3A DNA methyltransferase in AML patients cause both loss and gain of function and differential regulation by protein partners. *J Biol Chem*. 2019. doi:10.1074/jbc.RA118.006795.

38 Feinberg AP. The Key Role of Epigenetics in Human Disease Prevention and Mitigation. *N Engl J Med*. 2018;378(14):1323-1334. doi:10.1056/NEJMra1402513.

39 Dawson MA, Kouzarides T. Cancer epigenetics: from mechanism to therapy. *Cell*. 2012;150(1):12-27. doi:10.1016/j.cell.2012.06.013.

40 Holliday R, Pugh JE. DNA modification mechanisms and gene activity during development. *Science*. 1975;187(4173):226-232.
41 Dawson MA, Kouzarides T, Huntly BJP. Targeting epigenetic readers in cancer. *N Engl J Med*. 2012;367(7):647-657. doi:10.1056/NEJMra1112635.
42 Sun Y, Chen B-R, Deshpande A. Epigenetic Regulators in the Development, Maintenance, and Therapeutic Targeting of Acute Myeloid Leukemia. *Front Oncol*. 2018;8:41. doi:10.3389/fonc.2018.00041.
43 Ley TJ, Miller C, Ding L, et al. Genomic and epigenomic landscapes of adult de novo acute myeloid leukemia. *N Engl J Med*. 2013;368(22):2059-2074. doi:10.1056/NEJMoa1301689.
44 Gujar H, Weisenberger DJ, Liang G. The Roles of Human DNA Methyltransferases and Their Isoforms in Shaping the Epigenome. *Genes (Basel)*. 2019;10(2). doi:10.3390/genes10020172.
45 Koya J, Kurokawa M. Functional role of DNMT3A mutation in acute myeloid leukemia. *Rinsho Ketsueki*. 2018;59(5):602-610. doi:10.11406/rinketsu.59.602.
46 Marcucci G, Metzeler KH, Schwind S, et al. Age-related prognostic impact of different types of DNMT3A mutations in adults with primary cytogenetically normal acute myeloid leukemia. *J Clin Oncol*. 2012;30(7):742-750. doi:10.1200/JCO.2011.39.2092.
47 Kanwal R, Gupta K, Gupta S. Cancer epigenetics: an introduction. *Methods Mol Biol*. 2015;1238:3-25. doi:10.1007/978-1-4939-1804-1_1.
48 Bewersdorf JP, Shallis R, Stahl M, Zeidan AM. Epigenetic therapy combinations in acute myeloid leukemia: what are the options? *Ther Adv Hematol*. 2019;10:2040620718816698. doi:10.1177/2040620718816698.
49 Kim J, Guermah M, McGinty RK, et al. RAD6-Mediated transcription-coupled H2B ubiquitylation directly stimulates H3K4 methylation in human cells. *Cell*. 2009;137(3):459-471. doi:10.1016/j.cell.2009.02.027.
50 Barski A, Cuddapah S, Cui K, et al. High-resolution profiling of histone methylations in the human genome. *Cell*. 2007;129(4):823-837. doi:10.1016/j.cell.2007.05.009.
51 Sims RJ, Nishioka K, Reinberg D. Histone lysine methylation: a signature for chromatin function. *Trends Genet*. 2003;19(11):629-639. doi:10.1016/j.tig.2003.09.007.
52 Yang Y, Bedford MT. Protein arginine methyltransferases and cancer. *Nat Rev Cancer*. 2013;13(1):37-50. doi:10.1038/nrc3409.
53 Caligiuri MA, Strout MP, Lawrence D, et al. Rearrangement of ALL1 (MLL) in acute myeloid leukemia with normal cytogenetics. *Cancer Res*. 1998;58(1):55-59.
54 McGrath J, Trojer P. Targeting histone lysine methylation in cancer. *Pharmacol Ther*. 2015;150:1-22. doi:10.1016/j.pharmthera.2015.01.002.
55 Varier RA, Timmers HTM. Histone lysine methylation and demethylation pathways in cancer. *Biochim Biophys Acta*. 2011;1815(1):75-89. doi:10.1016/j.bbcan.2010.10.002.
56 Hamamoto R, Saloura V, Nakamura Y. Critical roles of non-histone protein lysine methylation in human tumorigenesis. *Nat Rev Cancer*. 2015;15(2):110-124. doi:10.1038/nrc3884.
57 Gažová I, Lengeling A, Summers KM. Lysine demethylases KDM6A and UTY: The X and Y of histone demethylation. *Mol Genet Metab*. 2019. doi:10.1016/j.ymgme.2019.04.012.
58 Li J, Ahn JH, Wang GG. Understanding histone H3 lysine 36 methylation and its deregulation in disease. *Cell Mol Life Sci*. 2019. doi:10.1007/s00018-019-03144-y.
59 Lowe BR, Maxham LA, Hamey JJ, Wilkins MR, Partridge JF. Histone H3 Mutations: An Updated View of Their Role in Chromatin Deregulation and Cancer. *Cancers (Basel)*. 2019;11(5). doi:10.3390/cancers11050660.
60 Qin J, Wen B, Liang Y, Yu W, Li H. Histone Modifications and their Role in Colorectal Cancer (Review). *Pathol Oncol Res*. 2019. doi:10.1007/s12253-019-00663-8.
61 Han M, Jia L, Lv W, Wang L, Cui W. Epigenetic Enzyme Mutations: Role in Tumorigenesis and Molecular Inhibitors. *Front Oncol*. 2019;9:194. doi:10.3389/fonc.2019.00194.
62 Han D, Huang M, Wang T, et al. Lysine methylation of transcription factors in cancer. *Cell Death Dis*. 2019;10(4):290. doi:10.1038/s41419-019-1524-2.
63 McCabe MT, Mohammad HP, Barbash O, Kruger RG. Targeting Histone Methylation in Cancer. *Cancer J*. 2017;23(5):292-301. doi:10.1097/PPO.0000000000000283.

64 Schenk T, Chen WC, Göllner S, et al. Inhibition of the LSD1 (KDM1A) demethylase reactivates the all-trans-retinoic acid differentiation pathway in acute myeloid leukemia. *Nat Med*. 2012;18(4):605-611. doi:10.1038/nm.2661.

65 Hanahan D, Weinberg RA. Hallmarks of cancer: the next generation. *Cell*. 2011;144(5):646-674. doi:10.1016/j.cell.2011.02.013.

66 Cashen AF, Schiller GJ, O'Donnell MR, DiPersio JF. Multicenter, phase II study of decitabine for the first-line treatment of older patients with acute myeloid leukemia. *J Clin Oncol*. 2010;28(4):556-561. doi:10.1200/JCO.2009.23.9178.

67 Stahl M, DeVeaux M, Montesinos P, et al. Hypomethylating agents in relapsed and refractory AML: outcomes and their predictors in a large international patient cohort. *Blood Adv*. 2018;2(8):923-932. doi:10.1182/bloodadvances.2018016121.

68 Esteller M. Epigenetics in cancer. *N Engl J Med*. 2008;358(11):1148-1159. doi:10.1056/NEJMra072067.

69 Kosugi H, Towatari M, Hatano S, et al. Histone deacetylase inhibitors are the potent inducer/enhancer of differentiation in acute myeloid leukemia: a new approach to anti-leukemia therapy. *Leukemia*. 1999;13(9):1316-1324.

70 Glass JL, Hassane D, Wouters BJ, et al. Epigenetic Identity in AML Depends on Disruption of Nonpromoter Regulatory Elements and Is Affected by Antagonistic Effects of Mutations in Epigenetic Modifiers. *Cancer Discov*. 2017;7(8):868-883. doi:10.1158/2159-8290.CD-16-1032.

71 Castelli G, Pelosi E, Testa U. Targeting histone methyltransferase and demethylase in acute myeloid leukemia therapy. *Onco Targets Ther*. 2018;11:131-155. doi:10.2147/OTT.S145971.

72 Rau RE, Rodriguez BA, Luo M, et al. DOT1L as a therapeutic target for the treatment of DNMT3A-mutant acute myeloid leukemia. *Blood*. 2016;128(7):971-981. doi:10.1182/blood-2015-11-684225.

73 Zheng Y-C, Yu B, Chen Z-S, Liu Y, Liu H-M. TCPs: privileged scaffolds for identifying potent LSD1 inhibitors for cancer therapy. *Epigenomics*. 2016;8(5):651-666. doi:10.2217/epi-2015-0002.

74 Preclinical characterization of a potent and selective inhibitor of the histone demethylase KDM1A for MLL leukemia. *J Clin Oncol;*2013.

75 Fiskus W, Sharma S, Shah B, et al. Highly effective combination of LSD1 (KDM1A) antagonist and pan-histone deacetylase inhibitor against human AML cells. *Leukemia*. 2017;31(7):1658. doi:10.1038/leu.2017.77.

76 Margueron R, Reinberg D. The Polycomb complex PRC2 and its mark in life. *Nature*. 2011;469(7330):343-349. doi:10.1038/nature09784.

77 Shahid Z, Simpson B, Singh G. *StatPearls: Genetics, Histone Code*. Treasure Island (FL); 2019.

78 Cao R, Wang L, Wang H, et al. Role of histone H3 lysine 27 methylation in Polycomb-group silencing. *Science*. 2002;298(5595):1039-1043. doi:10.1126/science.1076997.

79 Ding X, Wang X, Sontag S, et al. The polycomb protein Ezh2 impacts on induced pluripotent stem cell generation. *Stem Cells Dev*. 2014;23(9):931-940. doi:10.1089/scd.2013.0267.

80 Tan J-z, Yan Y, Wang X-x, Jiang Y, Xu HE. EZH2: biology, disease, and structure-based drug discovery. *Acta Pharmacol Sin*. 2014;35(2):161-174. doi:10.1038/aps.2013.161.

81 Lund K, Adams PD, Copland M. EZH2 in normal and malignant hematopoiesis. *Leukemia*. 2014;28(1):44-49. doi:10.1038/leu.2013.288.

82 Plath K, Fang J, Mlynarczyk-Evans SK, et al. Role of histone H3 lysine 27 methylation in X inactivation. *Science*. 2003;300(5616):131-135. doi:10.1126/science.1084274.

83 Di Croce L, Helin K. Transcriptional regulation by Polycomb group proteins. *Nat Struct Mol Biol*. 2013;20(10):1147-1155. doi:10.1038/nsmb.2669.

84 Hu S, Yu L, Li Z, et al. Overexpression of EZH2 contributes to acquired cisplatin resistance in ovarian cancer cells in vitro and in vivo. *Cancer Biol Ther*. 2010;10(8):788-795.

85 Zhang Y, Yu X, Chen L, Zhang Z, Feng S. EZH2 overexpression is associated with poor prognosis in patients with glioma. *Oncotarget*. 2017;8(1):565-573. doi:10.18632/oncotarget.13478.

86 Behrens C, Solis LM, Lin H, et al. EZH2 protein expression associates with the early pathogenesis, tumor progression, and prognosis of non-small cell lung carcinoma. *Clin Cancer Res*. 2013;19(23):6556-6565. doi:10.1158/1078-0432.CCR-12-3946.

87 Kleer CG, Cao Q, Varambally S, et al. EZH2 is a marker of aggressive breast cancer and promotes neoplastic transformation of breast epithelial cells. *Proc Natl Acad Sci U S A*. 2003;100(20):11606-11611. doi:10.1073/pnas.1933744100.

88 Varambally S, Dhanasekaran SM, Zhou M, et al. The polycomb group protein EZH2 is involved in progression of prostate cancer. *Nature*. 2002;419(6907):624-629. doi:10.1038/nature01075.

89 Bachmann IM, Halvorsen OJ, Collett K, et al. EZH2 expression is associated with high proliferation rate and aggressive tumor subgroups in cutaneous melanoma and cancers of the endometrium, prostate, and breast. *J Clin Oncol*. 2006;24(2):268-273. doi:10.1200/JCO.2005.01.5180.

90 Raman JD, Mongan NP, Tickoo SK, Boorjian SA, Scherr DS, Gudas LJ. Increased expression of the polycomb group gene, EZH2, in transitional cell carcinoma of the bladder. *Clin Cancer Res*. 2005;11(24 Pt 1):8570-8576. doi:10.1158/1078-0432.CCR-05-1047.

91 Kondo Y, Shen L, Suzuki S, et al. Alterations of DNA methylation and histone modifications contribute to gene silencing in hepatocellular carcinomas. *Hepatol Res*. 2007;37(11):974-983. doi:10.1111/j.1872-034X.2007.00141.x.

92 Lee HW, Choe M. Expression of EZH2 in renal cell carcinoma as a novel prognostic marker. *Pathol Int*. 2012;62(11):735-741. doi:10.1111/pin.12001.

93 Matsukawa Y, Semba S, Kato H, Ito A, Yanagihara K, Yokozaki H. Expression of the enhancer of zeste homolog 2 is correlated with poor prognosis in human gastric cancer. *Cancer Sci*. 2006;97(6):484-491. doi:10.1111/j.1349-7006.2006.00203.x.

94 Ougolkov AV, Bilim VN, Billadeau DD. Regulation of pancreatic tumor cell proliferation and chemoresistance by the histone methyltransferase enhancer of zeste homologue 2. *Clin Cancer Res*. 2008;14(21):6790-6796. doi:10.1158/1078-0432.CCR-08-1013.

95 Ma R, Wei Y, Huang X, et al. Inhibition of GSK 3β activity is associated with excessive EZH2 expression and enhanced tumour invasion in nasopharyngeal carcinoma. *PLoS ONE*. 2013;8(7):e68614. doi:10.1371/journal.pone.0068614.

96 Abd Al Kader L, Oka T, Takata K, et al. In aggressive variants of non-Hodgkin lymphomas, Ezh2 is strongly expressed and polycomb repressive complex PRC1.4 dominates over PRC1.2. *Virchows Arch*. 2013;463(5):697-711. doi:10.1007/s00428-013-1428-y.

97 van Galen JC, Muris JJF, Oudejans JJ, et al. Expression of the polycomb-group gene BMI1 is related to an unfavourable prognosis in primary nodal DLBCL. *J Clin Pathol*. 2007;60(2):167-172. doi:10.1136/jcp.2006.038752.

98 Morin RD, Johnson NA, Severson TM, et al. Somatic mutations altering EZH2 (Tyr641) in follicular and diffuse large B-cell lymphomas of germinal-center origin. *Nat Genet*. 2010;42(2):181-185. doi:10.1038/ng.518.

99 Bödör C, Grossmann V, Popov N, et al. EZH2 mutations are frequent and represent an early event in follicular lymphoma. *Blood*. 2013;122(18):3165-3168. doi:10.1182/blood-2013-04-496893.

100 Yap DB, Chu J, Berg T, et al. Somatic mutations at EZH2 Y641 act dominantly through a mechanism of selectively altered PRC2 catalytic activity, to increase H3K27 trimethylation. *Blood*. 2011;117(8):2451-2459. doi:10.1182/blood-2010-11-321208.

101 Sneeringer CJ, Scott MP, Kuntz KW, et al. Coordinated activities of wild-type plus mutant EZH2 drive tumor-associated hypertrimethylation of lysine 27 on histone H3 (H3K27) in human B-cell lymphomas. *Proc Natl Acad Sci U S A*. 2010;107(49):20980-20985. doi:10.1073/pnas.1012525107.

102 Ernst T, Chase AJ, Score J, et al. Inactivating mutations of the histone methyltransferase gene EZH2 in myeloid disorders. *Nat Genet*. 2010;42(8):722-726. doi:10.1038/ng.621.

103 Nikoloski G, Langemeijer SMC, Kuiper RP, et al. Somatic mutations of the histone methyltransferase gene EZH2 in myelodysplastic syndromes. *Nat Genet*. 2010;42(8):665-667. doi:10.1038/ng.620.

104 Guglielmelli P, Biamonte F, Score J, et al. EZH2 mutational status predicts poor survival in myelofibrosis. *Blood*. 2011;118(19):5227-5234. doi:10.1182/blood-2011-06-363424.

105 Xu B, On DM, Ma A, et al. Selective inhibition of EZH2 and EZH1 enzymatic activity by a small molecule suppresses MLL-rearranged leukemia. *Blood*. 2015;125(2):346-357. doi:10.1182/blood-2014-06-581082.

106 Basheer F, Giotopoulos G, Meduri E, et al. Contrasting requirements during disease evolution identify EZH2 as a therapeutic target in AML. *J Exp Med*. 2019;216(4):966-981. doi:10.1084/jem.20181276.

107 Vick B, Rothenberg M, Sandhöfer N, et al. An advanced preclinical mouse model for acute myeloid leukemia using patients' cells of various genetic subgroups and in vivo bioluminescence imaging. *PLoS ONE*. 2015;10(3):e0120925. doi:10.1371/journal.pone.0120925.

108 Mulholland CB, Ryan J, Qin W, et al. *TET1 drives global DNA demethylation via DPPA3-mediated inhibition of maintenance methylation*; 2018.

109 Bradford MM. A rapid and sensitive method for the quantitation of microgram quantities of protein utilizing the principle of protein-dye binding. *Anal Biochem*. 1976;72:248-254.

110 Mulholland CB, Smets M, Schmidtmann E, et al. A modular open platform for systematic functional studies under physiological conditions. *Nucleic Acids Res*. 2015;43(17):e112. doi:10.1093/nar/gkv550.

111 Soumillon M, Cacchiarelli D, Semrau S, van Oudenaarden A, Mikkelsen TS. *Characterization of directed differentiation by high-throughput single-cell RNA-Seq*; 2014.

112 Parekh S, Ziegenhain C, Vieth B, Enard W, Hellmann I. zUMIs - A fast and flexible pipeline to process RNA sequencing data with UMIs. *Gigascience*. 2018;7(6). doi:10.1093/gigascience/giy059.

113 Dobin A, Davis CA, Schlesinger F, et al. STAR: ultrafast universal RNA-seq aligner. *Bioinformatics*. 2013;29(1):15-21. doi:10.1093/bioinformatics/bts635.

114 Ritchie ME, Phipson B, Di Wu, et al. limma powers differential expression analyses for RNA-sequencing and microarray studies. *Nucleic Acids Res*. 2015;43(7):e47. doi:10.1093/nar/gkv007.

115 Robinson MD, McCarthy DJ, Smyth GK. edgeR: a Bioconductor package for differential expression analysis of digital gene expression data. *Bioinformatics*. 2010;26(1):139-140. doi:10.1093/bioinformatics/btp616.

116 Glueck DH, Mandel J, Karimpour-Fard A, Hunter L, Muller KE. Exact calculations of average power for the Benjamini-Hochberg procedure. *Int J Biostat*. 2008;4(1):Article 11. doi:10.2202/1557-4679.1103.

117 Büchner T, Berdel WE, Schoch C, et al. Double induction containing either two courses or one course of high-dose cytarabine plus mitoxantrone and postremission therapy by either autologous stem-cell transplantation or by prolonged maintenance for acute myeloid leukemia. *J Clin Oncol*. 2006;24(16):2480-2489. doi:10.1200/JCO.2005.04.5013.

118 Herold T, Metzeler KH, Vosberg S, et al. Isolated trisomy 13 defines a homogeneous AML subgroup with high frequency of mutations in spliceosome genes and poor prognosis. *Blood*. 2014;124(8):1304-1311. doi:10.1182/blood-2013-12-540716.

119 Wouters BJ, Löwenberg B, Erpelinck-Verschueren CAJ, van Putten WLJ, Valk PJM, Delwel R. Double CEBPA mutations, but not single CEBPA mutations, define a subgroup of acute myeloid leukemia with a distinctive gene expression profile that is uniquely associated with a favorable outcome. *Blood*. 2009;113(13):3088-3091. doi:10.1182/blood-2008-09-179895.

120 Taskesen E, Bullinger L, Corbacioglu A, et al. Prognostic impact, concurrent genetic mutations, and gene expression features of AML with CEBPA mutations in a cohort of 1182 cytogenetically normal AML patients: further evidence for CEBPA double mutant AML as a distinctive disease entity. *Blood*. 2011;117(8):2469-2475. doi:10.1182/blood-2010-09-307280.

121 Hothorn T LB. On the exact distribution of maximally selected rank statistics. *Computational Statistics & Data Analysis*.

122 Papaemmanuil E, Gerstung M, Malcovati L, et al. Clinical and biological implications of driver mutations in myelodysplastic syndromes. *Blood*. 2013;122(22):3616-27; quiz 3699. doi:10.1182/blood-2013-08-518886.

123 Stief SM, Hanneforth A-L, Weser S, et al. Loss of KDM6A confers drug resistance in acute myeloid leukemia. *Leukemia*. 2019. doi:10.1038/s41375-019-0497-6.

124 Makishima H, Jankowska AM, Tiu RV, et al. Novel homo- and hemizygous mutations in EZH2 in myeloid malignancies. *Leukemia*. 2010;24(10):1799-1804. doi:10.1038/leu.2010.167.

125 Rinke J, Müller JP, Blaess MF, et al. Molecular characterization of EZH2 mutant patients with myelodysplastic/myeloproliferative neoplasms. *Leukemia*. 2017;31(9):1936-1943. doi:10.1038/leu.2017.190.

126 Booth CAG, Barkas N, Neo WH, et al. Ezh2 and Runx1 Mutations Collaborate to Initiate Lympho-Myeloid Leukemia in Early Thymic Progenitors. *Cancer Cell*. 2018;33(2):274-291.e8. doi:10.1016/j.ccell.2018.01.006.

127 Wu H, Min J, Lunin VV, et al. Structural biology of human H3K9 methyltransferases. *PLoS ONE*. 2010;5(1):e8570. doi:10.1371/journal.pone.0008570.

128 Wang X, Dai H, Wang Q, et al. EZH2 mutations are related to low blast percentage in bone marrow and -7/del(7q) in de novo acute myeloid leukemia. *PLoS ONE*. 2013;8(4):e61341. doi:10.1371/journal.pone.0061341.

129 Poepsel S, Kasinath V, Nogales E. Cryo-EM structures of PRC2 simultaneously engaged with two functionally distinct nucleosomes. *Nat Struct Mol Biol*. 2018;25(2):154-162. doi:10.1038/s41594-018-0023-y.

130 Papaemmanuil E, Gerstung M, Bullinger L, et al. Genomic Classification and Prognosis in Acute Myeloid Leukemia. *N Engl J Med*. 2016;374(23):2209-2221. doi:10.1056/NEJMoa1516192.

131 Göllner S, Oellerich T, Agrawal-Singh S, et al. Loss of the histone methyltransferase EZH2 induces resistance to multiple drugs in acute myeloid leukemia. *Nat Med*. 2017;23(1):69-78. doi:10.1038/nm.4247.

132 Ott HM, Graves AP, Pappalardi MB, et al. A687V EZH2 is a driver of histone H3 lysine 27 (H3K27) hypertrimethylation. *Mol Cancer Ther*. 2014;13(12):3062-3073. doi:10.1158/1535-7163.MCT-13-0876.

133 Mallo M, Wellik DM, Deschamps J. Hox genes and regional patterning of the vertebrate body plan. *Dev Biol*. 2010;344(1):7-15. doi:10.1016/j.ydbio.2010.04.024.

134 O'Carroll D, Erhardt S, Pagani M, Barton SC, Surani MA, Jenuwein T. The polycomb-group gene Ezh2 is required for early mouse development. *Mol Cell Biol*. 2001;21(13):4330-4336. doi:10.1128/MCB.21.13.4330-4336.2001.

135 Abramovich C, Humphries RK. Hox regulation of normal and leukemic hematopoietic stem cells. *Curr Opin Hematol*. 2005;12(3):210-216.

136 Fuller JF, McAdara J, Yaron Y, Sakaguchi M, Fraser JK, Gasson JC. Characterization of HOX gene expression during myelopoiesis: role of HOX A5 in lineage commitment and maturation. *Blood*. 1999;93(10):3391-3400.

137 Buske C, Feuring-Buske M, Antonchuk J, et al. Overexpression of HOXA10 perturbs human lymphomyelopoiesis in vitro and in vivo. *Blood*. 2001;97(8):2286-2292. doi:10.1182/blood.v97.8.2286.

138 Thorsteinsdottir U, Mamo A, Kroon E, et al. Overexpression of the myeloid leukemia-associated Hoxa9 gene in bone marrow cells induces stem cell expansion. *Blood*. 2002;99(1):121-129. doi:10.1182/blood.v99.1.121.

139 Collins CT, Hess JL. Role of HOXA9 in leukemia: dysregulation, cofactors and essential targets. *Oncogene*. 2016;35(9):1090-1098. doi:10.1038/onc.2015.174.

140 Chen S, Yu J, Lv X, Zhang L. HOXA9 is critical in the proliferation, differentiation, and malignancy of leukaemia cells both in vitro and in vivo. *Cell Biochem Funct*. 2017;35(7):433-440. doi:10.1002/cbf.3293.

141 Chen J, Li J, Han Q, et al. Enhancer of zeste homolog 2 is overexpressed and contributes to epigenetic inactivation of p21 and phosphatase and tensin homolog in B-cell acute

lymphoblastic leukemia. *Exp Biol Med (Maywood)*. 2012;237(9):1110-1116. doi:10.1258/ebm.2012.012075.

142 Ito T, Teo YV, Evans SA, Neretti N, Sedivy JM. Regulation of Cellular Senescence by Polycomb Chromatin Modifiers through Distinct DNA Damage- and Histone Methylation-Dependent Pathways. *Cell Rep*. 2018;22(13):3480-3492. doi:10.1016/j.celrep.2018.03.002.

143 Dhawan S, Tschen S-I, Bhushan A. Bmi-1 regulates the Ink4a/Arf locus to control pancreatic beta-cell proliferation. *Genes Dev*. 2009;23(8):906-911. doi:10.1101/gad.1742609.

144 Bracken AP, Dietrich N, Pasini D, Hansen KH, Helin K. Genome-wide mapping of Polycomb target genes unravels their roles in cell fate transitions. *Genes Dev*. 2006;20(9):1123-1136. doi:10.1101/gad.381706.

145 Chen H, Gu X, Su I-h, et al. Polycomb protein Ezh2 regulates pancreatic beta-cell Ink4a/Arf expression and regeneration in diabetes mellitus. *Genes Dev*. 2009;23(8):975-985. doi:10.1101/gad.1742509.

146 Gil J, Peters G. Regulation of the INK4b-ARF-INK4a tumour suppressor locus: all for one or one for all. *Nat Rev Mol Cell Biol*. 2006;7(9):667-677. doi:10.1038/nrm1987.

147 Gibbs JD, Liebermann DA, Hoffman B. Egr-1 abrogates the E2F-1 block in terminal myeloid differentiation and suppresses leukemia. *Oncogene*. 2008;27(1):98-106. doi:10.1038/sj.onc.1210627.

148 Nguyen HQ, Hoffman-Liebermann B, Liebermann DA. The zinc finger transcription factor Egr-1 is essential for and restricts differentiation along the macrophage lineage. *Cell*. 1993;72(2):197-209. doi:10.1016/0092-8674(93)90660-i.

149 Tanaka S, Miyagi S, Sashida G, et al. Ezh2 augments leukemogenicity by reinforcing differentiation blockage in acute myeloid leukemia. *Blood*. 2012;120(5):1107-1117. doi:10.1182/blood-2011-11-394932.

150 Mallen-St Clair J, Soydaner-Azeloglu R, Lee KE, et al. EZH2 couples pancreatic regeneration to neoplastic progression. *Genes Dev*. 2012;26(5):439-444. doi:10.1101/gad.181800.111.

151 Grubach L, Juhl-Christensen C, Rethmeier A, et al. Gene expression profiling of Polycomb, Hox and Meis genes in patients with acute myeloid leukaemia. *Eur J Haematol*. 2008;81(2):112-122. doi:10.1111/j.1600-0609.2008.01083.x.

152 Wen S, Wang J, Liu P, et al. Novel combination of histone methylation modulators with therapeutic synergy against acute myeloid leukemia in vitro and in vivo. *Cancer Lett*. 2018;413:35-45. doi:10.1016/j.canlet.2017.10.015.

153 Fujita S, Honma D, Adachi N, et al. Dual inhibition of EZH1/2 breaks the quiescence of leukemia stem cells in acute myeloid leukemia. *Leukemia*. 2018;32(4):855-864. doi:10.1038/leu.2017.300.

154 Sashida G, Harada H, Matsui H, et al. Ezh2 loss promotes development of myelodysplastic syndrome but attenuates its predisposition to leukaemic transformation. *Nat Commun*. 2014;5:4177. doi:10.1038/ncomms5177.

155 Voz ML, Mathys J, Hensen K, et al. Microarray screening for target genes of the proto-oncogene PLAG1. *Oncogene*. 2004;23(1):179-191. doi:10.1038/sj.onc.1207013.

156 Landrette SF, Kuo Y-H, Hensen K, et al. Plag1 and Plagl2 are oncogenes that induce acute myeloid leukemia in cooperation with Cbfb-MYH11. *Blood*. 2005;105(7):2900-2907. doi:10.1182/blood-2004-09-3630.

5.3. Single Letter Codes for Amino Acids

Single letter code	Amino Acid
nonpolar	
A	Alanine (Ala)
V	Valine (Val)
L	Leucine (Leu)
I	Isoleucine (Ile)
M	Methionine (Met)
P	Proline (Pro)
G	Glycine (Gly)
polar hydrophylic	
S	Serine (Ser)
T	Threonine (Thr)
C	Cysteine (Cys)
N	Asparagine (Asn)
E	Glutamic acid (Glu)
negatively charged	
Q	Glutamine (Gln)
D	Aspartic acid (Asp)
positively charged	
K	Lysine (Lys)
R	Arginine (Arg)
H	Histidine (His)
aromatic	
F	Phenylalanine (Phe)
Y	Tyrosine (Tyr)
W	Tryptophan (Trp)

5.4. Abbreviations

%	Percentage
°C	Degree Celsius
µ	Micro
A	Ampère
ALL	Acute Lymphoblastic Leukaemia
AraC	Cytarabine
ASXL1	ASXL Transcriptional Regulator 1
AZA	Azacytidine
bp	Basepair/basepairs
BSA	Bovine serum albumine
cDNA	Complementary DNA
CML	Chronic Myeloid Leukaemia
CN	Cytogenetically normal
CR	Complete remission
CRISPR	Clustered Regularly Interspaced Short Palindromic Repeat
DAC	Decitabine
Del	deletion
Dest	Distilled
DMEM	Dulbecco´s Modified Eagle Medium
DMSO	Dimethyl Sulfoxide
DNA	Deoxyribonucleic acid
DNMT	DNA methyltransferase
DNMT3A	DNA methyltransferase 3 alpha
DNR	Daunorubicin
dNTP	deoxynucleotide triphosphate
dsDNA	Double-stranded DNA
DSMZ	German Collection of Microorganisms and Cell Cultures
DTT	Dithiothreitol
e.g.	for example
ECL	Enhanced chemoluminescence
EDTA	Ethylene diamine tetraacetic acid
EED	Embryonic Ectoderm Development Protein
EGR1	Early growth response protein 1

ELN	European LeukaemiaNet
ESC	Embryonic stem cell
EZH2	Enhancer of zeste homolog 2
FAB	French-American-British classification system
FACS	Fluorescence activated cell sorter
FBS	Fetal bovine serum
FLT3	Fms-like tyrosine kinase 3
FOR	Forward
g	Gram, genomic
GFP	Green fluorescent protein
GOF	Gain of function
h	Hours
H	Histone, Histidine
H3K27me1	Histone 3 lysine 27 mono-methylation
H3K27me2	Histone 3 lysine 27 di-methylation
H3K27me3	Histone 3 lysine 27 tri-methylation
HBS	Hepes-buffered saline
HMT	Histone methyltransferase
HOX	Homeobox
HRP	Horseradish peroxidase
HSC	Haematopoietic stem cell
i.v.	Intravenous
IC_{50}	Half-inhibitory concentration
IL-3	Interleukin 3
IL-6	Interleukin 6
inv	Inversion
ITD	Internal tandem duplication
kb	Kilo base pairs
Kd	Knockdown
kDa	Kilodalton(s)
Kg	Kilogram
KO	Knockout
l	Liter
LOF	Loss of function

LSC	Leukemic stem cell
M	Molar (mol/l)
m	Milli
MDR	Multidrug-resistance
MDS	Myelodysplastic syndrome
min	Minute(s)
MLL	Mixed Lineage Leukaemia
MLPA	Multiplex Ligation-dependent Probe Amplification
MPN	Myeloproliverative neoplasm
MRD	Minimal residual disease
mRNA	Messenger RNA
Mut	Mutated
n.s.	Not significant
Nano	Nano
NGS	Next-generation sequencing
NMP1	Nucleophosmin-1
OS	Overall survival
PAGE	Polyacrylamide gel electrophoresis
PB	PiggyBac
PBS	Phosphate buffered saline
PCR	Polymerase chain reaction
PDX	Patient-derived xenograft
PMSF	Phenylmethylsulfonyl fluoride
PRC1	Polycomb repressive complex 1
PRC2	Polycomb repressive complex 2
RB/AP46	Histone-binding protein RBBP4
REV	Reverse
RFS	Relapse free survival
rh	Recombinant human
RNA	Ribonucleic acid
RNAi	RNA interference
rpm	Rounds per minute
RPMI	Roswell Park Memorial Institute
RT	Room temperature,

SAH	S-adenosyl homocysteine
SAM	S-adenosyl-L-methionine
sAML	secondary AML
SCF	Stem cell factor
SDS	Sodium dodecyl sulfate
sec	Second
SET	Su(var)3-9, Enhancer-of-zeste and Trithorax
sgRNA	Single guide RNA
S-HAM	Sequential high dose AraC with mitoxantrone
siRNA	Small interfering RNA
SNP	Single nucleotide polymorphism
t	Translocation
t-AML	Therapy-related AML
TBS	Tris-buffered saline
TET2	Tet methylcytosine dioxygenase 2
Tm	Primer Melting Temperature
UPN	Unique Patient Number
V	Volt
VAF	Variant allele frequency
WB	Western Blot
WHO	World Health Organization
wt	Wildtype
α	Alpha, Anti
β	Beta

5.5. Figure Legend

5.6. Table Legend

5.7. Acknowledgements

Throughout my research work I have received a great deal of support and assistance for which I wish to thank. My deepest gratitude goes to my first supervisor Prof. Dr. Karsten Spiekermann, whose expertise was invaluable during my research work. His support and willingness to help in any kind of situation was irreplaceable.
Additionally, my deepest thank goes to Prof. Dr. rer. nat. Gunnar Schotta who agreed to support me as doctoral supervisor and supported during experimental project planning, and who was always ready to help.
My deepest thank also goes to Dr. Oliver Weigert who supported my project by participating my TAC. His great input and discussion guided the project essentially.

I would also like to thank the whole Spiekermann lab group. Dr. Sophie Stief, Dr. Harald Polzer, Maike Roas, Sabrina Weser, Anna Vetter and Belay Tizazu were a wonderful team and working family. They supported me during the daily routine and each time, motivation was necessary.

Special thank therefore goes to Dr. Sophie Stief, Maike Roas, Anna Vetter and Georg Leubolt. Their mental and practical support was invaluable during my work in the laboratory.

I also want to thank Michael Bartoschek, Prof. Dr. Irmela Jeremias, Dr. Binje Vick, Kerstin Völse and Dr. Tobias Herold for their great support during scientific cooperation and their kindful assistance.

I thank Sabrina Weser for processing and evaluating of all mRNA expression work described in this thesis.

To finish, lovely thanks go to Dr. Kristi König, Dr. Lisa Kempf, Raphael Graf, Sebastian Schmidt and all of my friends. Their mental support was irreplaceable.